Title

Adapting to Wildfire Risk in the California Electric Power Sector

Author

Warner, Cody

Publication Date

2024

Peer reviewed|Thesis/dissertation

Adapting to Wildfire Risk in the California Electric Power Sector

by

Cody Warner

A dissertation submitted in partial satisfaction of the

requirements for the degree of

Doctor of Philosophy

in

Energy and Resources

in the

Graduate Division

of the

University of California, Berkeley

Committee in charge:

Professor Duncan Callaway, Co-chair
Professor David Anthoff, Co-chair
Professor Meredith Fowlie
Professor Judson Boomhower

Summer 2024

Adapting to Wildfire Risk in the California Electric Power Sector

Abstract

Adapting to Wildfire Risk in the California Electric Power Sector

by

Cody Warner

Doctor of Philosophy in Energy and Resources

University of California, Berkeley

Professor Duncan Callaway, Co-chair

Professor David Anthoff, Co-chair

In recent years, the risk of catastrophic wildfire has escalated rapidly in the Western U.S. and globally. Earlier spring snowmelt and increasing moisture deficits have caused a dramatic rise in burned area. Climate warming does not act alone, however, in the explanation of rising wildfire risk. Population migration to high-risk areas and historical fire suppression policies have also contributed to the uptick in risk. These factors, in combination with aging electric utility infrastructure, have left the electric-power sector acutely vulnerable to catastrophic wildfire risk. In California, electric utilities are investing significant resources to buy down their exposure to wildfire and adapt to a future with more climate extremes. The research described in the following chapters dives into the costs and risk implications of such high-stakes electric-power sector adaptation investments. Probabilistic machine-learning models are trained and evaluated alongside econometric methods to address the low-probability, high-consequence nature of wildfire outcomes. Spatially-granular, robustly estimated measures of risk are shown to be fundamental ingredients to effective analysis of wildfire risk, management, and policy. One of the overarching findings is that cost-effective adaptation in the electric-power sector hinges crucially on the level of adaptation outside the electric-power sector. Overall, cross-sector collaboration across all levels of wildfire risk management is necessary to ensure electric-power sector adaptation investments deliver their intended risk reduction benefits and mitigate the threat of catastrophic wildfire damages.

"Examine each question in terms of what is ethically and aesthetically right, as well as what is economically expedient. A thing is right when it tends to preserve the integrity, stability, and beauty of the biotic community. It is wrong when it tends otherwise."

- Aldo Leopold, *A Sand County Almanac*, 1949

"I recognize the right and duty of this generation to develop and use the natural resources of our land; but I do not recognize the right to waste them, or to rob, by wasteful use, the generations that come after us[...] The farmer is a good farmer who, having enabled the land to support himself and to provide for the education of his children, leaves it to them a little better than he found it himself. I believe the same thing of a nation."

- Theodore Roosevelt, August 31, 1910

Contents

List of Figures

List of Tables

Acknowledgments

I am grateful for the many advisors and the academic community at UC Berkeley who have been invaluable in guiding me on this intellectual journey. Duncan Callaway and Meredith Fowlie have both generously dedicated their time to the ideas and analyses laid out in the following chapters. I am thankful for the many opportunities they have given me to share these findings with broader audiences and engage publicly. Their encouragement and thoughtful guidance has improved all levels of the research presented here, and I thank them both for that. I am also grateful to David Anthoff and Judd Boomhower for serving on my dissertation committee. They provided essential motivation and support at early and midway stages of the dissertation development. The Energy and Resources Group (ERG) community has been unrelenting in its goal of maintaining an inclusive space to pursue intellectual growth. It cannot be understated how valuable it is explore new ideas in an environment that is both welcoming and challenging. I appreciate how the ERG community strives to be a model for inclusive and interdisciplinary research, recognizing this is a continuously evolving goal. The academic staff at ERG, specifically Candace Groskreutz and Kay Burns, has provided me with valuable assistance when I have needed it most (and usually on late notice). Lastly, I am indebted to my family and friends for their unconditional support throughout the last six years and more. To my wife, Helen, none of this would have been possible without you. I thank you for your steadfast belief in seeing this through, despite the own sacrifices you have taken. To my parents, Cathie and Chris, thank you for showing me the importance of education and opening my eyes to the beauty of the California coast, woodlands, and mountains. Your passion for civic engagement has no doubt inspired my research at the intersection of policy, the environment, and economics. And to my brother, Christopher, thank you for ushering in the creativity and improvisation in life, something that is not lost on me amidst the technical nature of economic research.

Chapter 1

Introduction

1.1 Motivation

The research presented here is motivated by the overarching question: *what policies and investments can lead us to cost-effectively adapt to wildfire risk?* Unequivocally, wildfire risk has increased in recent years, particularly in the western forests of the United States [1–3]. Anthropogenic climate change has played a prominent role in this increase, but it is not the sole actor. Population migration to the wildland urban interface (WUI), where ignition rates are higher and fire behavior is more extreme, has caused an uptick in wildfire risk [4]. Policy has played a role, too. The institutionalized federal forest policy of suppressing wildfires and protecting the nation's timber resources has caused a dearth of low-intensity "good" fire [5].

Adapting to wildfire, like other climate change-fueled natural disasters, will be challenging and involve many levels of stakeholders. However, the task is not impossible. Unlike other natural disasters, such as hurricanes or winter storms, the vast majority of wildfires are caused by humans [6]. Moreover, their severity can be feasibly altered through known and effective management strategies, such as prescribed burns and mechanical thinning of fuels [7]. This makes wildfire a compelling setting to study adaptation strategies, policy, and economics.

The research presented here focuses on the nexus between wildfire and the electric-power sector, and in particular, the electric utility industry of California. The state is on the front lines of climate change, both in terms of policy and the impacts of rising temperatures. Despite the focus on California, the findings of this research inform ongoing policy discussions across the world. Many other regions face similar escalations in wildfire risk caused by aging electric distribution and transmission infrastructure. Australia, Hawaii, Texas, Canada, and Southern Europe are recent examples of regions experiencing catastrophic wildfire outcomes caused by electrical equipment.

I focus on the electric-power sector because a disproportionate share of wildfire damages

observed in California has been caused by the electric grid. As discussed in the next chapter, grid-caused ignitions frequently occur during strong wind events, when fires are more difficult to suppress, and in close proximity to structures [8–10]. Consequently, a significant flow of adaptation investment is being channeled through the electric-power sector in California. Electric utilities have proposed spending $9 billion annually on adapting to wildfire [11–13].

I also focus on the electric-power sector because the costs of adapting to wildfire in the electric-power sector have important implications for efforts to mitigate global greenhouse gas emissions. A core pillar of de-carbonization policy boils down to deploying low-carbon electric generating resources and "electrifying everything." Rising electricity costs, brought about by wildfire adaptation costs, threaten to undermine the incentives of this electrification strategy. Whether one lives in a high-fire risk area or not, all grid-connected, rate-paying electricity customers have a stake in ensuring cost-effective wildfire adaptation.

Lastly, from an economic perspective, studying wildfire risk is a fascinating and challenging task. The vast majority of wildfire ignitions do not lead to catastrophic outcomes. In fact, low-intensity wildfires create positive benefits to the ecosystem and can reduce future wildfire severity [5]. The risks associated with wildfire are thus concentrated in low-probability but extremely consequential events. Just one wildfire, the Camp fire, dealt approximately two-thirds of all of Pacific Gas and Electric Company's associated structure losses during the study period discussed in the next chapter. Developing probabilistic models that accurately capture the nature of such rare events data is a crucial ingredient to effective analysis of wildfire risk management and policy.

My hope is that this dissertation will inform policymakers, electric utilities, and communities that are grappling with a rapid rise in wildfire risk. In California, electric utilities have recently crafted plans and models to assess their exposure to wildfire risk. However, many electric utilities across the U.S. (and the world) do not have a clear accounting of their risk exposure[14]. The findings presented throughout can aid policymakers, utilities, and academic researchers who seek to develop rigorous risk models and evaluate the difficult trade-offs inherent to climate change adaptation.

1.2 Structure

Chapter 2, titled "Risk-Cost Trade-Offs in Electric Power-Sector Wildfire Adaptation," forms the key building block of the dissertation. Using empirical data on ignitions, wildfire sizes, adaptation investments, and costs, the chapter seeks to quantify the cost-effectiveness of electric-power sector wildfire adaptation investments made by the largest U.S. electric distribution utility. In doing so, the analysis combines machine-learning models and econometrics to identify the causal effects of different types of wildfire adaptation investments on ignition outcomes.

Overall, the analysis concludes that innovative grid management protocols can simulta-

neously reduce wildfire risk and decrease the need for capital-intensive adaptation measures. Burying powerlines underground, an archetype of system hardening, is shown to be less cost-effective than fast-trip settings, one example of innovative grid management protocols. However, electric utilities may prefer such capital-intensive system hardening due to more certain risk reductions and the incentives that rate of return regulation offers for capital investments.

The subsequent chapter, Chapter 3, is titled, "Measuring Uncertainty in the Cost-Effectiveness of System Hardening Investments." The analysis dives deeper into sources of uncertainty that determine the cost-effectiveness of system hardening investments. The probabilistic models developed in the preceding chapter form the basis of the methodological approach.

The analysis sets up a contrast between factors that are endogenous to the electric utility risk manager and factors that are exogenous. A point of emphasis is that exogenous factors, like the amount of protection property owners take to reduce structure losses, can change the cost-effectiveness of long-duration system hardening investments. This creates the potential for such investments to become "stranded assets," in which rate-paying customers are left paying for under-performing assets. On the other hand, the analysis finds that large and uncertain increases in extreme wildfire risk, which are also exogenous to the utility decision maker, can significantly improve cost-effectiveness. The study finds that regions with the largest uncertainty in wildfire behavior are also the regions where it is most cost-effective to bury powerlines, which suggests such investments may provide additional benefits by reducing extreme outcomes at the tail of the risk distribution. Overall, the findings of the chapter conclude that cross-sector collaboration across all levels of wildfire risk management is critical to ensuring cost-effective adaptation.

The final chapter, titled, "Charge Anxiety: The Effect of Wildfire-Induced Electricity Outages on Battery-Electric Vehicle Adoption," departs from the previous two and focuses on possible unintended consequences of wildfire adaptation investments in the electric-power sector. As explained in the introduction, such adaptation investments may come into conflict with broader de-carbonization goals, specifically building and transportation-sector electrification. The chapter explores the impact of wildfire-related electricity outages on electric vehicle adoption across the state of California.

In doing so, the analysis provides insight into a relatively understudied area of electric vehicle adoption called "charge anxiety." A close cousin of range anxiety, charge anxiety involves the potential for electric vehicle adopters to internalize the costs and frequency of electricity outages when making an adoption decision. The findings of the econometric analysis provide weak evidence that low-income customers and customers with long commute times are most susceptible to "charge anxiety." This echoes well-established energy justice concerns related to electricity reliability, electric vehicle adoption, and rate affordability.

Chapter 2

Risk-Cost Trade-Offs in Electric Power-Sector Wildfire Adaptation

2.1 Introduction

Wildfire is the fastest growing economic climate risk [15]. The destructive potential of wildfires ignited by electricity infrastructure is particularly high because these ignitions frequently occur during strong wind events and in close proximity to structures[8–10]. Some of the most destructive fires recorded have been traced to utility infrastructure, including the 2009 Black Saturday fires in Australia ($4.4B in losses)[16], the 2021 Dixie Fire in California (nearly one million acres burned)[17] and the 2023 wildfires in Maui (101 fatalities, the deadliest wildfire in the U.S. in the last century)[18, 19]. Faced with growing liabilities, utilities are spending billions of dollars to adapt to these increasing risks.

Recent reports suggest there is significant under-investment in climate change adaptation[20]. Factors that slow or impede cost-effective adaptation investments include a lack of quantifiable returns on investment and a dearth of evidence on the effectiveness of alternative adaptation strategies[21]. This study quantifies the effectiveness of a multi-faceted and multi-billion dollar effort to adapt to increasing wildfire risk. It presents an empirically tractable framework for evaluating the causal impacts of alternative wildfire risk management strategies on ignition outcomes, grid reliability, and ratepayer costs.

The central role that electric utilities play in climate change mitigation complicates the evaluation of wildfire risk management in the electric power sector. There is a global movement to decarbonize the sector and electrify end-uses that are currently powered by carbon-intensive fuels[22, 23]. If utility spending on wildfire risk management increases electricity rates, this will reduce incentives for households and firms to electrify. In addition, strategies that de-energize lines during high-risk conditions could slow the pace of electrification by reducing grid reliability. Utility decision-making must therefore strike a balance between wildfire risk adaptation and climate change mitigation efforts that will require affordable

and reliable electricity service.

The existing literature on climate change adaptation in the electricity sector has focused primarily on the investments to accommodate increases in electricity demand induced by rising temperatures and the need for cooling services[24–27]. Less attention has been paid to managing wildfire risks, despite the rising costs of wildfire risk mitigation. In California alone, the state's three largest utilities are proposing to spend $9 billion annually, up from $4.7 billion in 2019[11–13]. This utility spending far exceeds the amount that state and federal governments spend on fuel reduction treatments: The state of California budgeted less than $1 billion for the 2021-22 fiscal year on wildfire and forest resilience[28], and the 2025 U.S. Forest Service budget includes $207 million for hazardous fuel reductions[29].

This study also contributes to a nascent empirical literature on wildfire risk management[30–34]. Much of this research has focused on efforts outside the electric power sector, including building codes, fire suppression, and prescribed burns. In an electric power sector context, some studies have investigated the consequences of preventative power shutoffs, the cost implications of undergrounding, and the effect of vegetation management on outages[35–40]. Others have focused on electric utility planning and wildfire risk management[14, 41, 42]. Leveraging detailed data on powerline-caused ignitions in California, ours is the first to study ignition mitigation effectiveness, reliability impacts, and costs across a variety of strategies.

Wildfire Risk Reduction Strategies

An electric utility has several approaches at its disposal to reduce ignition risk on its distribution grid. These interventions can be classified into three categories.

System hardening includes measures such as undergrounding overhead powerlines, covering overhead bare conductors with insulated material, and replacing or reinforcing distribution poles. These types of measures require upfront capital investment and take time to deploy. Undergrounding can provide near permanent reductions in ignition risk, but capital costs are significant.

Vegetation management can substantially reduce ignitions caused by vegetation contact. "Enhanced" vegetation management removes all vegetation within twelve feet of overhead lines. The risk reduction benefits of enhanced vegetation management are not as permanent as system hardening investments because vegetation grows back over time.

Operational mitigations, including public safety power shutoffs (PSPS) and "fast-trip" settings, differ from other categories of mitigation activities in that they can be deployed in response to real-time wildfire conditions. PSPS events completely de-energize powerlines during hours of extreme wildfire risk and require inspections before re-energizing them. Fast-trip settings modify the sensitivity of existing protection equipment during periods of high fire risk[43]. This equipment senses when a fault occurs, notably when lines contact another

object. Faults lead to excess current flow, and protection equipment which senses that current interrupts all current flow on the line. This should reduce ignitions by quickly clearing faults[11], but there is limited empirical evidence. Although operational mitigations are inexpensive to enable, they introduce costs in the form of electricity outages and inspections when a fault does occur.

This chapter and the subsequent chapter focus on the wildfire mitigation activities of Pacific Gas & Electric Company (PG&E), the largest utility in the United States. Figure 2.1 shows the utility's service territory and the portions of its service territory that are characterized as high-fire threat districts (HFTD). HFTD areas are defined by the California Public Utilities Commission (CPUC) and denote locations where there is an increased risk for utility-associated wildfires to occur, to spread rapidly, and to cause damage to communities.

Figure 2.2 shows how PG&E's use of system hardening, vegetation management, and operational measures has evolved over time. After $30 billion in wildfire liabilities caused the utility to file for bankruptcy in 2019[44], the utility began to implement a range of wildfire risk reduction approaches, including enhanced vegetation management and proactively de-energizing (PSPS) lines during extreme wildfire conditions. In 2021, the utility piloted fast-trip settings on approximately half of its high-fire threat district (HFTD) distribution circuits, and the next year it expanded fast-trip settings to all HFTD circuits[11]. Over the long-term, the utility plans to underground ten thousand circuit-miles, which covers approximately 40% of the utility's HFTD[45]. This proposal is controversial given the high capital costs[46]. In 2020, PG&E's cost to underground one mile of overhead distribution line was $4.3 million[47]. The utility is projecting that these per-mile costs will drop to $2.8 million by 2026[48].

2.2 Data and Empirical Strategy

The following analysis makes extensive use of data on powerline-caused ignitions from the California Public Utilities Commission (CPUC) and regulatory filings made by PG&E[17]. Between 2015 and 2022, 95 percent of PG&E's 3,821 recorded ignitions occurred along distribution (versus transmission) lines. Because overhead distribution lines are typically uninsulated, contact with another object can readily produce ignitions. Table 2.2 shows that PG&E's distribution system comprises approximately 3,000 "circuits," or distinct radial paths that each connect a few hundred to a few thousand customers to the transmission system. PG&E's overhead distribution circuits span approximately eighty thousand miles, with twenty-five thousand miles (31%) in the HFTD. Our analysis focuses on 772 distribution circuits that lie, even partially, within the HFTD.

On average, circuits with at least one mile in the HFTD cause an ignition once every three years. In contrast, circuits outside of the HFTD cause an ignition once every ten years (see Table 2.3). The probability that an ignition from a distribution circuit causes large,

catastrophic wildfire outcomes is low. Table 2.3 shows that 95% of ignitions lead to wildfires less than ten acres, and only 0.5% of ignitions lead to wildfires exceeding 5,000 acres. This low-probability and high-consequence nature makes the task of wildfire risk management along powerlines particularly challenging to address.

Table 2.4 shows that between 2015 and 2022, 98% of PG&E's 1.3 million acres burned were ignited by vegetation contact (i.e., tree branch striking a powerline) in the HFTD. This is despite vegetation contact accounting for 19% of the utility's ignitions. Other causes of ignitions along powerlines include balloons contacting powerlines, vehicles knocking down distribution poles, or equipment failures. Since vegetation contact to powerlines represents the overwhelming share of the utility's total acres burned, this analysis focuses exclusively on ignitions produced by vegetation contact on circuits in the HFTD.

Presumably, utilities will target wildfire risk mitigation efforts at circuits with the greatest combination of ignition and wildfire risk. This non-random assignment of risk mitigation "treatments" complicates the estimation of causal impacts. A comparison of post-treatment ignition outcomes across treated versus untreated circuits could confound the effects of the intervention with differences in baseline risk. The empirical strategy addresses this selection problem in two steps. First, data collected before risk mitigation treatments were deployed is used to train a machine learning model to predict daily ignitions for all PG&E distribution circuits that overlap the HFTD. This model is used to predict "baseline" ignition risk for all circuit-days in our post-intervention period. Second, caliper matching is used to isolate comparisons between pairs of circuits with nearly identical levels of baseline ignition risk in the post intervention period, but received different risk mitigation treatments. For enhanced vegetation management, two tiers of treatment are defined, "high" and "moderate".

Ignition Risk Model

Fire weather variables, such as wind speed, are highly stochastic and may interact non-linearly to generate ignition events. To develop a measure of a circuit's daily ignition risk, a random forest model is trained using high-resolution weather data, topographic information, and circuit characteristics. The methodology closely follows the approach in [49].

In the random forest model, the positive class is an ignition event caused by vegetation contact on a given circuit-day. The ignition data are highly imbalanced, with the proportion of positive events to negative events being only 0.03%. The imbalanced nature of the ignition data is addressed by under-sampling the data. Models are evaluated based on the area under the receiver operator characteristic curve (AUC).

The model is trained with ignition data occurring between 2015 and 2019, prior to widespread implementation of PG&E's wildfire programs. 3-repeat 10-fold cross-validation is performed, and the training and testing data are split 75/25%. During this process, two hyperparameters are tuned: the number of decision trees and the number of features con-

sidered at each split. The ignition risk model produces an AUC value of 0.84 when used to predict ignition events in the testing data. Prediction models with AUC values between 0.8-0.9 are generally considered excellent[50]. The confusion matrix, using a classification threshold of 0.5, and ROC curve are shown in Figure 2.4a and 2.4b. Figure 2.5 provides a list of the top twenty most important variables that predict ignitions.

The output of the ignition risk model is the probability of an ignition occurring on a given circuit-day, and in all cases Bayes classification threshold of 0.5 is used to predict ignition counts. Because under-sampling creates bias in the posterior probability distribution[51], an adjustment is applied to the posterior probability estimates. The adjustment expresses the posterior probability of the positive class in the original dataset as a function of the posterior probability of the positive class after under-sampling and the proportion of negative class events in the under-sampled dataset. After calibrating the probabilities, the ignition risk model predicts 55 ignitions in the test data. The test data includes 45 actual ignitions. The recall of the model in the test data is 84% but the precision of the model is low (0.9%).

Matching

To identify effects of enhanced vegetation management on ignition outcomes, the matching strategy leverages documented "material shortcomings" in PG&E's approach to allocating these efforts. Monitoring inspections reports[52] have found that, as the company rolled out its enhanced vegetation management program, it did not prioritize wildfire risk reduction according to its highest risk circuits[53]. These shortcomings generated variation in treatment across circuits with the same baseline ignition risk.

The matching strategy identifies circuits that would have faced the same ignition risk in the post-intervention period, but received different levels of enhanced vegetation management treatment. For each treated circuit, we use caliper matching to identify the two nearest control circuits within a minimum distance – measured in terms of average daily ignition risk – to a treated circuit as potential matches. Because the treatment effects may be heterogeneous across the amount of enhanced vegetation management performed on each circuit, the caliper matching process is executed twice for two tiers of the vegetation management treatment. The first treatment level consists of circuits that received "high" amounts of enhanced vegetation management (50% or more of total circuit length), and the second treatment level consists of "moderate" amounts of enhanced vegetation management (between 10% and 50% of total circuit length). Figure 2.3 shows how the sizes of each treatment tier evolve over time.

Figure 2.6 provides a visual summary of the matching strategy. The figure reveals that treated circuits with higher average ignition risk are less likely to successfully match to a control circuit with nearly identical ignition risk. This occurs because as a matter of prioritizing risk management, the utility generally does not leave high-risk circuits untreated. As a robustness check, the logistic regression model (described later) is run across the sample

that does not drop these high-risk circuits that do not successfully match to a control circuit (Table A.6). For a detailed list of steps to replicate the matching strategy, see Appendix A.

To identify the effects of fast-trip settings, the matching strategy must be modified. PG&E deployed fast-trip settings to all circuits in the HFTD in 2022, so the within-time period matching approach described above is not possible for fast-trip settings. Instead, the matching strategy for fast-trip settings relies on an inter-temporal comparison and the fact that fast-trip settings are a recent innovation.

Because PG&E did not use fast-trip settings prior to its partial pilot deployment in 2021, the matching strategy compares similar high-risk location-days across the pre- and post-intervention periods. The inter-temporal comparisons restrict the sample only to circuit-days when wildfire risk was sufficiently high that the criteria for fast-trip enablement would have been met, even in the pre-period when fast-trip settings had not been deployed yet. One might be concerned that risk factors are distributed differently in the pre- and post-intervention periods. Tables A.1 and A.2 test for differences in the pre- and post-intervention periods, and Table A.2 finds similar conditions during high-risk days in the pre- and post-period. This increases the confidence that differences in ignition outcomes are caused by risk mitigation versus confounding factors. For more detail on how the fast-trip dataset is constructed and the criteria the utility uses to enable fast-trip settings, see Appendix A.

No identification strategy is pursued to isolate the causal effects of undergrounding and PSPS treatments on ignition outcomes; when a line is placed underground or de-energized, its probability of causing an ignition by vegetation-contact is plausibly zero. The empirical results, discussed in the next section, support this prior expectation. For covered conductor, low deployment levels (see Figure 2.2) prevent a tractable identification strategy.

Logistic Regression Model

The conditional probability of a vegetation-caused ignition at location i on day t is modeled as a function of variables X_{it} and unknown or unobserved factors ϵ_{it}. A logistic regression model assumes the ϵ_{it} are drawn from a standard logistic distribution. This yields the following closed form expression for the conditional ignition probabilities:

$$G(X_{it}\beta) = \frac{exp(X_{it}\beta)}{1 + exp(X_{it}\beta)} \tag{2.1}$$

$$\begin{gathered} X_{it}\beta = \alpha_0 + \alpha_1\theta_{it} + \beta_1 F_{it} + \\ \beta_2(D_{i,\text{Veg=Hi.}} * T_{it,\text{Post=1}}) + \beta_3(D_{i,\text{Veg=Med.}} * T_{it,\text{Post=1}}) + \\ \beta_4 D_{i,\text{Veg=Hi.}} + \beta_5 D_{i,\text{Veg=Med.}} + \beta_6 \text{UG}_{it} + \beta_7 Z_{it,\text{PSPS=1}} + \\ \beta_8 \text{CC}_{it} + \beta_9(F_{it} * D_{i,\text{Veg=Hi.}} * T_{it,\text{Post=1}}) + \beta_9(F_{it} * D_{i,\text{Veg=Med.}} * T_{it,\text{Post=1}}) \end{gathered} \tag{2.2}$$

Explanatory variables in the model include a binary variable indicating whether fast-trip settings were enabled on a given circuit-day (F_{it}) and binary variables indicating the circuit-level vegetation management treatment (D_i). Vegetation management treatments are defined across two levels, high and moderate, as described previously. Vegetation management treatments are interacted with a treatment indicator (T_{it}) to capture the effect of the treatment in the post-intervention period. Predicted ignition risk probability (θ_{it}), miles of undergrounding (UG_{it}) and covered conductors (CC_{it}), an indicator for PSPS events (Z_{it}), and an intercept term (α_0) are included.

2.3 Results

Effectiveness of Fast-Trip Settings and Enhanced Vegetation Management

Parameter estimates are reported in Table 2.5. In the case of fast-trip settings, the estimated incidence rate of -0.72 in the third column (β_1) implies that enabling a circuit's fast-trip settings on a high-risk day reduces the circuit's probability of causing an ignition by 72% (54%-83% confidence interval), on average. Circuits with high levels of vegetation management cause 57% (2%-82% confidence interval) fewer ignitions (β_2) on high-risk days than similarly risky circuits with minimal amounts of vegetation management.

For comparison, the first column of Table 2.5 displays estimation results for all HFTD circuits without applying the matching strategies to isolate the causal effects of either mitigation type. The estimates in this first column likely confound the effects of risk mitigation with differences in baseline risk, which is supported by the positive and statistically significant treatment group effects (β_4 and β_5). Once the vegetation management strategy is applied in the second column, and again when the data is filtered to high-risk days in the third column, these coefficients attentuate to zero and are no longer significant.

The estimating equation also includes interactions between vegetation management and fast-trip indicators. If a utility has cleared significant amounts of vegetation around an overhead line and deployed fast-trip settings, risk reduction may be greater than either measure can deliver independently. Consistent with this intuition, Table 2.5 shows that combining enhanced vegetation management with fast-trip settings (β_9) reduces ignition risk by 92% on average.

In Figure 2.7, the coefficients from the logistic regression model are used to assess how the utility's efforts have reduced ignition risk over the study period. The figure shows that in 2022 the utility's powerlines would have caused four times as many ignitions absent its wildfire mitigation efforts. A substantial share of the reduction in ignitions came from fast-trip settings because, unlike capital-intensive system hardening, the utility could deploy this operational measure rapidly across the distribution grid in response to hazardous conditions.

Cost-Effectiveness

Next, parameter estimates are combined with a cost model that implicates multiple sources of uncertainty (e.g., the rate at which wildfire risk will escalate over the life of a capital investment, unit costs, reliability impacts) and multiple cost dimensions (e.g. capital costs, operating costs, reliability impacts). The results of this model are used in Figure 2.8 to assess the relative cost-effectiveness of these adaptation strategies. Appendix A describes the cost modeling in closer detail. Cost-effectiveness results for PSPS measures are omitted because of a lack of confidence in reported costs.

Costs and avoided ignitions are measured as net present values over the lifetime of the measure relative to a baseline that deploys routine vegetation management. Routine vegetation management costs are avoided when a line is placed underground. The key costs included in the analysis are utility-reported capital and operating costs and customer reliability costs. A value of lost load (VoLL) framework is used to value customer reliability costs (see Figure 2.8 caption and Appendix A). The base case assumes ignition risk will increase linearly to a 50% increase in 2050 and continues to increase at a linear rate thereafter. See Appendix A for additional information.

Undergrounding cost-effectiveness estimates are constructed to reflect two different perspectives. The first ("social") cost perspective considers upfront capital investment costs and variable maintenance costs. The second ("regulator") cost perspective includes the rate of return on capital investment that the utility is authorized to earn as a cost. Uncertainty in a variety of parameters is captured by error bars around the central estimate.

There are three takeaways from the cost-effectiveness analysis summarized in the left panel of Figure 2.8. First, bearing in mind that fast-trip settings do not eliminate all ignitions, fast-trip settings are far more cost-effective at reducing ignitions than vegetation management or undergrounding. Crucially, this includes the additional costs to customers that fast-trip settings impose in the form of electricity outages. VoLL estimates are highly uncertain and heterogeneous, but Figure 2.8 shows that the size of this uncertainty is unlikely to alter the conclusion that fast-trip settings are more cost-effective than vegetation management and undergrounding. See Appendix A for additional background on customer reliability costs.

Second, despite the significant capital costs, undergrounding powerlines is more cost-effective than vegetation management. This is primarily because undergrounding fully eliminates vegetation-caused ignition risk well into the future. Unlike with undergrounding, the cost-effectiveness of enhanced vegetation management is highly susceptible to assumptions about how long its benefits will last (e.g., when will vegetation grow back).

Third, estimates of the cost-effectiveness of undergrounding differ significantly between the "social" and "regulator" perspectives. Because undergrounding is highly capital intensive, utilities earn a rate of return on these investments that is financed by electricity rate

increases[54]. To put this return in perspective, PG&E is authorized to spend $3.6 billion in capital on undergrounding 1,230 miles over the period 2023-2026[48]. Over an assumed 40-year lifetime and straight-line depreciation, our "regulator" cost perspective estimates that the utility collects an additional $2.9 billion (net present value) from ratepayers via its 7.28% rate of return[55] on its capital base (see Appendix A). While some of this return reflects the utility's true cost of capital, previous research shows that the regulated rate of return is often set above the true cost of capital[56]. When this is the case, a utility will substitute capital for other inputs[57], leading to a more capital-intensive and possibly less cost-effective wildfire mitigation strategy.

The right panel of Figure 2.8 moves beyond ignitions to understand how these measures may reduce the destructive potential of powerline-caused ignitions. To do so, wildfire perimeters are simulated across numerous ignition points and weather conditions. To contain the computational complexity of the simulations, the analysis focuses on a six-thousand mile subset of distribution circuits, roughly comprising (1) the region of Napa, Sonoma, and Lake counties and (2) the central Sierra foothills. Both regions experienced destructive grid-caused wildfires during the study period.

The simulations are then used estimate the number of residential and commercially-zoned parcels burned, per acre, for a representative set of ignitions and fire risk days. These parcel per acre estimates are then multiplied by the historical size distribution of powerline-caused wildfires over the study period. To capture variation in the destructive intensity of wildfires due to factors outside of the electric power sector, such as fire suppression efficacy and home hardening, the proportion of structures burned per parcel are varied. See Appendix A for more detail on simulating and calibrating wildfire perimeters. In addition, Chapter 3 extends this analysis to all high-risk distribution circuits in the utility's service territory and explores key drivers of heterogeneity.

The right panel of Figure 2.8 shows that fast-trip settings retain their cost-effectiveness advantage over the other measures when assessed in terms of structures burned. In these cost calculations, estimates are strongly dependent on assumptions about the share of structures destroyed per burned parcel. This underscores the crucial role of mitigation actions outside the electric power sector (e.g., suppression, home hardening) in determining wildfire risk outcomes and cost-effectiveness within the electric power sector. Chapter 3 identifies regions where cost-effectiveness estimates are more or less sensitive to such mitigation actions taken outside of the electric-power sector.

The different strategies this chapter investigates represent different tradeoffs between cost, wildfire risk mitigation, and deployability considerations. For example, fast-trip settings provide a relatively inexpensive way to reduce ignition risk and can be rapidly deployed across the distribution grid. However, current fast-trip protocols leave 28% of vegetation-caused ignitions unmitigated on average. In contrast, undergrounding is much more expensive and requires years to deploy, but is completely effective at reducing vegetation-caused ignitions.

Because circuits differ significantly in terms of baseline ignition risks, there is no one-size-fits-all risk mitigation strategy. Moreover, the optimal strategy at a given location can evolve as new mitigation approaches are developed and refined. During the study period, for example, the introduction of fast-trip settings as a viable risk mitigation regime altered the frame of reference for other risk mitigation alternatives.

Figure 2.9 explores the implications for undergrounding. The vertical axis measures costs per avoided ignition. The horizontal axis measures miles of distribution lines in ascending order of baseline risk. The costs and ignition reduction benefits of undergrounding are assessed against two baselines. The solid lines show how estimated undergrounding costs per avoided ignition vary across line segments relative to a baseline regime that incorporates only routine vegetation management. The higher the baseline risk at a location, the more ignitions avoided, the lower the cost per avoided ignition, all else equal. The broken lines show undergrounding costs relative to the baseline regime that includes both routine vegetation management and fast-trip settings. Against this updated baseline, undergrounding delivers smaller benefits in terms of avoided ignitions. The costs that undergrounding eliminates (i.e., vegetation management, fast-trip costs, and outage impacts) are relatively small, so the implied costs per avoided ignition increase significantly under the "with fast-trip settings" baseline.

Figure 2.9 illustrates how incorporating fast-trip settings into standard practice significantly reduces the amount of undergrounding investment needed to achieve a given ignition risk reduction target. Consider, for example, PG&E's ten-thousand mile target. If one assumes that the utility is planning to underground the highest risk circuits, the ignition risk model estimates a remaining risk of approximately 1,200 discounted ignitions along the line miles that are not undergrounded if the baseline for comparison deploys only routine vegetation management. Using the alternative baseline that enables fast-trip settings, the miles of undergrounding required to achieve the same reduction in ignitions is significantly reduced (arrows denote this reduction).

2.4 Discussion

As the frequency and intensity of wildfire and other extreme weather events increases, the private sector will play an essential role in financing adaptation investments. To date, empirical evidence on the impacts and relative effectiveness of adaptation investments has been limited. Electric utilities are currently experimenting with a variety of measures to adapt to heightened wildfire risk. These are high-stakes experiments with potentially significant implications for affordability, reliability, and safety. This chapter develops an empirically tractable framework for evaluating the effectiveness of these investments and for analyzing tradeoffs between wildfire risks and consumer costs.

Operational measures like fast-trip settings can be deployed quickly and dynamically in

response to evolving wildfire conditions at relatively low capital costs. The results indicate that fast-to-deploy measures have played a vital role in cost-effective adaptation strategies to date. Electric utilities around the world that face rapidly escalating wildfire risk and rising electricity costs may benefit substantially from the deployment of dynamic operational measures. However, the analysis finds that the fast-trip protocols that have been demonstrated in California leave an estimated 28 percent of ignition risk unmitigated, on average. This stands in contrast to capital-intensive measures, like undergrounding, which are slower to deploy, significantly more expensive, but eliminate risk with more assurance in the locations they are deployed. The results do not point to the superiority of one mitigation measure over another, however they do elucidate some key tradeoffs and illustrate how important innovations in wildfire risk adaptation strategies can significantly change the cost-calculus that guides private-sector investment choices.

The analysis comes with caveats. There are many sources of uncertainty in the cost-effectiveness estimates, and the measures of avoided wildfire damages are model-dependent. Innovative drilling techniques may reduce undergrounding costs greater than forecasted. On the other hand, costs could exceed forecasts if the utility has targeted the most favorable, cost-effective sites first. The deployment of fast-trip settings during the study period represents the utility's initial efforts; operational risk mitigation strategies are being refined in ways that could reduce costs and increase risk reduction effectiveness. While this analysis estimates that the economic outage costs of fast-trip settings are small compared with the additional investment costs of undergrounding, there are shortcomings when relying on point estimates of the value of lost load to do this quantification. These considerations notwithstanding, the results demonstrate how ongoing experimentation with low-cost operational measures can avoid significant capital outlays, and the deployability of such operational measures may especially benefit utilities with nascent wildfire mitigation programs.

The extent to which fast-trip settings– and future operational innovations– deliver real cost reductions will depend in part on utility incentives. Regulated utilities, especially in the electric power sector, are routinely authorized to earn generous returns on capital investments[56]. These incentives will lead utilities to favor capital-intensive mitigation options over operational ones. Liability rules and public relations considerations encourage utilities to drive electric power sector ignitions to zero. To the extent that these utility incentives are misaligned with the best interests of consumers, regulatory oversight will be critical in the negotiation of tradeoffs between risk reduction benefits and the societal costs of wildfire mitigation. This paper provides a framework for thinking more systematically about these risk-cost tradeoffs, and demonstrates how publicly available data and causal inference methods can be used to evaluate the cost-effectiveness of adaptation efforts. In no other sector is the measurement of adaptation impact and cost-effectiveness more critical than in the electric power sector, where adaptation investments, electricity costs, and decarbonization policies are linked so tightly.

2.5 Figures and Tables

Table 2.1: Data Sources

Data Type	Variables	Resolution	Source
Climate	Minimum relative humidity, wind velocity, wind direction, accumulated precipitation, maximum temperature, downward surface shortwave radiation, evapotranspiration, vapor pressure deficit	4 km	gridMET, Climatology Lab, University of California, Merced [58]
Climate	Air temperature, hourly precipitation, relative humidity, wind speed, wind direction	RAWS weather station	Mesowest, University of Utah [59]
Fuels	100-hour and 1000-hour dead fuel moisture, energy release component	4 km	gridMET, Climatology Lab, University of California, Merced [60]
Fuels	Live fuel moisture	RAWS weather station	Mesowest, University of Utah [59]
Topography	Mean forest canopy height, maximum forest canopy height, elevation above sea-level	30-meter	LANDFIRE, USDA and U.S. Department of the Interior [61]
Circuit Characteristics	Installed year, length in HFTD-Tier 2, Tier 3, and non-HFTD	Circuit	PG&E 2020 Wildfire Mitigation Plan [62]
High-Fire Threat District	Perimeters of HFTD Tiers 2 & 3	Spatial polygon	California Public Utilities Commission [63]
Ignitions	Location, voltage, cause, date, time, size, fire potential index	Lat/long position	California Public Utilities Commission [17], PG&E 2023 Wildfire Mitigation Plan [64]
Public Safety Power Shutoffs	Circuit name, date, outage start and end, outage duration, customers impacted	Circuit	California Public Utilities Commission [65]
Fast-Trip Outages	Circuit name, outage start and end, customers impacted, ignitions occurring during fast-trip enablement	Circuit	PG&E 2023 Wildfire Mitigation Plan[66, 67], PG&E 2022 Wildfire Mitigation Plan [68, 69]
Vegetation management & system hardening	Enhanced vegetation management, undergrounding, and covered conductor	Circuit-miles	PG&E 2020, 2021, 2022, and 2023 Wildfire Mitigation Plans [70–74]
Residential and commercial parcels	Perimeters of parcels, zoning classifications	Spatial polygon	County GIS Services
Costs	Undergrounding, enhanced and routine vegetation management, fast-trip settings	Per mile and aggregate	PG&E 2023 General Rate Case [47, 48, 75]

Table 2.2: Length and Count of PG&E Distribution Circuits

	Non-HFTD	**HFTD**
Circuits (N)	2,279	772
Total length (miles)	40,340	40,095
Total length in HFTD (miles)	-	25,308
Mean length per circuit (miles)	18	52
Standard dev. per circuit (miles)	(25)	(51)

Notes: Circuits are assigned to HFTD if they intersect, even partially, the HFTD perimeter. Of the utility's 772 circuits that intersect the HFTD, 25 thousand miles are located within the HFTD and another 15 thousand miles (40 thousand miles - 25 thousand miles) are located outside the HFTD.

Table 2.3: PG&E Distribution Grid Ignitions

	Non-HFTD	**HFTD**
Ignitions per circuit-year (mean)	0.10	0.33
Acres burned per ignition (mean)	6	751
Acres burned per ignition (median)	< 1	< 1
Percent of ignitions >10 acres	2.6%	4.5%
Percent of ignitions >300 acres	0.3%	1.3%
Percent of ignitions >5,000 acres	0%	0.5%

Notes: Using data from 2015-2022, circuits that overlap the HFTD cause an ignition once every three years. In contrast, circuits outside the HFTD cause ignitions at a much lower rate– once every ten years. Less than 5% of ignitions in the HFTD spread to more than 10 acres.

Figure 2.1: Map of High-Fire Threat District (HFTD)

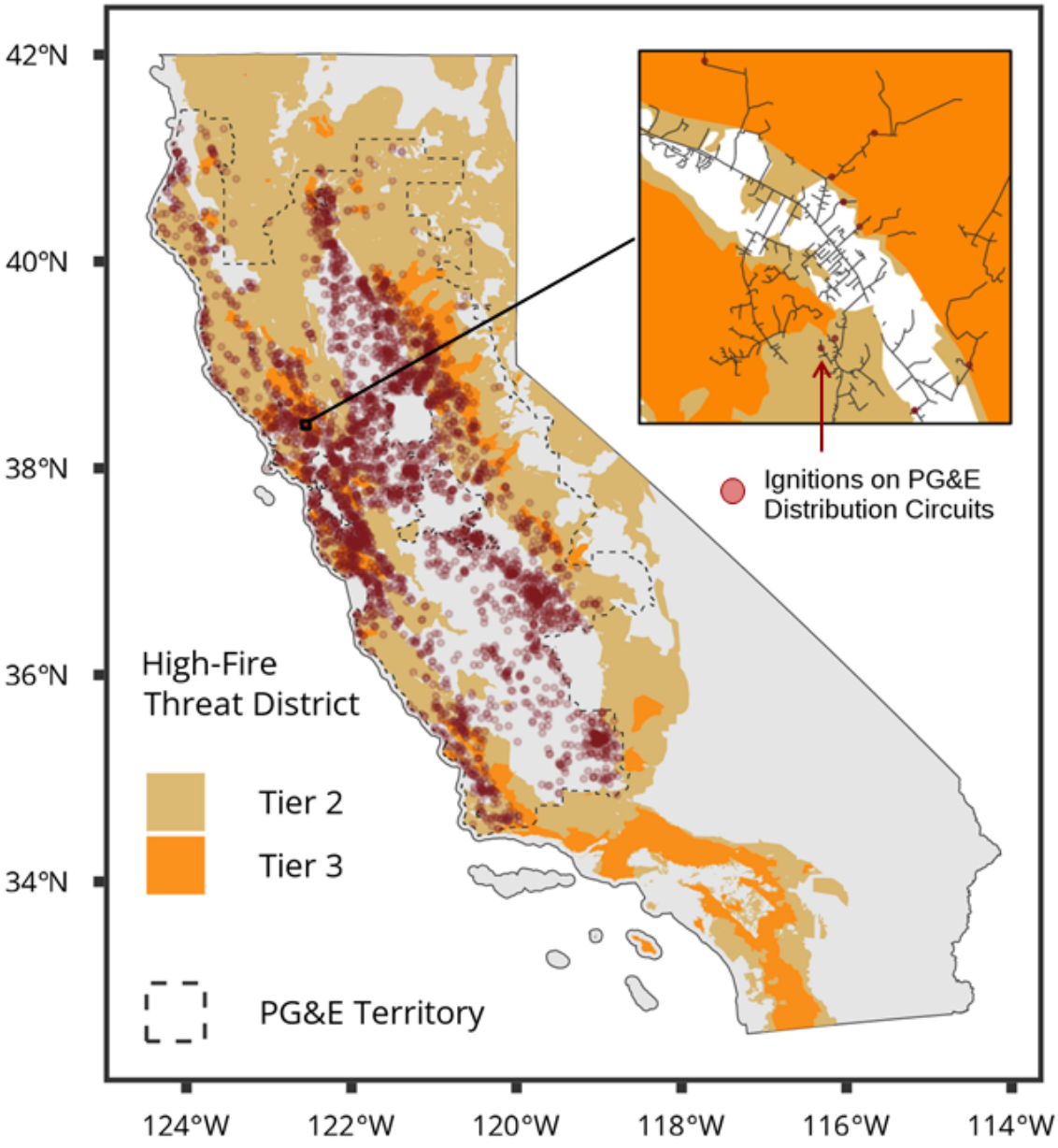

Notes: The map of the high-fire threat district ("HFTD") shows areas where there is an increased risk for utility-associated wildfires to occur, to spread rapidly, and to cause damage to communities. HFTD areas are defined by the California Public Utilities Commission. Tier 3 features more severe wildfire risk than Tier 2. Overlaid in red are ignitions caused by PG&E distribution circuits between 2014 and 2022. The map inset displays an example distribution circuit and the locations of ignitions associated with the circuit during the study period.

Table 2.4: Ignitions and Acres Burned by PG&E Distribution Circuits

	Non-HFTD	**HFTD**
Ignitions Caused by Veg. Contact		
Total	332	697
Mean per circuit-year	0.02	0.13
Standard dev. per circuit-year	0.14	0.42
Ignitions by Other Causes		
Total (2015-2022)	1,640	951
Mean per circuit-year	0.09	0.18
Standard dev. per circuit-year	(0.33)	(0.47)
Acres Burned by Veg. Contact		
Total (2015-2022)	325	**1,278,068**
Mean per ignition	1	**1,891**
Standard dev. per ignition	(2)	(37,328)
Acres Burned by Other Causes		
Total (2015-2022)	11,503	10,998
Mean per ignition	7	12
Standard dev. per ignition	(91)	(121)

Notes: The table indicates that an overwhelming share of acres burned from the utility's distribution circuits are caused by vegetation contact ignitions in the HFTD (98%), despite such ignitions accounting for 19% of total ignitions. Excluding the Dixie Fire, which burned nearly one million acres, lowers this share slightly to 93%.

Figure 2.2: Deployment of Wildfire Prevention Measures

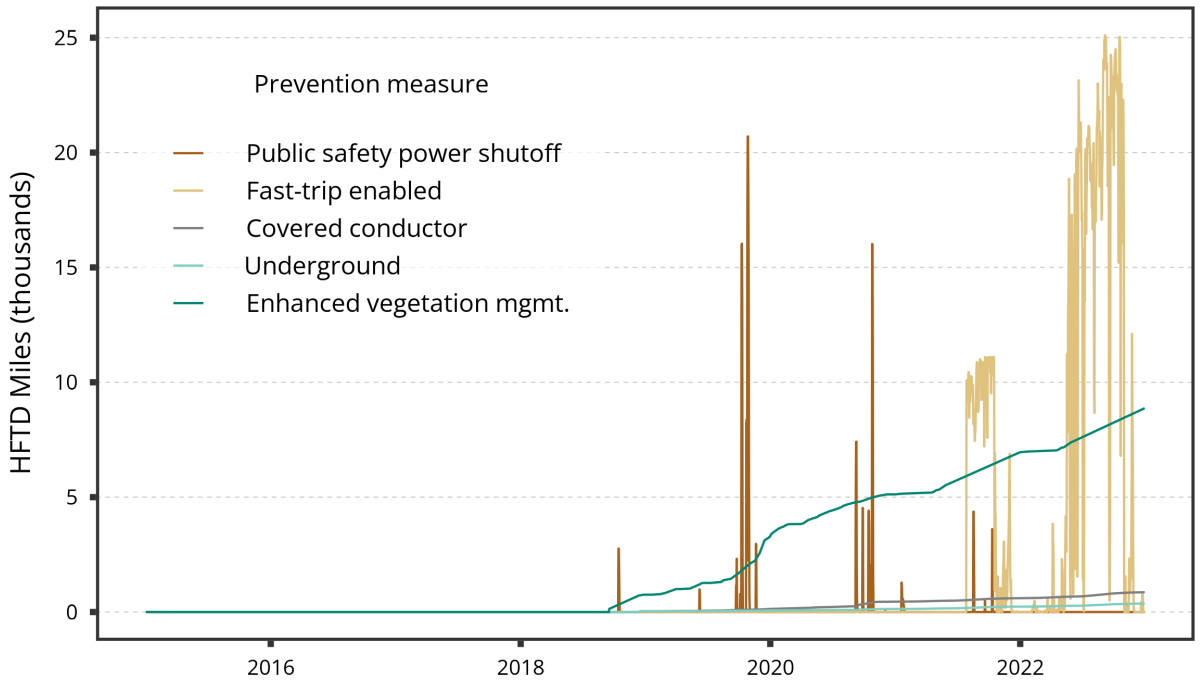

Notes: The vertical axis shows the deployment of select wildfire prevention measures measured in thousands of circuit-miles. The miles deployed of operational mitigations are measured on a daily basis, while grid hardening and vegetation management investments are shown on a cumulative basis. When the utility calls a PSPS de-energization event on a given circuit, we assume all of the circuit's HFTD miles are de-energized, though in practice fewer miles may be de-energized due to grid architecture and installed sectionalizing devices.

Figure 2.3: Deployment of Enhanced Vegetation Management, by High and Moderate Treatment Definition

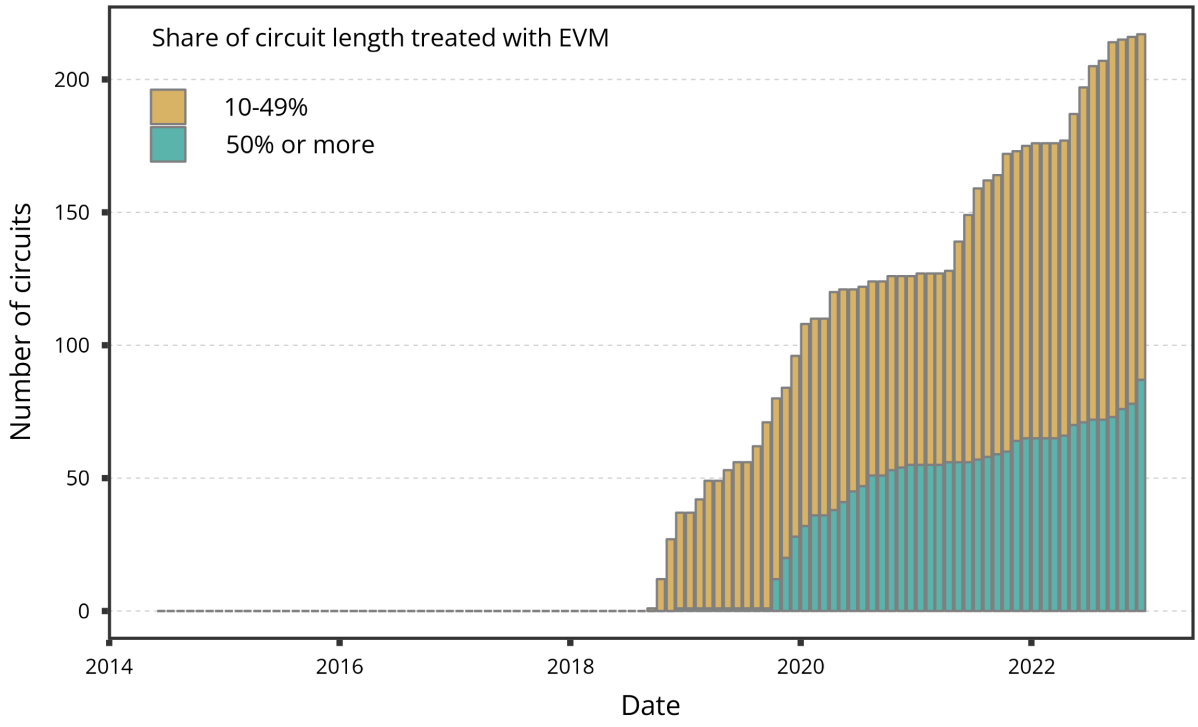

Notes: Circuits that received enhanced vegetation management equal to 10-49% of their circuit length (in miles) by the end of the study period are assigned to the "moderate" enhanced vegetation management treatment group. Circuits that received over 50% are assigned to the "high" treatment group.

Figure 2.4: Ignition Risk Model, Confusion Matrix, and Receiver Operating Characteristic Curve

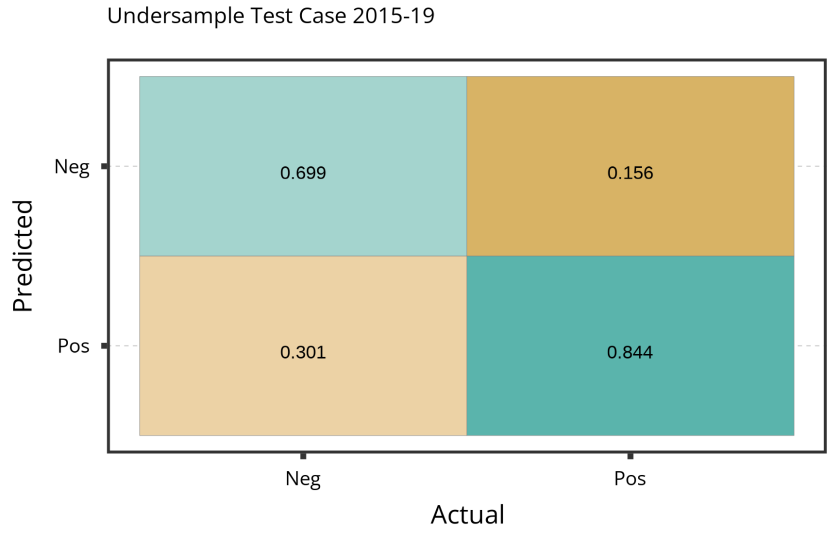

(a) Confusion Matrix

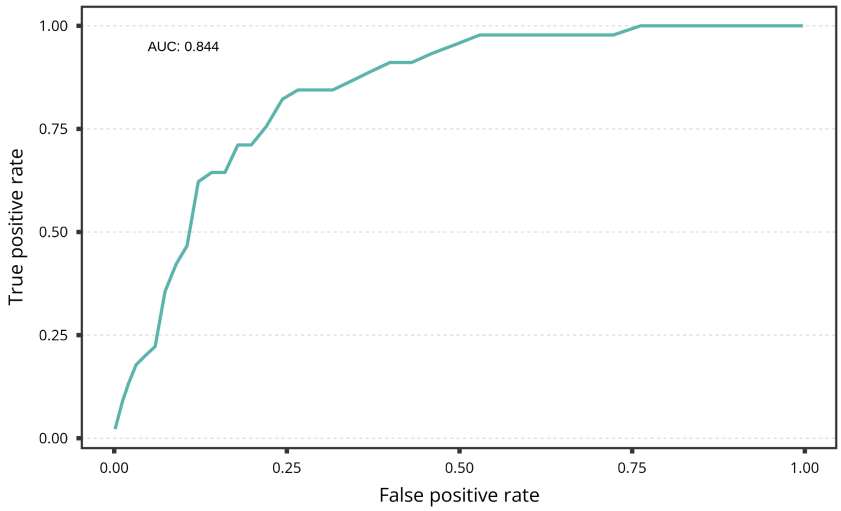

(b) Receiver Operating Characteristic Curve

Notes: (a) Plots the confusion matrix of the ignition risk model on the sample of testing data using a classification threshold of 0.50. (b) Plots the receiver operating characteristic (ROC) curve, which produces an area under the ROC curve of 0.844.

Figure 2.5: Ignition Risk Model Feature Importance

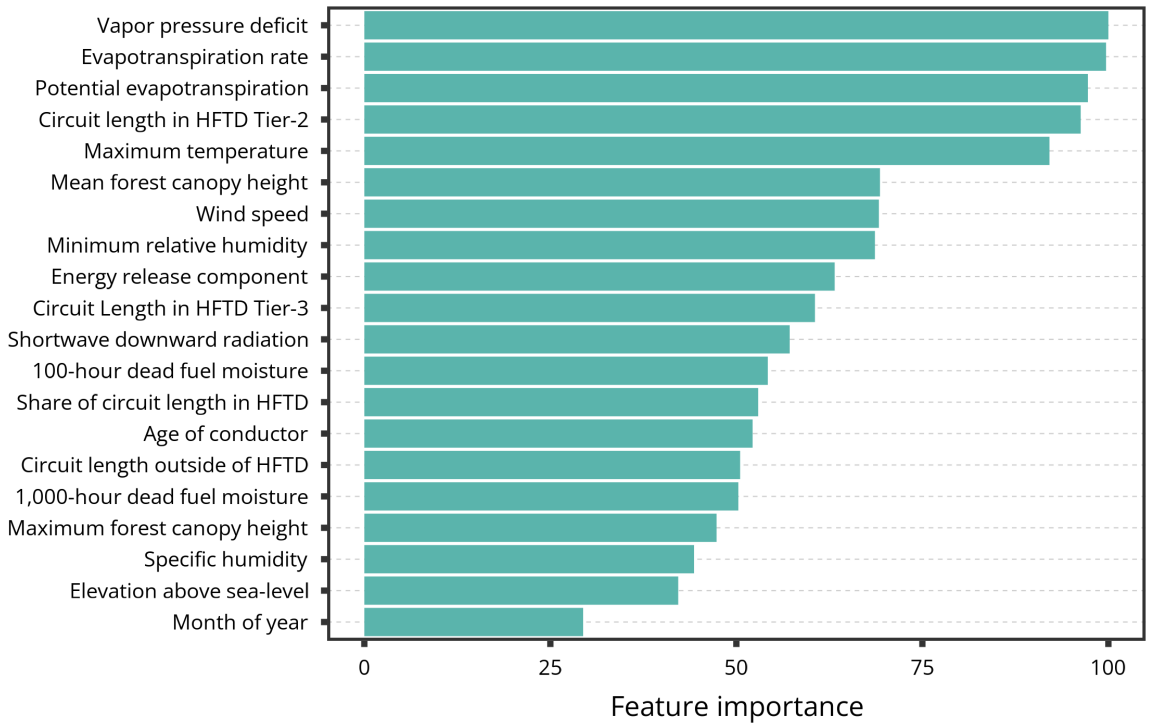

Notes: The figure ranks the twenty most important features in the ignition risk model by feature importance. Feature importance reflects the decrease in accuracy of the model when the variable is excluded from training and testing the model. Vapor pressure deficit, which captures how dry the air is and is similar to relative humidity, is shown to be the most important predictor of ignition risk in our model.

Figure 2.6: Matching on Predicted Ignition Risk

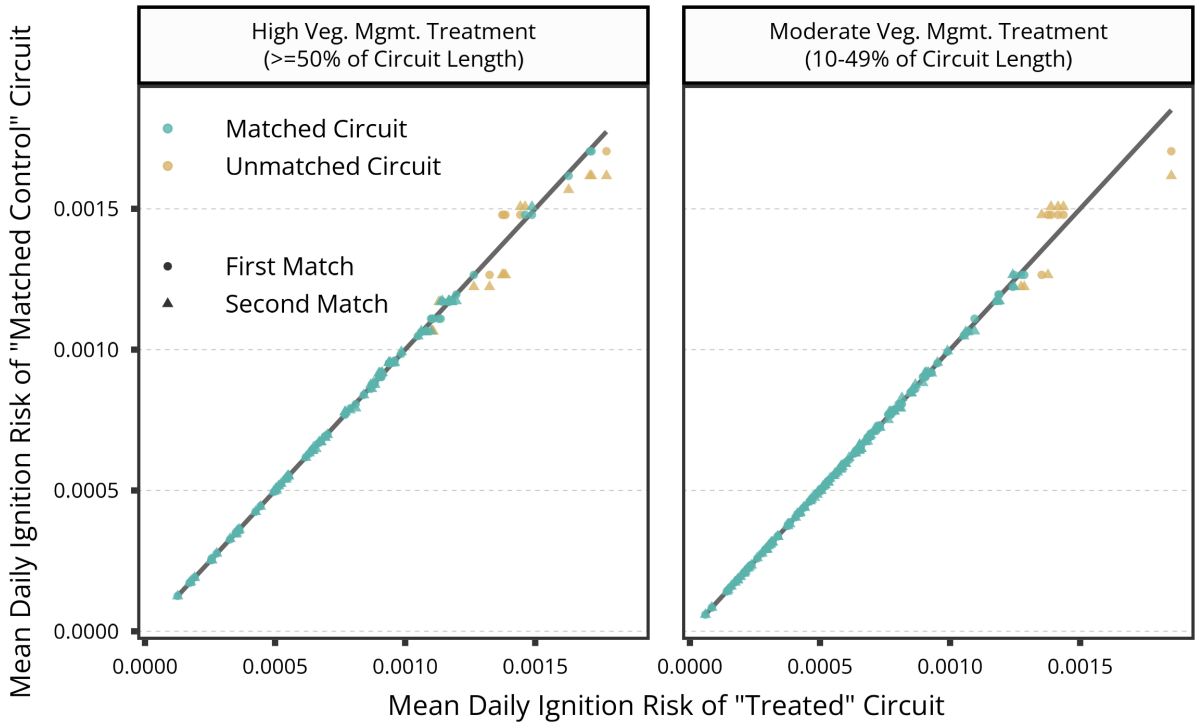

Notes: The horizontal axis plots the average daily ignition risk score of each circuit treated with vegetation management. The vertical axis plots the same metric but for the two control circuits with the nearest average daily ignition risk scores. If treatment and control circuits had identical baseline risk scores, they would fall on the 45 degree line (in gray). The effect of caliper matching is visible in the different color of points that fall sufficiently far off of the 45 degree line. If the absolute difference between a treated and control circuit's average daily ignition risk score is more than 10% of the standard deviation of the sample's risk score, then it is deemed an unsuccessful match. If both of a treated circuit's two nearest neighbors exceed this caliper, then the treated circuit is discarded from the analysis. The plot shows that it is more difficult to find successful matches for higher risk circuits because most high risk circuits receive enhanced vegetation management treatment.

Table 2.5: Effects of Wildfire Prevention Measures on Ignition Probability

	Incidence Rate - Vegetation-Caused Ignitions		
	No Matching	Matching	Matching & High Fire Risk
	(1)	(2)	(3)
β_1: Fast-Trip (F_{it})	−0.27	−0.60*	−0.72*
	(−0.58, 0.26)	(−0.75, −0.33)	(−0.83, −0.54)
β_2: Veg. Mgmt. (D_i=High x T_{it}=Post)	−0.62*	−0.57*	−0.57*
	(−0.79, −0.29)	(−0.77, −0.20)	(−0.82, −0.02)
β_3: Veg. Mgmt. (D_i=Moderate x T_{it}=Post)	−0.03	−0.01	0.26
	(−0.27, 0.29)	(−0.27, 0.34)	(−0.14, 0.86)
β_4: Veg. Mgmt. (D_i=High)	1.18*	0.02	0.12
	(0.77, 1.70)	(−0.17, 0.26)	(−0.12, 0.42)
β_5: Veg. Mgmt. (D_i=Moderate)	1.23*	0.05	0.05
	(0.87, 1.67)	(−0.11, 0.25)	(−0.17, 0.32)
β_9: Combined Effect (D_i=High x F_{it} x T_{it}=Post)	−0.89	−0.87	−0.92
	(−1.00, 1.89)	(−0.99, 2.27)	(−1.00, 1.72)
β_{10}: Combined Effect (D_i=Moderate x F_{it} x T_{it}=Post)	−0.77	−0.81	−0.88
	(−0.97, 0.94)	(−0.98, 0.88)	(−0.99, 0.38)
Risk-score matching	No	Yes	Yes
High-fire risk days only	No	No	Yes
Matched control neighbors (N)	-	2	2
Region FEs	No	No	No
Risk-score, undergrounding, PSPS, and covered conductor controls	Yes	Yes	Yes
AUC	0.782	0.798	0.745
Observations	2,400,342	1,890,015	665,868
Log Likelihood	−6,776.30	−8,168.87	−4,610.30

Notes: In all three columns, the dependent variable is a binary variable indicating whether vegetation contact caused an ignition on a given circuit on a given day. The estimated coefficients are transformed to incidence rates for ease of interpretation. 95% confidence intervals constructed using heteroskedasticity-consistent standard errors are shown in parentheses below the incidence rate estimates. Asterisks (*) denote statistical significance at the 95% level. The sample in column (1) includes all circuits with non-zero HFTD circuit-miles. Column (2) restricts the sample only to circuits that are treated with high (>=50% circuit length) or moderate (10-49%) amounts of vegetation management and control circuits that are matched to each treated circuit (see Methods). The sample in column (3) uses the same matched sample in column (2) but further restricts the sample to days when wildfire conditions are elevated. Vegetation management effects are shown for both the high and moderate treated groups. The first pair of vegetation management coefficients estimates the effect of the treatment after the treatment has taken place. The second pair describes a group-specific effect. The third and final pair of vegetation management effects describes the combined interaction between vegetation management and fast-trip enablement. For example, comparing the incidence rate estimate of -0.92 for the combined effect with the -0.57 estimate for fast-trip enablement suggests ignitions are 35% less likely when a utility both enables fast-trip settings and deploys high levels of vegetation management. In all three columns, we condition on our ML-derived measure of daily ignition risk. To provide a sense of the regression model's goodness of fit, we report the area under the receiver operating characteristic curve (AUC).

Figure 2.7: Ignitions Avoided by Wildfire Mitigation Investments

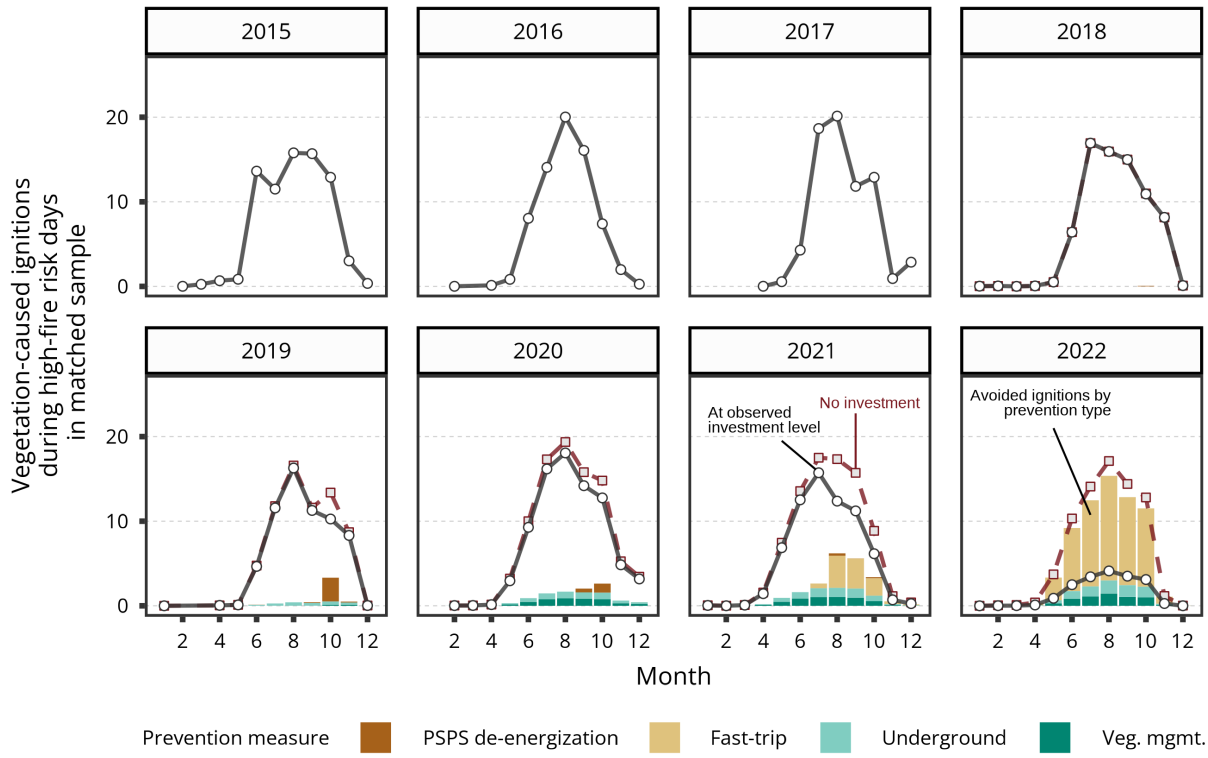

Notes: The vertical axis shows the number of ignitions predicted by our logistic regression model on high-fire risk days. The circuits included in this analysis are ones that received high amounts of vegetation management or control circuits that were matched to these treated circuits based on similar ignition risk. Using the coefficients reported in column (3) of Table 1, the gray line predicts the number of ignitions in each month assuming the utility invested in wildfire prevention measures at observed levels. The stacked vertical bars represent the contributions of each key prevention measure to overall ignition reductions. These measure-specific contributions to risk reduction are estimated by deploying each wildfire measure in isolation, holding the deployment of all other measures at zero. Note that the sum of the stacked bars may not equal the difference between the red dashed line and the gray line. This is because the ignition reductions of each wildfire prevention measure are compared to a baseline of no other wildfire prevention measures. If a circuit produces 3.0 ignitions over the period without any wildfire measures, then fully undergrounding this circuit would reduce ignitions to zero and enabling fast-trip settings would reduce ignitions to 0.8 [(3 * (100%-72%)] over the period. However, the sum of these two in isolation would produce a total ignition reduction of 3.8, which cannot exceed 3.0 ignitions.

Figure 2.8: Cost Efficiency of Electric Utility Wildfire Mitigation

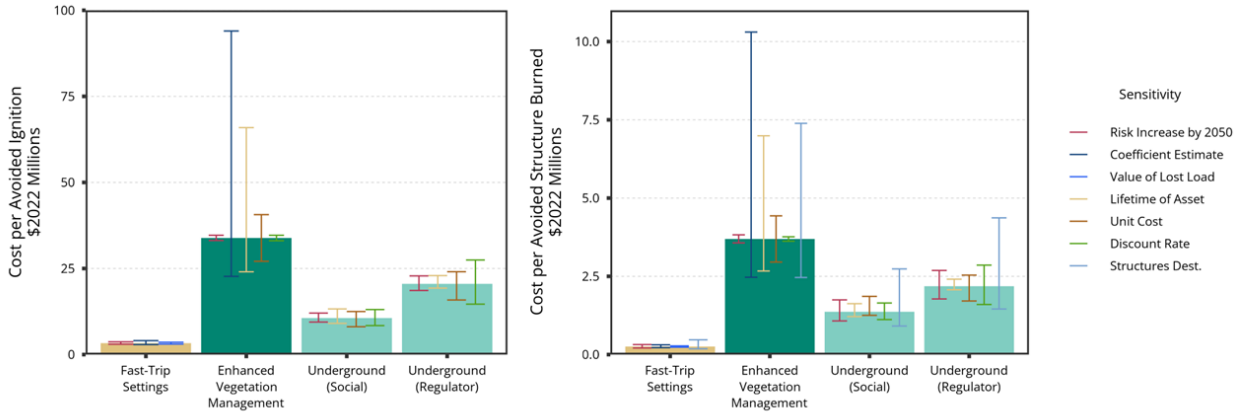

Notes: The figure plots estimated electric utility investment costs per avoided ignition and per avoided structure burned for each wildfire mitigation measure deployed across all HFTD circuits. For fast-trip settings, we include estimated reliability costs borne by customers by applying a value of lost load to electric service interruptions. In our central case, we assume a constant \$5/kWh value of lost load. We vary this parameter choice between \$2.5/kWh and \$7.5/kWh. For undergrounding, we consider two different cost structures. The first, called the "social" perspective, only considers the per-mile costs of undergrounding and discounts future benefits in terms of avoided ignitions using a real social discount rate. The second, called the "regulator" perspective, adds in the return the utility earns on capital investment under rate of return regulation as a cost. See Methods and Appendix A for more detail.

Figure 2.9: Implications of Operational Measures, Risk Reduction, and Shifting Underground Capital Investment

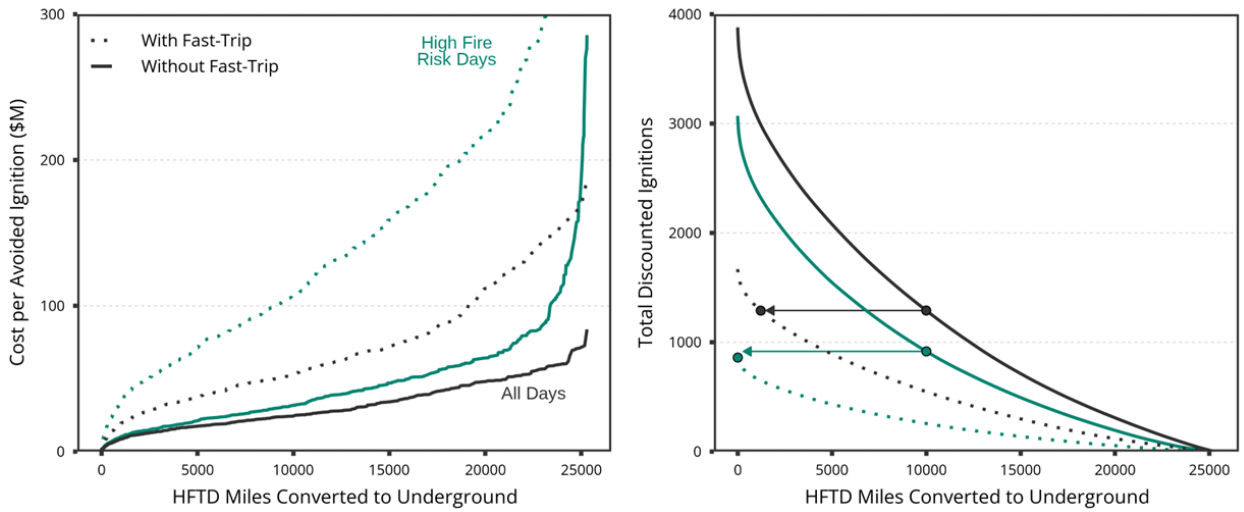

Notes: The plot on the left describes how our estimates of the cost per avoided ignition for a given undergrounding investment vary across circuits. Specifically, the horizontal axis corresponds to hypothetical levels of undergrounding investment across the HFTD, with the left side of the axis corresponding to zero miles of undergrounding (0% of HFTD) and the right side corresponding to 25 thousand miles of undergrounding (100% of HFTD). Ten thousand miles of undergrounding is used as a reference point, which has been proposed publicly by PG&E. The plot on the left is constructed by ordering circuits in terms of cost-effectiveness assuming all miles of the circuit are placed underground. See Methods and Appendix A for additional detail on the cost analysis. The solid line plots cost per avoided ignition for undergrounding under the assumption that no fast-trip settings (or other wildfire mitigation measures) are deployed. However, when we plot the dashed line, we model the impact that fast-trip settings have on reducing ignition risk during high-fire risk days on circuit-miles that are not placed underground. In addition, the scenario depicted by the dashed line accounts for cost savings that undergrounding produces in terms of reducing fast-trip program costs, reliability impacts, and routine vegetation management. The plot on the right shows the total discounted ignitions over the lifetime of the undergrounding investment. As 100% of the HFTD is placed underground on the right of the horizontal axis, total discounted ignitions are zero.

Figure 2.10: Comparison of Predicted and Actual Wildfire Spread Sizes, by Month

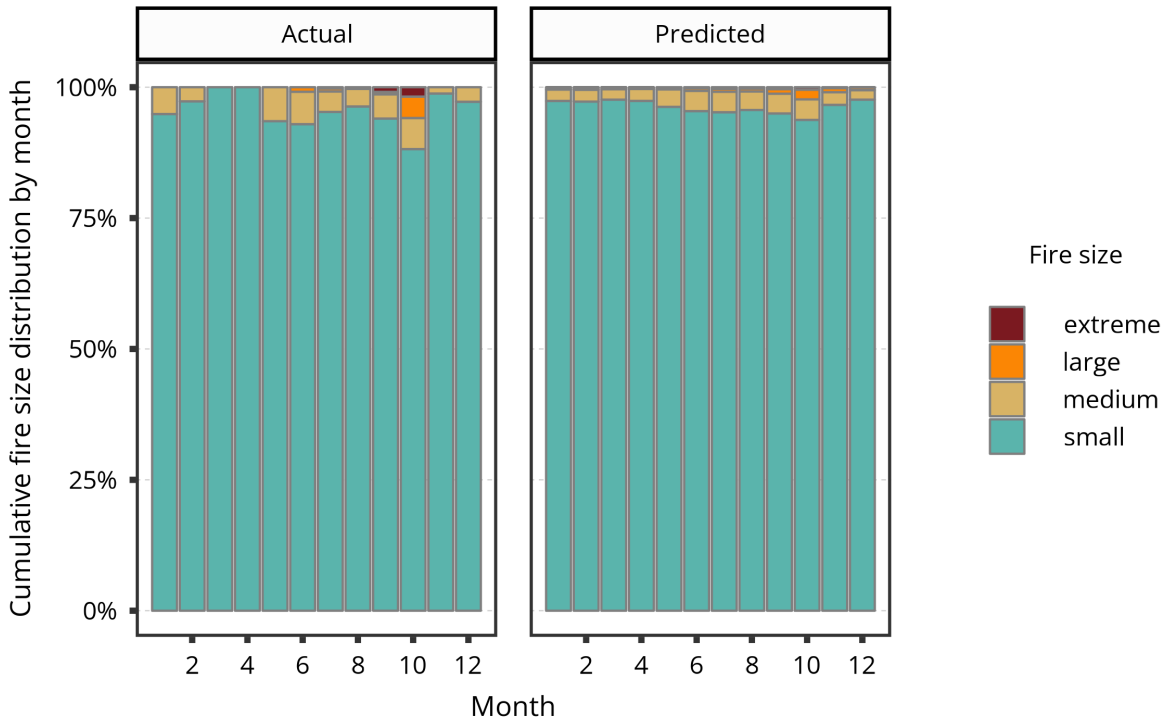

Notes: The left panel of the figure plots the distribution of actual wildfires ignited by PG&E distribution lines between 2015 and 2022. Small fires are defined as less than 10 acres. Medium fires are defined as greater than or equal to 10 acres and less than 300 acres in size. Large fares are defined as greater than or equal to 300 acres and less than 10,000 acres. Extreme fires are defined as greater than or equal to 10,000 acres. The plot on the right shows the predicted distribution of wildfire sizes using the random forest model we train on 75% of actual wildfire ignitions by PG&E distribution circuits.

Figure 2.11: Predicted Probability of Wildfire Spread Size

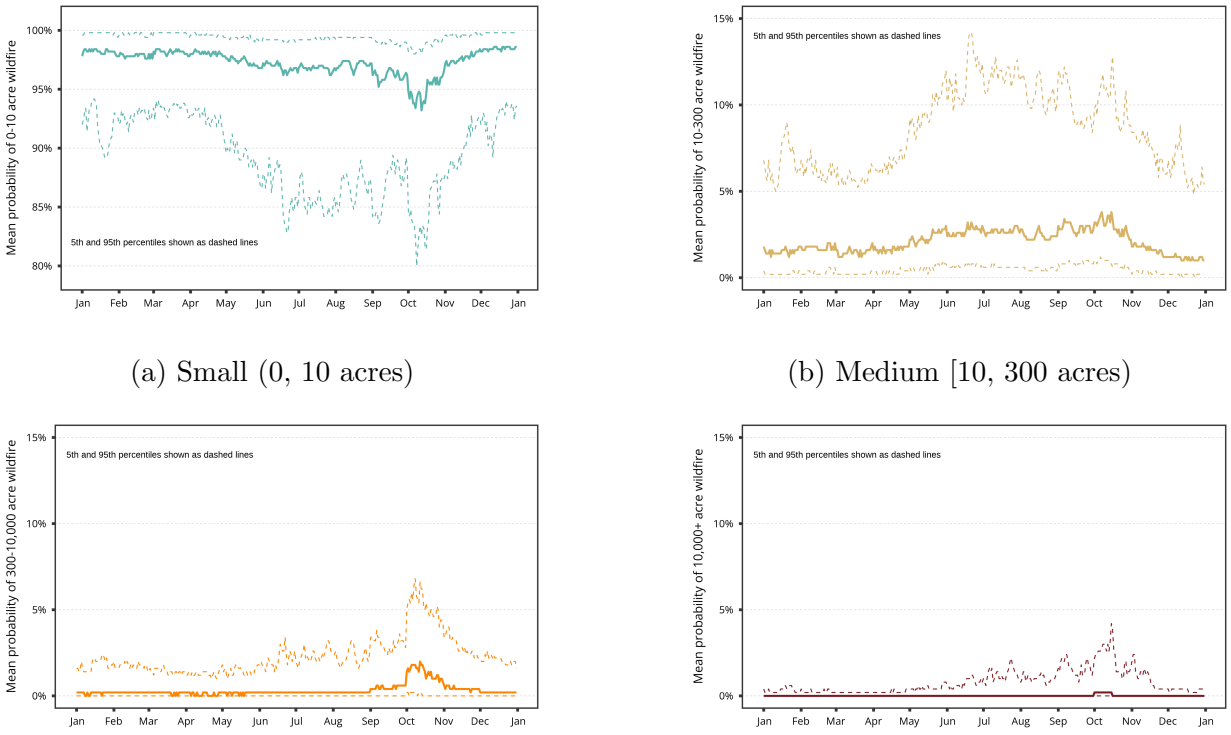

(a) Small (0, 10 acres)

(b) Medium [10, 300 acres)

(c) Large [300, 10,000 acres)

(d) Extreme [10,000, ∞)

Notes: Each plot shows the average predicted probability of a given wildfire size class (e.g., "small": less than 10 acres, "extreme": greater than or equal to 10,000 acres), averaged across each circuit and each day of the year during our study period. In addition to the average, the dashed lines plot the 5th and 95th percentiles.

Chapter 3

Measuring Uncertainty in the Cost-Effectiveness of System Hardening Investments

3.1 Introduction

Adapting to the risks of wildfire in the electric power sector involves many levels of wildfire risk management beyond the electric power sector itself. The expected returns on a utility's investment in system hardening depend on a fire district's defensible space policies, the ability of firefighters to suppress wildfires, and the amount of fuel treatments applied to the landscape to reduce wildfire severity. If forest management professionals deploy widespread fuel treatments in the future that reduce wildfire severity, then the avoided damages from a system hardening investment made today would be lowered. This nexus between the electric power sector and the broader set of wildfire risk mitigation policies creates uncertainty in the payoffs of electric power sector adaptation efforts.

All levels of wildfire risk management face uncertainty when making investment decisions, but this uncertainty may affect the electric power sector uniquely because it is held financially liable for the damages it causes from igniting wildfires. In California, public utilities face strict liability for igniting wildfires due to inverse condemnation, allowing citizens to sue public utilities for damages incurred to their private property regardless if the utility is found negligible or not in its operations that led to the ignition [76]. In contrast, firefighters are shielded from legal action if they are unable to prevent structure loss, and forest professionals would not typically be sued if their fuel treatment projects proved ineffective. Property owners face a financial incentive to protect their structures from wildfire damages, but market failures in the insurance industry may reduce this incentive [77].

In the face of large potential liabilities and uncertainty in the amount of adaptation outside the electric power sector, electric utilities may over-invest in wildfire adaptation to

reduce expected losses. This may not be consequential for short-run adaptation investments; the utility or regulator can update its wildfire mitigation strategy as new information about non-electric power sector investments is learned each year. However, system hardening investments with longer lifetimes, like burying overhead powerlines, could become "stranded".

"Stranded assets" are ones that lose economic value well ahead of their anticipated useful lives, whether that is a result of changes in market forces, environmental shocks, or other factors [78]. Stranded assets have been a focus of the literature on the electric and gas utility industry [79–83]. The analysis described in this chapter contributes to this broader literature on aging infrastructure and efforts to decarbonize the economy. One study finds that the push to electrify buildings may leave customers who remain connected to the gas distribution network stuck paying for legacy utility costs [82]. In a similar fashion, electric distribution customers could be left paying for uneconomical system hardening investments if their intended risk reduction benefits do not deliver in future periods.

The goal of this chapter is to decompose key sources of uncertainty that affect the returns on an electric utility's long-duration wildfire adaptation investments. Three categories of uncertainty are considered: (1) factors outside the electric power sector, such as changes in extreme wildfire risk, (2) factors within the electric power sector, such as the effectiveness of operational mitigations, and (3) other economic and social factors, such as the discount rate. Each of these categories is analyzed spatially across the varied landscape and fire regimes of Pacific Gas and Electric Company's service territory. In doing so, this analysis aims to guide electric power sector adaptation investments to locations where they are cost-effective and least likely to fall victim to becoming stranded assets.

The analysis finds that burying overhead powerlines may be most cost-effective in interior regions of the utility's service territory, where ignition and extreme wildfire risk is highest. This is despite the lower structure density found in these regions. Uncertainty in extreme wildfire risk is also highest in these interior regions bordering the Sierra Nevada Mountains and Southern Cascades. To reduce the potential for extreme outcomes at the tail of the risk distribution, system hardening investments may be best targeted to these regions.

Second, the possibility for underground powerlines to become "stranded" is significant. An improvement in grid management protocols that reduces ignition risk, such as fast-trip settings, can more than double the costs of undergrounding when assessed on the basis of avoided structures burned. Similarly, a one standard deviation decrease in structure risk, possibly caused by defensive actions taken by property owners, could raise the costs of undergrounding by nearly 50%. These findings point to the importance of cross-sector coordination across all levels of wildfire risk management to ensure electric utility customers are not left paying for an uneconomical wildfire adaptation portfolio.

3.2 Data

The majority of the electric power sector data used in this analysis is previously described at length in the previous chapter and Appendix A. New sources of data include those from the"Wildfire Risk to Communities" project (WRC), a joint collaboration between the U.S. Forest Service's Rocky Mountain Research Station, Pyrologix, LLC, and Headwaters Economics.

Electric Utility Infrastructure

The analysis focuses on distribution circuits in Pacific Gas and Electric Company's (PG&E) high-fire threat district (HFTD). Specifically, the sample of circuits included in the analysis is limited to circuits that span at least ten miles in the HFTD. There are 449 of these circuits and they account for a total of 24,347 HFTD miles, which represents approximately 96% of the utility's high-risk distribution lines.

Table 3.1 shows the count and length of circuits by region. Regions are defined using the protection districts from the California Department of Forestry and Fire Protection (CALFire). See Figure 3.3 for a map of the boundaries of each region. On average, each region contains 24 circuits and 1,300 miles of distribution lines. These regions aggregate areas with similar fire regimes.

Data on operational mitigations, namely public-safety power shutoffs (PSPS) and fast-trip settings, is included in the analysis. These mitigations are described at length in both Chapters 2 and 4. Table 3.1 shows how the incidence of these measures varies across region. Three regions (Amador-El Dorado, Nevada-Yuba-Placer, and Sonoma-Lake-Napa) account for over half of all PSPS customer-hours.

Ignition Risk and Wildfire Spread

Ignition risk is evaluated using the machine-learning ignition risk model described in Chapter 2. It represents the probability of a vegetation-caused ignition occurring on a given day for a given circuit. The rightmost column of Table 3.2 transforms daily ignition probability per circuit to show the expected number of ignitions per circuit in a given fire season (defined May 15 to November 15) by region.

Average circuit ignition risk tends to be highest in regions in the Northern Sierra Nevada Mountains and Southern Cascades. Circuits in the Tehama-Glenn region, Amador-El Dorado region, and Madera-Mariposa-Merced region all produce an ignition about once every three years. Circuits along the central coast of California see much lower ignition risk of about once every ten years.

The probability of wildfire spread model is also discussed at length in the previous chapter and Appendix A. See Figures 2.10 and 2.11. This model estimates the probability that an

ignition on a given distribution circuit would reach a given size in acres. The model is trained used empirical data on PG&E-caused wildfires [17]. Table 3.2 shows that the probability of extreme electric utility-caused wildfire spread (larger than 10,000 acres) is highest in Southern Cascads (Lassen-Modoc region and Shasta-Trinity region) and generally lower in more coastal and urban regions (Marin region, San Mateo-Santa Cruz region, and San Luis Obispo region). This reflects the historical pattern of wildfire risk in the utility's service territory.

Table 3.2 contains additional summary statistics on key variables that inform the prediction of ignition risk and wildfire spread in the machine-learning models. These variables include vapor pressure deficit, average forest canopy height along the circuit, dead-fuel moisture (100 hour and 1,000 hour time lags are used), and energy release component. Figure 2.5 shows additional variables that are important determinants of ignition risk.

Wildfire Risk to Communities (WRC) Project

The Wildfire Risk to Communities (WRC) project provides national geospatial data products on wildfire hazard [84]. It was developed in collaboration with the U.S. Forest Service, Pyrologix, LLC, and Headwaters Economics. This analysis relies on two key geo-spatial products from the WRC dataset: (1) building counts in raster format and (2) conditional risk to potential structures in raster format.

The building count data is created by combining two independent sets of building footprints, one from ONEGEO and another from Oak Ridge National Laboratory and the Federal Emergency Management Agency. The WRC project filters out small polygons that represent sheds or may reflect the shadows of rocks (footprint less than 40 m^2). Footprints that overlap uninhabitable land cover such as open water or permanent snow are removed. This produces a raster dataset at a pixel size of 30 meters x 30 meters that contains the count of buildings in each pixel.

The second key geo-spatial product is called conditional risk to potential structures (cRPS). This product represents the potential consequences of a fire to a structure if both a fire were to occur and a structure was located in that pixel. Its values range from zero to 100, with zero indicating no damage to a structure and 100 indicating complete structure loss. The measure is developed by estimating flame length probability classes across the landscape and assigning response function values based on flame length and vegetation type. Importantly, cRPS reflects the potential risk to a generic residential structure and does not account for actions taken by property owners to protect their homes. See WRC documentation for more details on methods [85].

Table 3.3 summarizes the building count data and conditional risk to potential structures by region. The data is further summarized by wildfire class sizes (small, medium, large, and extreme) corresponding to the wildfire spread model discussed earlier (see Figure 2.11).

Additional details on wildfire sizes are described in the Methods section next. The first panel of Table 3.3 shows that structure density decreases with larger wildfire sizes. This is driven by powerlines generally being located close to structures, so as fires spread further from powerlines structure density decreases.

The middle panel of Table 3.3 shows that conditional risk to potential structures (cRPS) tends to be highest in regions in the Central Sierra. The three regions with the highest average cRPS (Nevada-Yuba-Placer, Tuolumne-Calaveras, and Amador-El Dorado) have an average cRPS of 0.44. The three regions with the lowest average cRPS (Santa Clara, Marin, and San Mateo-Santa Cruz) are urban and coastal regions (mean 0.25 cRPS).

The third and final panel of Table 3.3 multiplies structures per acre by cRPS to calculate expected structures burned per acre. Here, the regions with the highest values are located in more urban and coastal areas that feature high structure densities (Marin, Santa Clara, and San Luis Obispo).

3.3 Methods

To evaluate the key sources of uncertainty that affect the returns on electric power sector wildfire adaptation (i.e., undergrounding), the following five steps are taken. Additional detail on each step is described next.

1. Calculate expected structure damages from ignition points along each circuit, calibrating to observed wildfire sizes and structure losses during the historical period.
2. Create a 40-year sample of circuit and weather data by randomly sampling historical data (2015 to 2022), and combine the 40-year sample with expected structure damages.
3. Calculate the system hardening costs of undergrounding each circuit, the avoided structure losses, and other avoided costs associated with system hardening (e.g., customer outages, fast-trip and PSPS costs), discounting them over the 40-year lifetime to net present value.
4. Rank each circuit in terms of cost-effectiveness (total cost per avoided structure loss), and record the point at which 80% of total structures are avoided as a benchmark.
5. Repeat above steps after shifting key variables by one standard deviation (i.e., ignition probability) and compare changes in cost-effectiveness across regions.

Calculating Expected Structure Loss

Deriving a measure of expected structure loss at the circuit level that varies with daily changes in fire weather is central to this analysis. The threat of structure loss along circuits

can vary considerably due to differences in topography, vegetation type, wind velocity, fuel moisture, structure density, firefighting resources, structure hardening, and mitigating actions taken by the electric utility. The following model takes these factors into consideration when calculating expected structure loss.

It is worth underscoring that structure loss represents one source of damages caused by wildfires. Several studies have demonstrated that public health losses from wildfire smoke likely dwarf the damages to structures[86–88]. Other costs associated with wildfires include direct fatalities, changes to ecosystem services, firefighting expenses, and disruptions to economic activity and recreation [7]. This analysis will focus solely on structure loss because it is the largest source of damages utilities are held liable for (utilities are also held liable for firefighting expenses and direct fatalities). Future research should aim to incorporate the damages from air quality impacts into the evaluation of electric power sector wildfire adaptation efforts.

Calculation of expected structure loss (Y_{it}) at circuit i on day t takes the following form[1]:

$$Y_{it} = \Pr(I = 1|X_{it}, C_i, Z_{it}) * \sum_{s}^{S} \Pr(s|X_{it}, C_i) * \delta_{is} * \bar{\text{A}}_s \tag{3.1}$$

The first term of Equation 3.1 represents the probability of an ignition occurring for a given circuit on a given day. The ignition risk model is described at length in Chapter 2. Importantly, the probability of an ignition is adjusted to account for operational mitigations the utility may take to reduce ignition risk (Z_{it}). The two operational mitigations considered are fast-trip settings and PSPS events. In the central case, when fast-trip settings are enabled, ignition probability decreases by 72%. PSPS events are assumed reduce ignition probability by 100%.

Next, the second term of Equation 3.1, $\Pr(s|X_{it}, C_i)$, reflects the probability of an ignition spreading into a wildfire of size s. These wildfire class size probabilities are also discussed at length in Chapter 2 and Appendix A. They are estimated by training a machine-learning prediction model on historical wildfire sizes from PG&E fire ignition data. Fire suppression is not explicitly modeled in this analysis, though the wildfire spread model implicitly controls for fire suppression because it is trained on empirical wildfire sizes. The four wildfire class sizes (s) considered are:

1. Small: $<$ 10 acres
2. Medium: [10 acres, 300 acres)

[1]This equation is similar to the one used in the wildfire simulations in Chapter 2 and Appendix A, but offers several improvements. Ignition probability and wildfire class size probability are identical to the previous approach. Structures burned per acre is estimated with improved data from the cRPS data product and then calibrated to historical structure losses.

3. Large: [300 acres, 10,000 acres)
4. Extreme: [10,000 acres, ∞)

The third term of Equation 3.1 (δ_{is}) captures the number of structures burned per acre by a wildfire of size s. Figure 3.1 provides an illustration of how δ_{is} is calculated for an example circuit. First, ignition points are randomly sampled along each distribution circuit because wildfire risk can vary depending on where the ignition occurs along the circuit. The circuits included in the analysis span 50 miles, on average, and therefore can intersect a variety of vegetation types and structure densities. Five ignition points are sampled for each circuit.

Buffers equal to the average wildfire footprint ($\bar{A}_s$) of each wilfire class size (s) are then drawn around each ignition point. These buffers are shown surrounding each ignition point in Figure 3.1. Each buffer is then intersected with the 30-meter raster data on (1) building counts, (2) conditional risk to potential structures, and (3) the product of the two raster datasets. Across all pixels intersected, δ_{is} is then calculated as the average of the product of building counts (B) and cRPS. δ_{is} is adjusted to a per-acre basis to account for the 30-meter pixel sizes equaling approximately 0.22 acres. Standard deviations of δ_{is} are recorded across pixels for the uncertainty analysis. Equation 3.2 shows this mean calculation, where p denotes pixels, $B_{i,s,p}$ represents building count in pixel p intersected by fire size s, and $\text{cRPS}_{i,s,p}$ similarly represents cRPS in a pixel intersected by a given wildfire size.

$$\delta_{is} = \frac{\sum_p^P B_{i,s,p} * \text{cRPS}_{i,s,p}}{P} * \frac{1}{0.22} \tag{3.2}$$

Lastly, the fourth term of Equation 3.1 ($\bar{A}_s$) is the average wildfire footprint for a given class size, using historical data from PG&E ignition data. Average wildfire footprint sizes are multiplied by expected structure loss per acre (δ_{is}) to obtain total structure loss for wildfire class size s at circuit i in Equation 3.1. In addition, the average wildfire footprint sizes are used to draw buffers around ignition points for each wildfire class size (see Figure 3.1).

1. $\bar{A}_{s=\text{Small}}$: 1 acre
2. $\bar{A}_{s=\text{Medium}}$: 150 acres
3. $\bar{A}_{s=\text{Large}}$: 2,000 acres
4. $\bar{A}_{s=\text{Extreme}}$: 20,000 acres

Finally, expected structure losses are calibrated to historical data on structure losses from PG&E-caused wildfires using a calibration factor α. Using incident-specific reports

from CALFire, total structure losses from PG&E-caused wildfires during the 2015 to 2022 period are approximately 27,000[2], denoted by μ. The Camp fire accounts for 18,804 of the approximately 27,000 structures lost. Exclusion of the Camp fire would reduce the calibration factor to 1.4.

$$\alpha = \frac{\mu}{\sum_{2015}^{2022} \sum_{i}^{N} Y_{it}} = \frac{27,271}{6,358} = 4.3 \tag{3.3}$$

Therefore, expected structure loss for a circuit i on day t is given by:

$$\hat{Y}_{it} = Y_{it} * \alpha \tag{3.4}$$

There are several advantages and disadvantages to this methodology that are important to highlight. First, estimating wildfire class size probabilities is subject to small sample bias. Extreme wildfire sizes are rare, 0.5% of all PG&E-caused ignitions, but drive a significant portion of structure losses. Just one wildfire, the Camp fire, accounts for two-thirds of observed structure losses. And yet, the Camp fire was only 15% of the size in acres of PG&E's largest wildfire, the Dixie fire. In short, Equation 3.1 inherently assumes an increasing relationship between wildfire size and structure loss, but this simplified relationship does not always hold with some of the state's most extreme wildfires.

An important advantage of this approach is that it leverages a structure damage response function (cRPS) at a highly granular 30-meter resolution. Rather than selecting a single parameter for this damage function (0.4 in the case of the wildfire simulations in Chapter 2), this approach captures how difficult it may be to fight fires and protect structures conditional on local topography, land cover, vegetation type, and fuels. In addition, because cRPS values are generated at a granular geo-spatial scale, a distribution of cRPS values can be created and drawn from for the uncertainty analysis.

A disadvantage of the methodology described comes from the construction of buffers around ignition points. In the wildfire simulations described in Chapter 2, wildfire perimeters were grown using the Minimum Travel Time method. As a result, wildfire footprints tended to grow in the direction of prevailing winds and follow the slopes and vegetation around the circuit. This produces wildfire footprints that closely resemble actual wildfire footprints (see Figure A.2). However, these wildfire simulations require significant computation time and were thus limited to subset of distribution circuits. In this analysis, circular buffers are drawn around each ignition point, which may not reflect the tendency of wildfires to grow in specific directions surrounding each circuit.

[2]Destroyed structures are assigned a value of 1 and damaged structures are assigned a value of 0.5. The Kincade fire is excluded because it was ignited by a transmission line. The Tubbs fire is excluded because it was ignited by private electrical equipment.

Creating the Circuit-Weather Sample

Next, a 40-year sample of weather data is constructed for each circuit included in the analysis. The data sample is restricted to the fire season, defined as May 15 to November 15. The sample is created by drawing randomly from the historical set of weather data from 2015 to 2022. The period of 40-years is based on the expected lifetime of underground powerline assets.

The key variables recorded when creating the circuit-weather sample include the probability of ignition, the probability of each wildfire class size, and the presence of fast-trip settings, PSPS events, and associated outage durations (Z_{it}). Ignition risk or wildfire risk is not assumed to increase in future years, however these variables are shifted up and down in the following uncertainty analysis.

System Hardening Costs and Benefits

The calculation of system hardening costs and benefits closely follows the approach described in Chapter 2 and Appendix A, with several changes. First, the analysis does not assume the utility earns a return on its capital investment. In this way, the costs presented here more resemble the"social" perspective shown in Figure 2.8. However, the cost analysis does assume there is some financing cost the utility faces. The interest rate is set at 2.5% above the real social discount rate. The central estimates assume a discount rate of 2.5% and an interest rate of 5%. In Chapter 2, the "social" perspective does not assume there is any financing cost for the undergrounding investment.

When an electric-utility undergrounds a powerline, it obviates the need to use operational mitigations such as fast-trip settings and PSPS events. The cost analysis includes these avoided operational costs as a benefit of undergrounding powerlines. Using historical data on fast-trip and PSPS costs, the analysis assumes $20 per customer-hour of fast-trip outages and $10 per customer-hour of PSPS outages. Customers also face an economic cost in the form of outages when operational mitigations are activated. The cost analysis assumes a value of lost load (VoLL) of $3 per kWh. See Chapter 2 and Appendix A for more details.

The cost model assumes a unit cost of $3 million per mile of undergrounding. See Appendix A for a detailed discussion of unit cost sources for undergrounding. Annual undergrounding costs, avoided structure losses, and other avoided costs such as outages are discounted to net present value terms using a real social discount rate of 2.5%.

Benchmarking Cost-Effectiveness

The next step combines net present costs with net present avoided structure losses to calculate cost per avoided structure burned. A benchmark is needed to assess cost-effectiveness across sensitivity analyses and across regions. The system-wide average cost per avoided

structure burned is not a useful benchmark because in some low-risk locations it is highly uneconomical to underground powerlines.

In this case, the benchmark used is the marginal cost per avoided structure burned at which 80% of total structure risk is mitigated. This parameter choice of 80% could be viewed as arbitrary, but it is useful to ground it in the "prices vs. quantities" concept of mitigating global greenhouse gas emissions [89]. In the absence of a full cost-benefit analysis, it is unknown at what marginal cost undergrounding becomes uneconomical. Instead, a target is set on total structure loss, akin to a target on emissions, and the marginal cost is observed at that target. This target of 80% risk reduction produces an undergrounding quantity result that tracks the utility's publicly stated goal of undergrounding 10,000 miles of powerlines [45]. However, the analysis could be replicated with lower or higher targets for robustness.

To construct the benchmark, circuits are ranked in terms of cost-effectiveness. The analysis assumes the utility deploys the most cost-effective projects first. The first set of results also reports that average cost per avoided structure burned at which 80% of structure risk is mitigated.

Uncertainty Analysis

Finally, the last step involves shifting key parameters up and down to observe how sensitive the cost-effectiveness benchmark is to each parameter. This decomposition analysis aims to identify what factors may play the largest role in affecting the returns on system hardening investments. Specifically, the goal of the analysis is to determine to what extent do exogenous influences outside of the electric power sector play a prominent role in driving the returns on electric power sector adaptation investments. A list of how each parameter is shifted follows:

1. *Ignition Probability*: Standard deviations are calculated for each circuit across all fire-season days. Ignition probabilities are then shifted both up and down for each circuit by one standard deviation. If ignition probability is equal to or less than zero, it is set to the minimum value of $1 * 10^{-6}$.

2. *Extreme Wildfire Spread*: Standard deviations of the probability of extreme wildfire spread ($\geq$ 10,000 acres) are calculated for each circuit using all fire-season days. The probability of extreme wildfire spread is then shifted up and down by one standard deviation. Because the probabilities across all wildfire class sizes must sum to 1, the corresponding increase or decrease in extreme wildfire spread probability is offset by even changes in small and medium wildfire class size probabilities.

3. *Structure Risk*: Figure 3.1 illustrates how each wildfire class buffer intersects many pixels. Standard deviations for expected structure loss per acre (δ) for each circuit are obtained through this variation across pixels. δ is then shifted up and down by one standard deviation.

4. *System Hardening Costs*: The central case assumes undergrounding costs of $3 million per mile. The uncertainty analysis uses $2 million per mile as the low case and $4 million per mile as the high case.

5. *Discount Rate and Interest Rate*: The central real social discount rate used is 2.5%. The low case uses 0.05% and the high case uses 4.5%. The corresponding low and high interest rates (shifted symmetrically with the discount rate) are 3% and 7%.

6. *Fast-Trip Settings*: In the central case, fast-trip settings are assumed to be 72% effective at reducing ignition risk when enabled. The low and high cases vary this effectiveness by 20%. No sensitivity analysis is provided for fast-trip program costs, PSPS program costs, or PSPS effectiveness.

7. *Value of Lost Load*: The central case assumes a VoLL of $3 per kWh. The low case assumes a VoLL of $1 per kWh and the high case assumes $5 per kWh.

Finally, Monte Carlo methods are used to construct 95% confidence intervals. For the Monte Carlo simulation, 100 runs are performed. For each run, a new 40-year sample of circuit-weather data is randomly drawn. In addition, for each run the parameters described above are randomly drawn from their corresponding distributions. Variation in the cost-effectiveness of undergrounding across each Monte Carlo run allows for construction of 95% confidence intervals shown in Figure 3.2.

3.4 Results

The next section discusses three sets of finding. The first provides an overview of undergrounding cost-effectiveness on a system-wide basis, similar to results discussed in Chapter 2 (Figures 2.8 and 2.9). These results improve upon those discussed in Chapter 2 by estimating cost-effectiveness across all high-risk circuits, in contrast to the two regions that wildfire simulations were performed in. The second set of results discusses regional heterogeneity in undergrounding cost-effectiveness and its likely causes. The third set of results focuses on decomposing the key sources of uncertainty that influence undergrounding cost-effectiveness.

System-Wide Cost-Effectiveness

The following sets of findings rely on a benchmark cost-effectiveness measure that is calculated as the marginal cost per avoided structure burned at which 80% of system-wide structure risk is mitigated. Figure 3.2b shows that the central estimate of this benchmark is $5.0 million per avoided structure burned with a 95% confidence interval of $2.8 to $8.8 million per avoided structure burned. While this cost is much higher than the median structure value in California, structure losses represent just one source of damages from wildfires and should not be used as the sole criterion in a cost-benefit analysis.

Both Figures 3.2a and 3.2b show that 80% of structure risk can be mitigated by undergrounding 8,900 miles of distribution lines. This suggests that 80% of the utility's structure risk is concentrated in 36% of the utility's distribution-circuit miles. This finding is consistent in the Monte Carlo simulation, producing a 95% confidence interval of 8,700 miles to 9,500 miles.

The total cost to mitigate 80% of structure risk is estimated at approximately $50 billion, assuming per-mile costs of $3 million per mile, a discount rate of 2.5%, and an interest rate of 5%. The Methods section and Appendix A discuss how additional costs are treated, including outage costs and avoided operational expenses. While the benchmark marginal cost per avoided structure burned for an 80% risk reduction is $5.0 million, the average cost across all 8,900 miles buried is approximately half the marginal cost ($2.5 million per avoided structure burned). This highlights the significant variation in cost-effectiveness across undergrounding projects.

Regional Heterogeneity

Next, the analysis finds that this benchmark cost-effectiveness measure of $5.0 million per avoided structure burned varies considerably across the regions of Northern and Central California. Burying powerlines is most cost-effective in regions to north of the utility's service territory that border the Sierra Nevada mountain range (See Figure 3.3).

In the Butte Unit (BTU), where the Camp fire was ignited, 80% of the region's structure risk can be mitigated at a low benchmark cost of approximately $1 million per avoided structure burned. This finding of high cost-effectiveness in the Butte region is consistent empirically. At the end of 2022, PG&E had directed one-third of its undergrounding investment to date to the Butte region, despite its distribution circuit miles accounting for less than 5% of the utility's total high-risk miles.[3]

The next three most cost-effective regions are all adjacent to the Butte region: Shasta-Trinity, Tehama-Glenn, and Lassen-Modoc. Marginal cost per avoided structure burned at which 80% of each region's structure risk is mitigated ranges from $2.0 million to $2.3 million.

Regions where undergrounding is least cost-effective are located generally along the coast. These regions span all the way to the utility's northern border (Humboldt-Del Norte) and to its southern border (Santa Barbara). Differences in ignition risk and extreme wildfire spread, as opposed to structure density and conditional risk to structures, likely explain the regional heterogeneity in cost-effectiveness. In coastal regions, the areas near high-risk distribution lines feature approximately double the structure density compared to the more cost-effective regions bordering the Northern and Central Sierra Nevada mountains. Despite the larger

[3]This may be explained partially by the necessary rebuild of the distribution network following the Camp fire.

structure count in coastal regions, ignition probability is less than half and the probability of extreme wildfire spread is 10% of the respective values in the Northern interior regions of the utility's service territory.

This finding confirms the importance of extreme wildfire probabilities in explaining catastrophic wildfire outcomes and heterogeneity across regions. While extreme wildfire sizes are very rare (0.5% of powerline-caused ignitions), they are a large driver of damages. Accurately measuring these probabilities is a difficult task given small sample sizes, but it is a crucial ingredient to effective deployment of adaptation investments. Tables 3.2 and 3.3 summarize ignition risk, wildfire spread probability, and structure risk variables for each region.

Uncertainty Analysis

In Figure 3.4, key parameters (i.e., ignition risk, undergrounding unit costs) are shifted upwards and downwards, and their impacts to cost-effectiveness are recorded. The first finding is that the unit cost of undergrounding, often a focus of regulatory proceedings and debate among stakeholders, does not have the largest impact on cost-effectiveness. Instead, parameters related to ignition risk, including the effectiveness of fast-trip settings at mitigating ignition risk, can produce a much larger impact.

Consider an improvement in undergrounding unit costs from $3 million per mile to $2 million per mile. This improvement would lower the cost per avoided structure burned by 42%. In contrast, an increase in the effectiveness of fast-trip settings from 72% to 92% would raise the cost per avoided structure burned by 140%. Similarly, a one standard deviation decrease in ignition risk, which can serve as a useful for proxy for other grid management technologies developed in the future, leads to a doubling of cost per avoided structure burned.

This finding highlights concerns about underground powerlines becoming "stranded assets". The cost-effectiveness of undergrounding investments made today can be eroded by future improvements in the effectiveness of operational mitigations deployed in later periods. Adaptation strategies that embrace innovation across a range of system hardening and operational measures provides the utility with portfolio diversity; committing to a single system hardening technology with a long lifetime may lead to the "stranded asset" problem and reduced cost-effectiveness.

The second finding from the uncertainty analysis is that a one standard deviation increase in the probability of extreme wildfire spread can cut the cost per avoided structure burned by more than half from $5.0 million to $2.25 million. As the climate warms and periods of drought intensify, wildfires may be more difficult to contain as drier fuels encourage extreme fire behavior. On the other hand, widespread use of fuel treatments (e.g., prescribed burns, mechanical thinning) and improved fire suppression resources could reduce the potential for extreme wildfire spread in the future. Extreme burn severity could produce a negative feedback on future wildfire spread[90]. The uncertainty analysis finds that this parameter, which

is exogenous from the utility's perspective, plays a significant role in the cost-effectiveness of its system hardening investments.

Figure 3.5 explores the extreme wildfire spread parameter in more depth by breaking out the effect of a one standard deviation increase across each region. The purpose of this task is to identify regions where undergrounding investments are subject to more uncertainty, and in doing so, can inform future investment. The results of the figure find that regions in the Northern Sierra Nevada mountains and Southern Cascades would experience the largest changes in cost-effectiveness caused by a one standard deviation increase in extreme wildfire spread. Specifically, the Butte region, the Nevada-Yuba-Placer region, and the Tehama-Glenn region would experience a 60-69% decrease in cost per avoided structure burned under a one standard deviation increase.

Given these three regions are already some of the most cost-effective areas to bury powerlines, targeting undergrounding investments here may deliver the most cost-effective undergrounding investments. Moreover, from the perspective of risk-averse wildfire manager, directing undergrounding investment towards these regions could reduce the risk of catastrophic outcomes at the tail of the risk distribution. The three regions where a one standard deviation increase in extreme wildfire spread produce the smallest changes to cost-effectiveness are to the south of the utility's service territory and along the coast (San Luis Obispo region, San Benito-Monterey region, and Santa Barbara region). For comparison, a one standard deviation increase produces a 12-30% reduction in cost per avoided structure burned.

Third, to simulate the potential for property owners to invest heavily in wildfire adaptation (e.g., defensible space, structure hardening), a similar exercise is undertaken with respect to structure risk in Figure 3.6. Comparing Figure 3.6 with Figure 3.5, the effect of a one standard deviation decrease in structure risk is on par with that of a one standard deviation increase in extreme wildfire spread. Across all regions, the former produces an average increase in cost per avoided structure burned of 48% while the latter produces a decrease of 47%.

The Lassen-Modoc region stands out as an outlier in terms of its vulnerability to uncertainty regarding structure risk. A one unit decrease in structure risk raises the cost per avoided structure burned by approximately 140%. This stems intuitively from the region displaying the largest variability in structures lost per acre across circuits and wildfire class sizes. One possible explanation for why the region sees the largest variability in this parameter is that the region has some of the lowest structure density (0.05 structures per acre in a 20,000 acre footprint around each circuit compared with territory average of 0.21 structures per acre; see Table 3.3). Despite the Lassen-Modoc region's high ignition and wildfire spread risk, its low structure density and accompanying uncertainty in structure risk makes the returns on undergrounding in the region less certain. This finding suggests that the deployment of system hardening investments should find an appropriate balance between

high risk versus densely populated areas.

3.5 Discussion

This chapter addresses a pressing question focused on uncertainty and sources of heterogeneity in the cost-effectiveness of adapting to wildfire risk in the electric power sector. This question is important to investigate because electric utilities are investing significant capital to buy down wildfire risk that has escalated rapidly in recent years, and in all likelihood, will continue to escalate.

Adaptation across all sectors, including the electric power sector, is needed critically [20]. However, capital investments with long lifetimes, such as burying powerlines, may fall victim to a "stranded assets" effect. If innovation produces new approaches to manage wildfire risk more cost-effectively, then the economics of burying powerlines may deteriorate and leave utility customers tied to higher electricity costs.

The concept of stranded assets in the electric power sector has been studied in the context of natural gas distribution and fossil-fuel generating facilities. However, existing literature on electric power sector adaptation to wildfire has not addressed the vulnerability of such investments to future uncertainty. The methodology used in this analysis provides a robust framework to approach the problem. Machine-learning models are trained on empirical data on powerline-caused ignitions and wildfire sizes. Evaluating these prediction models creates useful measures of ignition and wildfire size probabilities. The distribution of these two parameters are then used to study how uncertainty in ignition and wildfire risk influences cost-effectiveness.

A main limitation of the methodological approach is that the uncertainty in ignition risk and wildfire spread is derived using historical data. In future years, extreme autumn wildfires in California are projected to increase in severity [90, 91], and climate change in general will likely increase the occurrence of extreme weather events [92]. This suggests that the historical distribution of fire weather may not sufficiently capture the presence of extreme fire weather events that play an important role in determining the cost-effectiveness of adaptation investments.

Another limitation concerns the structure risk data. The underlying cRPS data developed by the U.S. Forest Service's Wildfire Risk to Communities project assumes all structures are a representative building. In doing so, it ignores local investments that property owners may have access to reduce potential losses. For example, some fire districts may enforce defensible space policies more strongly or have more local resources available to suppress fires. This analysis ignores these possibilities, and instead assumes structure risk is purely a function of probabilistic flame length and vegetation type.

The key findings of the analysis are threefold. First, 80% of the utility's structure risk

is concentrated in approximately one-third of its high-risk distribution lines. A regional decomposition analysis suggests that the most cost-effective locations to underground are located in the interior parts of the utility's service territory along the Northern Sierra Nevada mountains and Southern Cascades. The primary source of this heterogeneity stems from high ignition and wildfire risk, despite these regions showing lower average structure densities.

Second, there is potential for undergrounding invesments to become stranded assets. An improvement in the effectiveness of operational mitigations such as fast-trip settings can raise the cost per avoided structure burned of an undergrounding investment by 140%. Similarly, a one standard deviation decrease in ignition risk could double the cost per avoided structure burned. One recommendation that emerges from this finding is that long-lived system hardening investments like undergrounding should be evaluated carefully and continuously across their lifetimes. Through the establishment of methods to assess their cost-effectiveness, these adaptation investments can be deployed iteratively in future periods depending on how well they achieve their intended risk reduction benefits.

Third, the analysis quantifies two exogenous sources of uncertainty to the electric utility's wildfire adaptation strategy. Unlike parameters such as the probability that its equipment causes an ignition or the unit cost of system hardening, an electric utility wildfire risk manager has little control over extreme wildfire behavior or property owner actions taken to reduce structure loss. And yet, this analysis finds that these two exogenous sources of uncertainty play a significant role in influencing the cost-effectiveness of undergrounding. A one unit decrease in structure risk, possibly initiated by stricter building codes and defensible space policies in high-risk areas, can produce a near doubling of the cost per avoided structure burned associated with undergrounding.

Overall, the results of this analysis emphasize the need a coordinated approach to wildfire risk management across all levels of stakeholders. Electric utilities are held financially liable for the outcomes of wildfires ignited by their equipment, independent of the successes or failures of mitigation actions taken outside the electric power sector. Due to the large and uncertain liabilities electric utilities potentially face, they may seek to invest heavily in capital-intensive system hardening investments such as undergrounding. However, the cost-effectiveness of these long-duration capital investments are susceptible to future levels of adaptation outside the electric power sector. Without adequate cross-sector coordination of wildfire risk management, electric utility customers may be left paying for a high-cost and under-performing wildfire adaptation portfolio.

3.6 Figures and Tables

Figure 3.1: Illustration of Structure Risk Methodology

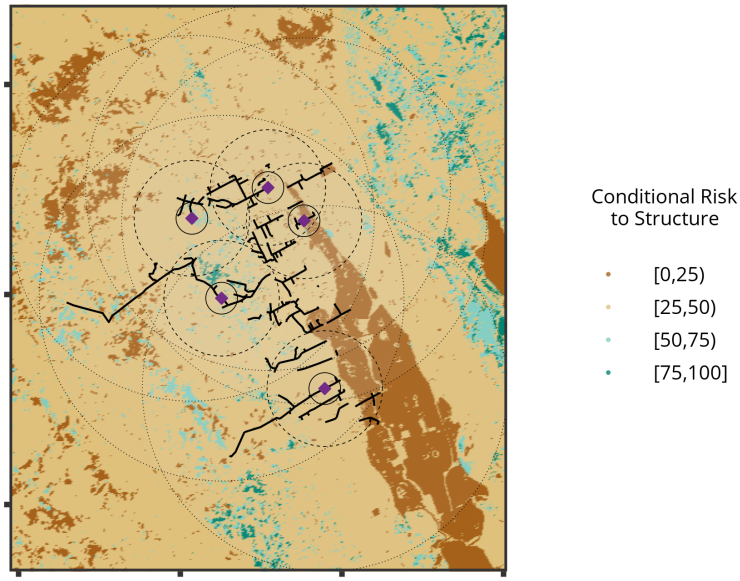

(a) Conditional Risk to Structures

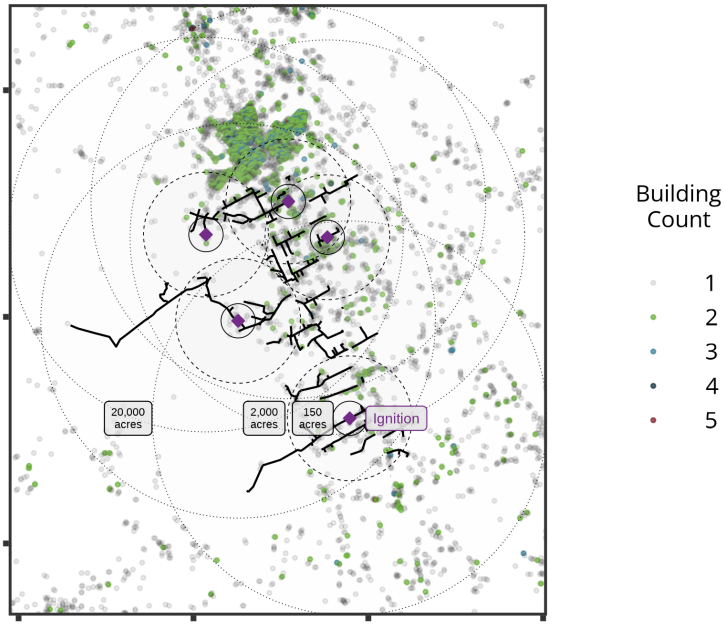

(b) Building Count

Figure 3.2: Estimated Structure Loss and Cost per Avoided Structure Burned

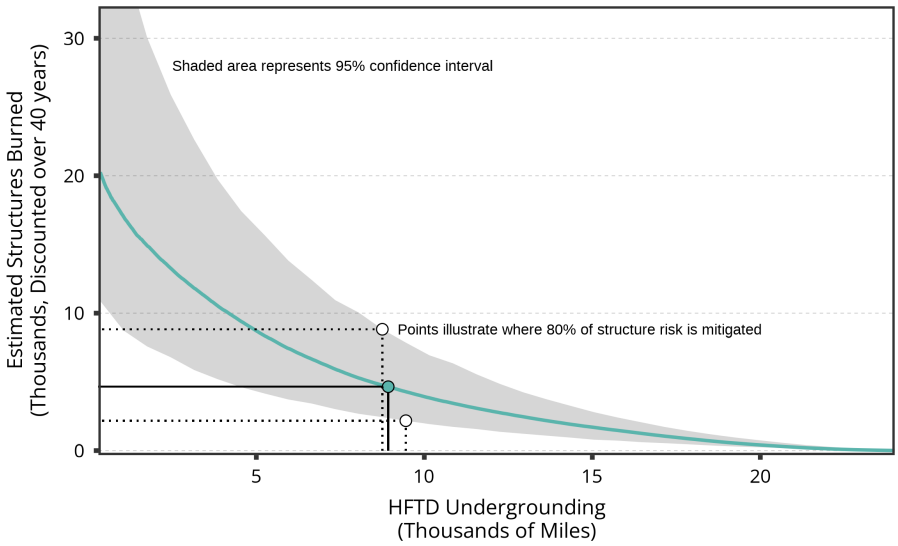

(a) Structure Curve

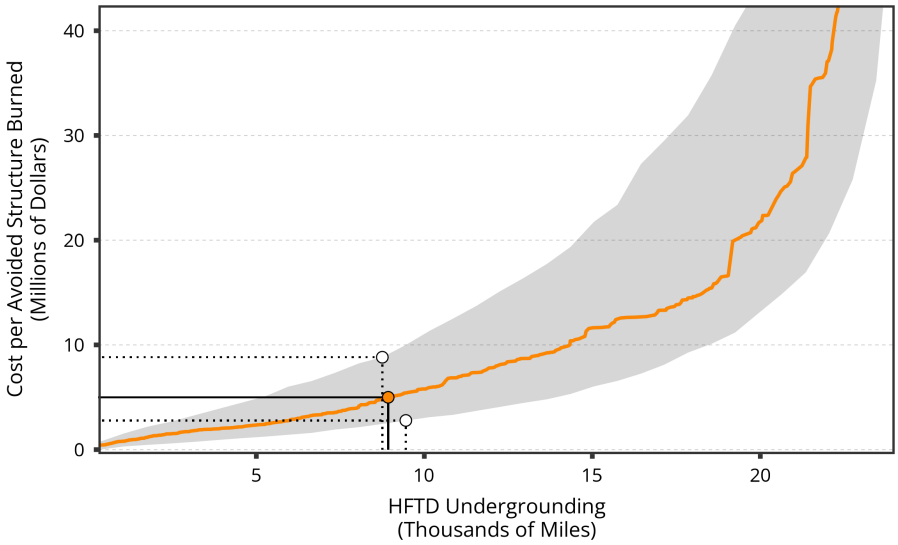

(b) Cost Curve

Notes: (b) The cost curve is constructed by ranking each circuit in terms of cost per avoided structure burned. See Methods for cost-modeling assumptions. (a) The structure curve shows how total estimated structures burned decreases with more undergrounding investment, assuming the most cost-effective circuits are prioritized first. 95% confidence intervals are derived using Monte-Carlo simulation.

Figure 3.3: Cost-Effectiveness Map

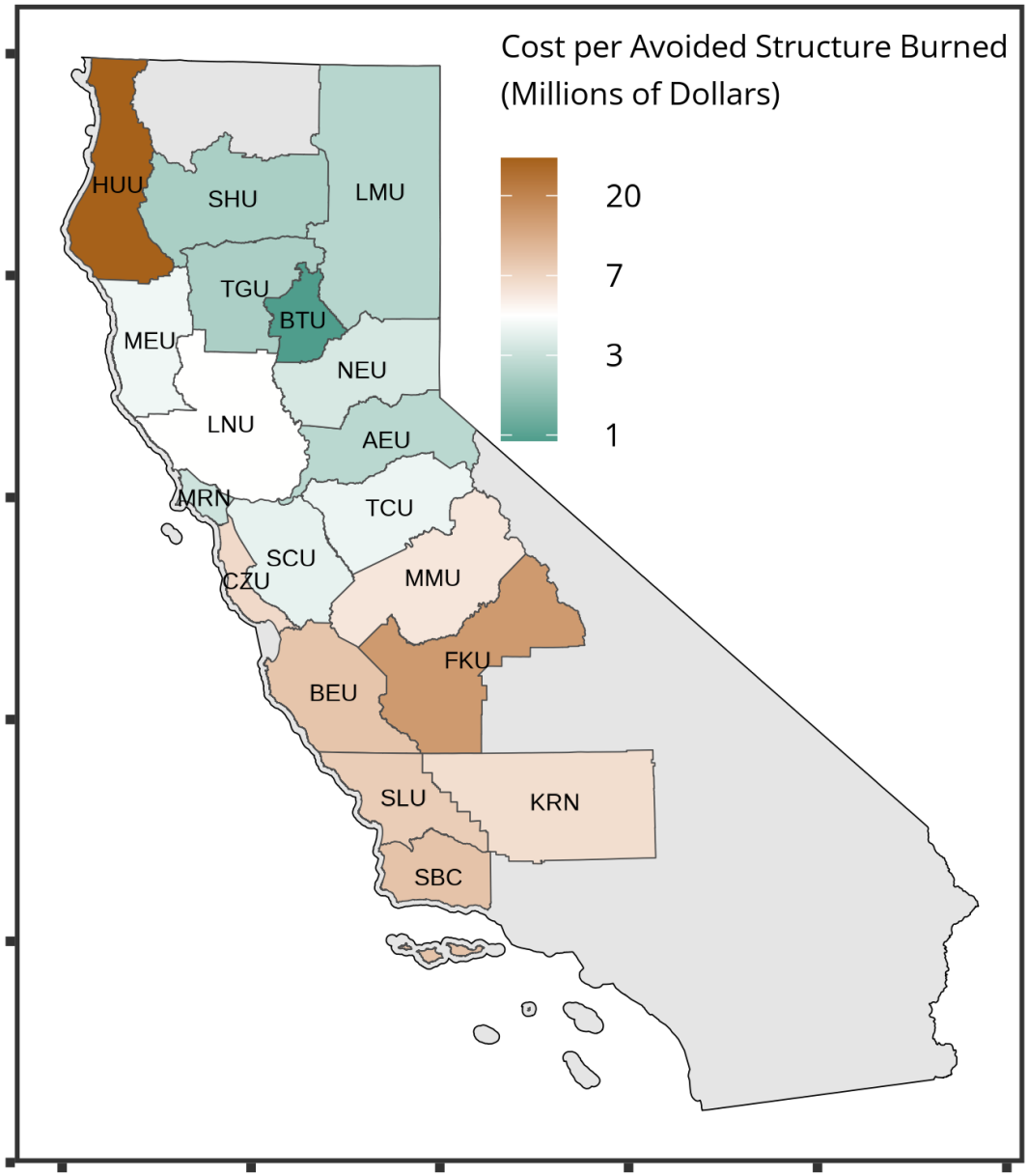

Notes: Cost per avoided structure burned represents the marginal cost at which 80% of each region's structure risk is mitigated. Regions are abbreviated as following: Amador-El Dorado (AEU), Butte (BTU), Frenso-Kings (FKU), Huboldt-Del Norte (HUU), Kern (KRN), Lassen-Modoc (LMU), Madera-Mariposa-Merced (MMU), Marin (MRN), Mendocino (MEU), Nevada-Yuba-Placer (NEU), San Benito Monterey (BEU), San Luis Obispo (SLU), San Mateo-Santa Cruz (CZU), Santa Barbara (SBC), Santa Clara (SCU), Shasta-Trinity (SHU), Sonoma-Lake-Napa (LNU), Tehama-Glenn (TGU), Tuolumne-Calaveras (TCU).

Figure 3.4: Tornado Chart

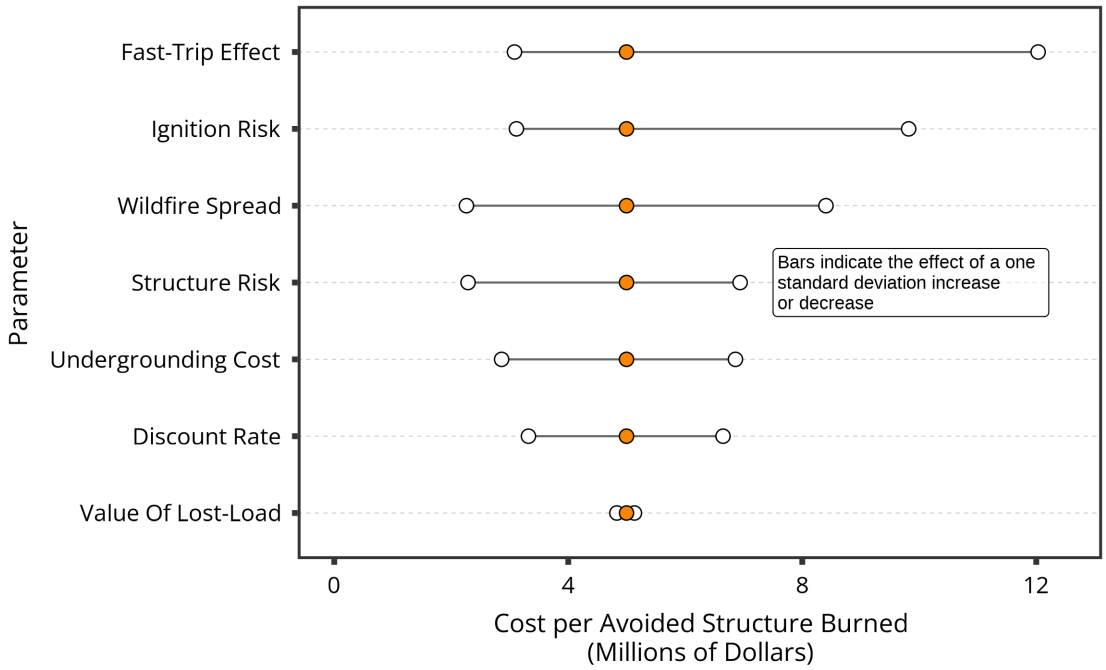

Notes: The central estimates of cost per avoided structure burned indicate the marginal undergrounding cost at which 80% of structure risk is mitigated. The error bars report the same value after shifting key parameters up and down. For ignition risk and wildfire spread, the error bars represent the effect of a one standard deviation change, where the standard deviation is measured at the circuit-month level. For wildfire spread, the probability of "extreme" wildfire class size is shifted up and down, and the opposite change in probability is applied to the probability of "small" wildfire class size to ensure the probabilities of all class sizes sum to one. For structure risk (structures burned per acre), standard deviations are obtained at the circuit-level and measured across pixels, fire size classes, and sampled ignition points along a circuit. The error bars for fast-trip settings are calculated assuming a high effect on ignition risk of 92% and a low effect of 52%. The range of undergrounding costs is \$2 million per mile to \$4 million per mile. The range of discount rates is 0.05% to 4.5%. The range of value of lost loads is \$1 per kWh to \$5 per kWh.

Table 3.1: Summary Statistics: Circuit Characteristics

Region	Circuits (N)	HFTD Miles	PSPS Duration	Fast-Trip Duration
Amador-Eldorado	36	2,793	16.2	1.1
Butte	17	952	6.7	0.2
Fresno-Kings	9	842	0.4	0.3
Humboldt-Del Norte	17	848	1.6	0.3
Kern	3	101	0.1	0
Lassen-Modoc	9	326	0.8	0.1
Madera-Mariposa-Merced	17	1,710	1.5	0.6
Marin	13	434	3.5	0.2
Mendocino	21	1,304	3.5	0.1
Nevada-Yuba-Placer	49	2,839	17.8	0.7
San Benito-Monterey	25	910	0.3	0.3
San Luis Obispo	24	1,247	0	0.4
San Mateo-Santa Cruz	24	1154	6.7	1.4
Santa Barbara	13	487	0	0.1
Santa Clara	41	988	5.7	1
Shasta-Trinity	28	1,589	6.6	0.2
Sonoma-Lake Napa	67	2,839	25.2	1.1
Tehama-Glenn	11	780	2.5	0.1
Tuolumne-Calaveras	25	2,204	9.5	1
Total	449	24,347	108.6	9.3

Notes: PSPS and fast-trip durations are measured in millions of customer-hours between 2018 and 2022. Fast-trip settings were piloted to half of HFTD circuits in 2021 and then deployed to all circuits in 2022. Only circuits with at least 10 miles in the HFTD are included in the analysis. Therefore, total HFTD miles above are slightly less than PG&E's total of 25,300 HFTD miles.

Table 3.2: Summary Statistics: Ignition Risk

Region	Vapor Pressure Deficit	Forest Canopy Height	Energy Release Comp.	Dead Fuel Moisture	**Probability of Wildfire Spread** Small	Med.	Large	Extr.	Circuit Ignition Risk
	kPa	m	Index	%					Ignitions
Amador-Eldorado	1.99	13.3	68.01	9.34	0.96	0.03	0	0.01	0.32
	(0.94)	(5.78)	(19.83)	(3.43)	(0.03)	(0.03)	(0.01)	(0.01)	(0.14)
Butte	2.1	14.59	69.45	9	0.94	0.04	0.01	0.01	0.27
	(0.99)	(5.11)	(20.82)	(3.65)	(0.04)	(0.03)	(0.01)	(0.02)	(0.1)
Fresno-Kings	2.18	9.32	74.18	8.18	0.9	0.09	0	0.01	0.27
	(0.97)	(4.42)	(16.99)	(2.66)	(0.04)	(0.04)	(0.01)	(0.02)	(0.12)
Humboldt-Del Norte	1.14	12.57	41.84	14.41	0.97	0.02	0	0	0.15
	(0.77)	(3.4)	(18.31)	(4.2)	(0.03)	(0.02)	(0)	(0)	(0.08)
Kern	2.47	0.82	81.51	6.95	0.88	0.11	0.01	0.01	0.09
	(1.01)	(0.62)	(14.81)	(2.12)	(0.06)	(0.06)	(0.01)	(0.02)	(0.01)
Lassen-Modoc	1.59	15.12	66.75	9.56	0.91	0.04	0.01	0.04	0.14
	(0.77)	(5.91)	(21.05)	(3.65)	(0.04)	(0.02)	(0.01)	(0.03)	(0.04)
Madera-Mariposa-Merced	2.1	11.16	70.98	8.71	0.92	0.06	0.01	0.01	0.31
	(0.93)	(4.82)	(16.91)	(2.74)	(0.04)	(0.03)	(0.01)	(0.01)	(0.16)
Marin	1.09	8.37	42.28	13.83	0.98	0.02	0	0	0.1
	(0.57)	(3.51)	(10.39)	(2.36)	(0.02)	(0.01)	(0.01)	(0)	(0.03)
Mendocino	1.24	10.44	43.68	14.01	0.97	0.02	0	0	0.18
	(0.85)	(4.32)	(18.74)	(4.1)	(0.03)	(0.02)	(0.01)	(0.01)	(0.07)
Nevada-Yuba-Placer	1.96	15.75	69.54	9.07	0.95	0.04	0	0.01	0.22
	(0.93)	(5.6)	(20.41)	(3.53)	(0.04)	(0.04)	(0.01)	(0.02)	(0.11)
San Benito-Monterey	1.32	6.43	49.08	12.69	0.95	0.04	0.01	0	0.11
	(0.82)	(5.53)	(15.41)	(2.92)	(0.04)	(0.03)	(0.02)	(0)	(0.06)
San Luis Obispo	1.31	4.09	47.32	13.18	0.96	0.03	0	0	0.12
	(0.76)	(2.22)	(12.66)	(2.39)	(0.03)	(0.03)	(0.01)	(0)	(0.1)
San Mateo-Santa Cruz	1.16	15.38	45.37	13.43	0.97	0.03	0.01	0	0.14
	(0.64)	(6.48)	(12.42)	(2.57)	(0.02)	(0.02)	(0.01)	(0)	(0.07)
Santa Barbara	1.33	2.3	45.97	13.43	0.92	0.07	0.01	0	0.1
	(0.66)	(0.71)	(10.21)	(1.84)	(0.03)	(0.03)	(0.01)	(0)	(0.04)
Santa Clara	1.37	7.74	52.29	11.82	0.97	0.02	0	0	0.08
	(0.74)	(4.96)	(13.8)	(2.64)	(0.03)	(0.02)	(0.01)	(0)	(0.03)
Shasta-Trinity	2.1	9.07	65.48	9.61	0.95	0.03	0	0.01	0.26
	(1.05)	(4.84)	(20.39)	(3.81)	(0.03)	(0.02)	(0.01)	(0.01)	(0.09)
Sonoma-Lake Napa	1.52	6.44	50.61	12.39	0.96	0.03	0.01	0	0.16
	(0.83)	(4.47)	(16.96)	(3.48)	(0.04)	(0.02)	(0.02)	(0.01)	(0.06)
Tehama-Glenn	2.31	4.85	68.33	8.93	0.95	0.04	0.01	0.01	0.35
	(1.08)	(2.98)	(18.59)	(3.28)	(0.04)	(0.03)	(0.01)	(0.01)	(0.1)
Tuolumne-Calaveras	1.9	13.25	66.69	9.56	0.94	0.05	0	0.01	0.25
	(0.89)	(6.52)	(18.72)	(3.21)	(0.05)	(0.04)	(0.01)	(0.01)	(0.11)
Mean	1.65	10.02	57.39	11.21	0.95	0.04	0.01	0.01	0.19

Notes: Reported values are means for each circuit by region, and values in parentheses are standard deviations. However, circuit ignition risk is measured as the total predicted count of ignitions during the fire season (May 15 to November 15) in that region. Standard deviations for ignition risk represent annual variation. Dead fuel moisture reported above is for 1,000 hour time-lag fuels, such as dead fallen trees.

Table 3.3: Summary Statistics: Structure Risk

	Structure Density per Acre				**Conditional Structure Risk**				**Structures Burned per Acre**			
Region	Sml.	Med.	Lrg.	Extr.	Sml.	Med.	Lrg.	Extr.	Sml.	Med.	Lrg.	Extr.
AEU	0.61	0.52	0.37	0.27	0.39	0.41	0.44	0.46	0.2	0.16	0.11	0.08
	(0.55)	(0.35)	(0.23)	(0.18)	(0.1)	(0.09)	(0.1)	(0.1)	(0.19)	(0.11)	(0.06)	(0.05)
BTU	0.5	0.49	0.38	0.25	0.35	0.36	0.36	0.36	0.13	0.14	0.1	0.06
	(0.56)	(0.38)	(0.29)	(0.17)	(0.09)	(0.1)	(0.09)	(0.08)	(0.15)	(0.11)	(0.08)	(0.04)
FKU	0.15	0.13	0.07	0.05	0.38	0.4	0.42	0.43	0.04	0.04	0.02	0.01
	(0.19)	(0.07)	(0.05)	(0.03)	(0.09)	(0.07)	(0.08)	(0.08)	(0.05)	(0.02)	(0.01)	(0.01)
HUU	0.6	0.29	0.1	0.05	0.29	0.29	0.3	0.31	0.15	0.08	0.03	0.01
	(0.59)	(0.21)	(0.09)	(0.07)	(0.04)	(0.04)	(0.05)	(0.06)	(0.15)	(0.05)	(0.02)	(0.01)
KRN	0.32	0.08	0.03	0.02	0.34	0.34	0.34	0.35	0.11	0.03	0.01	0.01
	(0.41)	(0.11)	(0.05)	(0.03)	(0.07)	(0.06)	(0.07)	(0.08)	(0.14)	(0.04)	(0.02)	(0.01)
LMU	0.4	0.27	0.09	0.04	0.37	0.39	0.4	0.4	0.2	0.11	0.03	0.01
	(0.8)	(0.37)	(0.11)	(0.05)	(0.11)	(0.13)	(0.15)	(0.15)	(0.46)	(0.18)	(0.04)	(0.02)
MMU	0.5	0.29	0.15	0.08	0.36	0.37	0.4	0.42	0.16	0.09	0.05	0.03
	(0.39)	(0.18)	(0.1)	(0.05)	(0.05)	(0.05)	(0.05)	(0.05)	(0.15)	(0.06)	(0.03)	(0.02)
MRN	2.26	1.66	1.19	0.72	0.27	0.26	0.26	0.26	0.57	0.42	0.29	0.16
	(1.64)	(1.03)	(0.76)	(0.49)	(0.03)	(0.02)	(0.02)	(0.04)	(0.42)	(0.26)	(0.19)	(0.11)
MEU	0.51	0.38	0.25	0.13	0.32	0.33	0.33	0.34	0.14	0.1	0.07	0.04
	(0.52)	(0.46)	(0.3)	(0.13)	(0.06)	(0.07)	(0.08)	(0.1)	(0.13)	(0.1)	(0.07)	(0.04)
NEU	0.44	0.44	0.31	0.23	0.44	0.47	0.5	0.52	0.15	0.14	0.1	0.07
	(0.47)	(0.4)	(0.29)	(0.19)	(0.13)	(0.13)	(0.14)	(0.14)	(0.17)	(0.12)	(0.08)	(0.05)
BEU	0.71	0.65	0.4	0.21	0.28	0.29	0.31	0.32	0.14	0.13	0.07	0.03
	(0.99)	(0.86)	(0.58)	(0.31)	(0.1)	(0.09)	(0.1)	(0.11)	(0.22)	(0.15)	(0.09)	(0.04)
SLU	1.21	1.08	0.63	0.32	0.3	0.3	0.31	0.32	0.32	0.28	0.15	0.07
	(1.24)	(1.13)	(0.6)	(0.22)	(0.05)	(0.05)	(0.06)	(0.07)	(0.35)	(0.31)	(0.15)	(0.05)
CZU	1.2	1.17	0.88	0.59	0.24	0.25	0.25	0.25	0.23	0.23	0.15	0.09
	(0.83)	(0.75)	(0.79)	(0.48)	(0.07)	(0.05)	(0.05)	(0.05)	(0.18)	(0.15)	(0.09)	(0.05)
SBC	0.65	0.41	0.29	0.16	0.32	0.33	0.35	0.37	0.18	0.11	0.08	0.04
	(0.72)	(0.45)	(0.37)	(0.13)	(0.05)	(0.03)	(0.03)	(0.03)	(0.18)	(0.11)	(0.09)	(0.03)
SCU	1.32	1.31	1.17	1.12	0.25	0.26	0.27	0.26	0.27	0.26	0.2	0.13
	(1.31)	(0.95)	(0.94)	(0.82)	(0.07)	(0.07)	(0.07)	(0.06)	(0.27)	(0.18)	(0.13)	(0.06)
SHU	0.56	0.29	0.2	0.15	0.35	0.37	0.38	0.39	0.17	0.09	0.06	0.04
	(0.77)	(0.29)	(0.19)	(0.17)	(0.08)	(0.1)	(0.1)	(0.1)	(0.23)	(0.08)	(0.05)	(0.04)
LNU	0.99	0.79	0.52	0.34	0.29	0.29	0.3	0.3	0.25	0.21	0.13	0.07
	(0.98)	(0.68)	(0.47)	(0.27)	(0.07)	(0.06)	(0.06)	(0.06)	(0.29)	(0.2)	(0.11)	(0.05)
TGU	0.56	0.46	0.31	0.18	0.3	0.3	0.32	0.34	0.11	0.1	0.07	0.04
	(0.77)	(0.47)	(0.36)	(0.14)	(0.06)	(0.05)	(0.05)	(0.05)	(0.11)	(0.09)	(0.07)	(0.03)
TCU	1.05	0.65	0.39	0.21	0.38	0.39	0.43	0.46	0.35	0.21	0.13	0.07
	(0.91)	(0.43)	(0.27)	(0.14)	(0.08)	(0.07)	(0.08)	(0.1)	(0.33)	(0.14)	(0.09)	(0.05)
Mean	0.82	0.68	0.48	0.33	0.33	0.34	0.35	0.36	0.21	0.17	0.11	0.07

Notes: Regions are abbreviated for table fit. See Figure 3.3 or Table 3.2 for definitions. Each value represents the mean value for each region, and standard deviations describe variation across circuits in each region. See Methods for definitions and relevant data sources. Each value is sub-divided into fire size classes (i.e., small, extreme). Small fires are less than 10 acres. Medium fires are 10-300 acres. Large fires are 300-5,000 acres. Extreme fires are larger than 5,000 acres.

Figure 3.5: Regional Sensitivity to Extreme Wildfire Spread

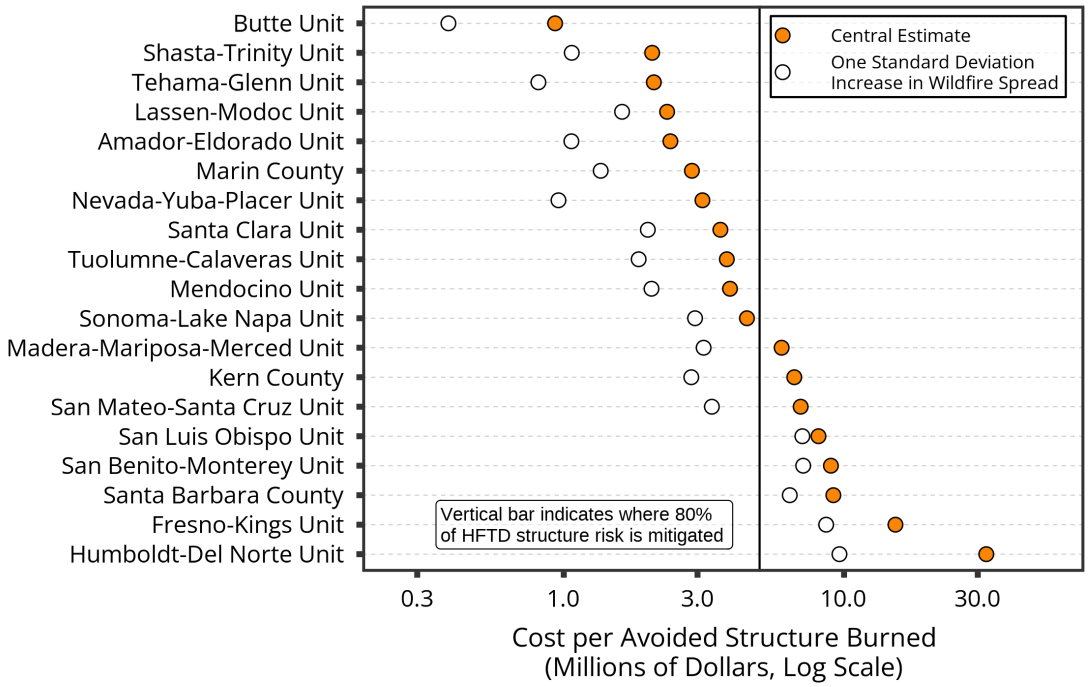

Notes: The central estimates indicate the cost per avoided structure burned at which 80% of a given region's total structure risk is mitigated. The vertical bar indicates the value across all regions. The open points denote the effect of a one standard deviation increase in extreme wildfire spread probability, where the standard deviation is measured at the circuit-month level within each region.

Figure 3.6: Regional Sensitivity to Structure Hardening

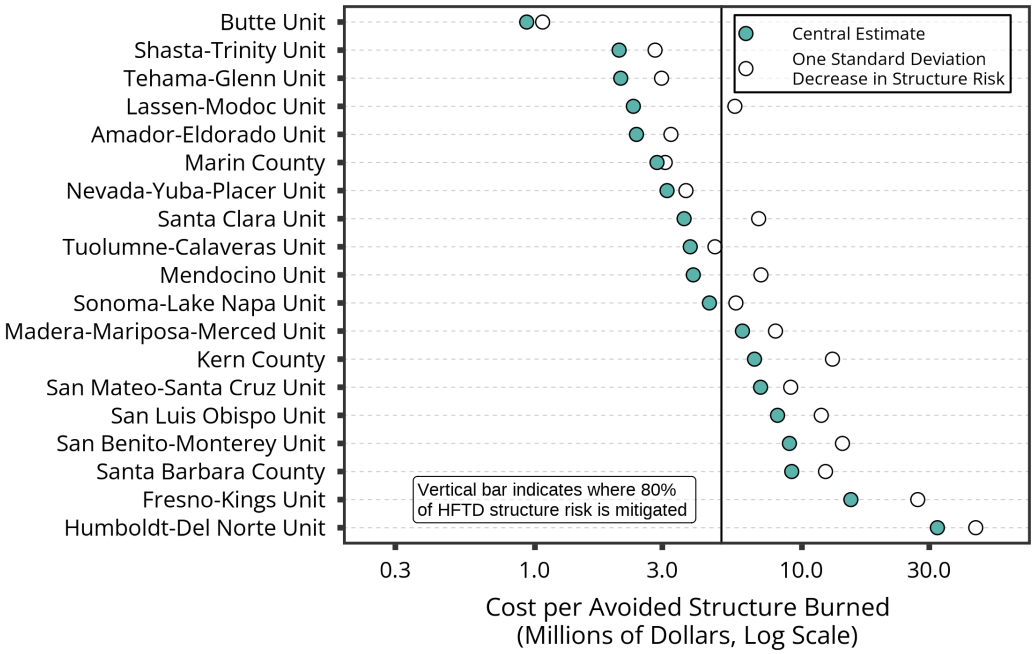

Notes: The central estimates indicate the cost per avoided structure burned at which 80% of a given region's total structure risk is mitigated. The vertical bar indicates the value across all regions. The open points denote the effect of a one standard deviation decrease in structure risk, where the standard deviation is measured at the circuit level across wildfire class sizes, sampled ignition points, and pixels intersected by wildfire class sizes. The decrease in structure risk can serve as a proxy for policies that encourage homeowners to harden their homes or maintain defensible space.

Chapter 4

Charge Anxiety: The Effect of Wildfire-Induced Electricity Outages on Battery-Electric Vehicle Adoption

4.1 Introduction

Globally, the transportation sector contributes approximately 25% of greenhouse gas emissions [93]. Widespread adoption of battery-electric vehicles (BEVs), paired with low-carbon electricity generation, plays an essential role in plans to de-carbonize the economy. The lowest-cost scenarios of the Net-Zero America study assume the electric vehicle stock grows to 96% of all light-duty vehicles by 2050 [94]. Recent policy support, such as the U.S. Inflation Reduction Act and the E.U. Net Zero Industry Act, aims to strengthen the uptake of BEVs. The International Energy Agency projects that every other car sold globally in 2035 will be electric based on today's energy, climate, and industrial policies [95].

Despite the importance of BEV adoption in achieving de-carbonization goals, barriers to widespread adoption remain. In the U.S., electric vehicle registrations grew by 40% in 2023 compared with 2022, slower in relative growth than the previous two years [95]. Two well-studied barriers to BEV adoption include range anxiety and price. Range anxiety arises from a consumer's perceived fear of completing a trip due to insufficient range or a lack of charging infrastructure along their route. Range anxiety may pose the most significant barrier to BEV adoption [96], and surveys of consumers have found that range anxiety and the presence of public charging infrastructure are important determinants of BEV purchase decisions [97–99].

High BEV purchase prices also discourage widespread adoption. In California, high-income households make up nearly 50% of early BEV adopters but only 3.6% of the population [100]. Low and middle-income households have been shown to repsond less to electric vehicle subsidies, and the top 10% of households filing taxes claim 60% of federal electric

vehicle subsidies [101, 102]. BEV manufacturers are addressing range anxiety and purchase price concerns, with average BEV ranges increasing by 75% between 2015 and 2023. Between 2018 and 2022, the average medium-sized BEV retail price fell by about 10% [95].

This study focuses on a different determinant of BEV adoption. While range anxiety and income effects are well-documented, little empirical evidence exists on the impact of electricity outages on demand for BEVs. Charge anxiety arises when a consumer fears that an electricity outage will interrupt their charging session, possibly leading to insufficient battery charge to complete a desired trip. Charge anxiety can also arise when a consumer lacks information on the reliability of public charging infrastructure. As climate change, aging infrastructure, and greater energy demand threaten to increase electricity outages [103, 104], it is critical to understand the relationship between electricity outages and BEV adoption.

To quantify the effect of charge anxiety on BEV adoption, this study uses a novel dataset on wildfire-related electricity outages in California. Wildfire-related electricity outages provide a compelling empirical setting to test the relationship between outages and BEV adoption. Unlike hurricanes or winter storms that cause outages across large portions of metropolitan areas, proactive power shutoffs to reduce wildfire ignition risk narrowly affect distinct neighborhoods depending on the locations of distribution circuits' protective devices. This means that one city block may experience an outage while a neighboring block does not.

Using data from 2015-2021 across the California's three largest electric utility service territories, this study takes advantage of quasi-experimental variation to compare electric vehicle adoption across adjacent census block groups before and after the policy was instituted to de-energize powerlines during periods of elevated wildfire risk. While the findings are specific to California, the empirical evidence suggests low-income households and ones with long commute times are influenced by electricity outages when considering the purchase of a BEV.

4.2 Background

Relevant Literature

Much of the literature on BEV adoption focuses on range anxiety, affordability, and consumer attitudes. One study shows that interactions between pro-environmental attitudes and technological interest are strong predictors of plug-in hybrid electric vehicle adoption, which may spillover to BEV adoption [105]. High levels of educational attainment, prior ownership of a hybrid vehicle, and environmentalist attitudes have also been demonstrated to explain BEV adoption [106].

The lack of empirical research on consumer behavior and attitudes toward charging qual-

ity forms an important gap in the literature. Existing studies investigate the optimal locations of charging infrastructure (as in [107] and [108]) and the optimal sizes of public charging stations (as in [109]). However, more research is needed to understand to what extent potential BEV purchasers internalize the dis-amenities of electricity outages when choosing to adopt a BEV or not. A recent field experiment in Calgary explores how financial incentives can nudge charging behavior [110], but the focus of the study is not on interruptions to charging sessions.

While this study contributes most directly to the literature on BEV adoption, it also contributes to a nascent body of literature on wildfire-related de-energization events. One study finds that climate change will lead to an increase in the population exposed to de-energization events [9]. Surveys of households affected by de-energization events find evidence of an increased willingness to adopt solar and battery storage, adopt fossil fuel backup generation, and change landscaping to mitigate wildfire risk [39, 40]. Notably, one of the surveys found that respondents who experienced a de-energization event were seven percentage points less likely to report that they planned to purchase an electric vehicle as their next vehicle. However, the authors of the study noted that this self-reported effect was only marginally statistically significant. Nevertheless, the survey results support the empirical findings of this study.

California's Powerline De-Energization Program

In recent years, prolonged periods of drought, historical fire management practices, and migration to high-hazard areas have contributed to some of California's most destructive wildfire seasons [4, 90, 91, 111]. Electricity infrastructure is responsible for nine of California's top twenty most destructive wildfires, with eight of those occurring in the last decade [112]

The California Public Utilities Commission (CPUC) first granted authority to San Diego Gas and Electric (SDG&E) to proactively de-energize its power lines due to wildfire risk in 2012 (this program is referred to as Public Power Safety Shutoffs) [113]. The utility requested the authority from the CPUC several years prior following the October 2007 Witch, Guejito, and Rice fires, which destroyed more than 1,500 homes and resulted in $5.6 billion in liabilites for SDG&E.

After destructive fires caused by electricity infrastructure in 2017, the CPUC expanded de-energization rules in July 2018 to California's two largest investor-owned utilities, Pacific Gas and Electric (PG&E) and Southern California Edison (SCE) [114]. The fundamental features of the de-energization rules include (1) a review of the reasonableness of the de-energization event, (2) requirements for reporting such events to the CPUC, and (3) requirements for notifying customers about potential de-energization events.

On October 23, 2017, SDG&E called its first de-energization event that affected residen-

tial customers, though its footprint was minimal. 60 residential customers and 31 commercial customers in the community of North Descanso lost power for a little under 48 hours. Less than two months later, SDG&E reported its first widespread de-energization event to the CPUC. One circuit lost power for six consecutive days, and all affected circuits lost power for an average of one and a half days.

PG&E proactively de-energized its first circuit nearly a year later in October 2018. This event led to approximately two million customer-hours of outages. However, the next year, the utility significantly expanded its use of PSPS, causing more than 100 million customer-hours of outages in the summer and fall of 2019. Though wildfire conditions and the number of customers served differs across each utility, SCE and SDG&E's de-energization programs resulted in fewer outage impacts in 2019, approximately five million and 1.3 million customer-hours, respectively. In 2020 and 2021, PG&E reduced the scope of its de-energization program to approximately 15 million customer-hours per year. This was in part due to natural climate variability and in part due to other wildfire mitigation efforts such as system hardening and vegetation management.

4.3 Data

Electric Vehicle Fleet Database

In partnership with the California Department of Motor Vehicles, the California Air Resources Board maintains an inventory of registered vehicles in the state. As of the end of 2021, the data contains approximately 14 million vehicle registrations in the state of which 3.1% are battery-electric vehicles [115]. This compares with 0.6% in 2015, the first year data is available. The database also tracks the registrations of plug-in hybrid electric vehicles (PHEV). In this study, plug-in hybrid electric vehicles are excluded because it is unlikely that charge anxiety plays a significant role in hybrid vehicle adoption.

The finest level of aggregation in the California Air Resources Board's fleet database is the census-block group (CBG). Census-block groups are larger in population than census blocks but finer than census tracts and the typical postal code. The U.S. Census Bureau designs CBGs to contain similar population sizes, so the area of a CBG will be larger in rural areas compared to urban areas. The average population of a CBG in California in 2021 is approximately 1,500. In 2020, the U.S. Census Bureau amended the boundaries of census-block groups as part of its decadal re-districting effort.

De-Energization Data (PSPS)

Under the CPUC's de-energization rules, electric utilities must submit reports after a wildfire-related de-energization event is called. The de-energization reports obtained from the CPUC identify de-energization events by circuit number, the time the circuit was de-energized, the

time power was restored, the total number of customers affected, and the number of residential, commercial, industrial, and medical baseline customers affected [65]

De-energization reports are matched to spatial data on the locations of distribution circuits using the name of the circuit. The locations of each utility's distribution circuits are obtained from wildfire mitigation reports that the utilities submitted in proceedings with the CPUC. In many cases, a circuit will span across multiple CBG boundaries. In these cases, de-energization events are allocated to CBGs based on the corresponding share of the circuit's length that overlaps with the CBG. This may produce some measurement error, particularly in cases where certain segments of a circuit are de-energized rather than the entire customer population served by the circuit.

Demographic Data

To complete the panel dataset, demographic characteristics obtained from the U.S. Census Bureau's American Community Survey (ACS) are merged with data on electric vehicle adoption and de-energization events. Specifically, data on race, median household income, age, educational attainment, and commute time are included.

4.4 Methods

One of the most widely used quasi-experimental estimators is the differences-in-differences estimator [116]. This estimator compares the evolution of outcomes in groups affected by a policy change against groups unaffected by the change– both before and after the policy intervention. Recent research has offered useful improvements to the standard differences-in-differences research design. Callaway and Sant'Anna (2021) propose a more flexible differences-in-differences estimator that is better equipped to handle settings where groups are exposed to the policy intervention in different time periods[117]. This approach avoids the potential pitfalls of the standard two-way fixed effects regression model.

The core mechanics of the estimator are described next in Equation 4.1. For additional detail, see [117]. The building block of the estimator is called a group-time average treatment effect. This parameter represents the effect of the policy intervention– in this case the de-energization program– for a specific treatment group G at a specific time period t. In this setting, a treatment group G refers to an annual cohort of CBGs that were all first exposed to a de-energization event in the same year g (i.e., CBGs served by PG&E that were first de-energized in 2019).

The group-time average treatment effect takes the following form:

$$ATT(g,t) = \mathrm{E}[(\frac{G_g}{\mathrm{E}[G_g]} - \frac{\frac{p(X)C}{1-p(X)}}{\mathrm{E}[\frac{p(X)C}{1-p(X)}]})(Y_t - Y_{g-1} - m_{g,t}(X))] \tag{4.1}$$

Estimating the group-time average treatment effects first requires estimating a propensity-score model. Propensity-scores, denoted $p(x)$, for control units C are then used as weights when comparing the evolution of BEV adoption in control units against treated units.

Weights for the treated and control units are then applied to the difference in electric vehicle adoption Y in year t compared to electric vehicle adoption in the year prior to de-energization exposure (Y_{g-1}). For further robustness against model misspecification, the "doubly-robust" approach leverages the fitted values from a linear regression model of electric vehicle adoption on the relevant covariates X. Hence, $m_{g,t}(x) = \mathrm{E}[Y_t - Y_{g-1}|X, C = 1]$. See [117] for additional detail.

A critical identifying assumption of the differences-in-differences model is the conditional parallel trends assumption [117, 118]. This assumption requires, in the absence of de-energization, that the electric vehicle market share of CBGs that were de-energized to have evolved similarly to control CBGs, conditional on covariates such as race, income, and commute times. The next section discusses the empirical strategy to estimate the effect of de-energization events on electric vehicle market share, including the spatial discontinuity research design, propensity-score estimation, and conditional parallel trends.

4.5 Empirical Strategy

One concern in this setting is the potential for selection bias. Specifically, if communities that were de-energized for wildfire risk exhibit different characteristics than communities that were never de-energized– and these characteristics are correlated with BEV adoption– then a naive comparison of pre- and post-BEV adoption across treated and control units may be susceptible to selection bias. As discussed in the literature review, such characteristics include household income, commute times, and other hard to measure beliefs like pro-environmental attitudes. To alleviate the potential for selection bias, the empirical strategy relies on two key features: (1) spatial discontinuity methods and (2) propensity-score weights.

Spatial Discontinuity

Spatial discontinuity methods compare the outcomes of treated and control units that are located on opposite sides of a discrete border that delineates treatment status. An advantage of using spatial discontinuity methods is that treated and control units located in close proximity to each other may share similar observable characteristics (i.e., household income, commute times) as well as difficult to observe characteristics (i.e., pro-environmental attitudes, willingness to adopt new technology) [119, 120]. However, if households can select into treatment status by observing where the discrete border is located, then spatial discontinuity methods may still be subject to selection bias.

In this setting, the spatial discontinuity approach compares BEV adoption outcomes for CBGs that were de-energized against adjacent CBGs that were never de-energized. In constructing the comparison group, the approach excludes any CBGs that do not share a border with a CBG that was de-energized. Given de-energization events are targeted to high-wildfire risk locations, this tends to exclude CBGs that are located in predominantly urban areas. Figure 4.1 illustrates an example of the spatial discontinuity research design. Throughout the rest of this article and its graphical elements, treated CBGs are referred to as "de-energized," control CBGs are referred to as "adjacent and not de-energized," and excluded CBGs are referred to as "not adjacent and not de-energized."

In the short-run, it is unlikely households observe the unique topology of their electric utility's distribution grid and subsequently make decisions on where to live on the basis of de-energization likelihood. In addition, due to the recent deployment of the de-energization program during the study period and natural variation in fire weather, it would be difficult for households to predict where each utility would call de-energization events. Therefore in the short-run, the spatial discontinuity approach offers quasi-experimental variation in de-energization status across CBGs. In the long-run, as utilities invest in more wildfire risk mitigation measures that make de-energization more predictable in specific locations, it is possible households consider the potential for de-energization when purchasing a home. However, other amenities and factors such as price are likely stronger considerations.

Propensity-Score Weighting

The second feature of the research design that alleviates selection bias is propensity-score weighting. As described previously, estimation of the group-time average treatment effects includes propensity-score weights. In general, the propensity-score describes the conditional probability of assignment to a treatment group given observed covariates [121–123]. In this setting, the propensity-score represents the probability that a CBG would be de-energized at any point during the study period conditional on demographics such as median household income, mean commute times, and educational attainment.

When estimating group-time average treatment effects, propensity-score weights assign greater weight to the outcomes of control units that have a high estimated likelihood of being de-energized but never were de-energized. This approach alleviates selection bias in the differences-in-differences estimator by prioritizing the outcomes of control units that share similar characteristics to treated units.

Propensity-scores are estimated using a machine-learning prediction model with 3-repeat 10-fold cross-validation. The target for the random forest model is a binary variable indicating if a CBG experienced a de-energization event at any time during the study period. Approximately 24% of CBGs in the three utility service territories– PG&E, SCE, and SDG&E– experienced a de-energization event during the study period. To alleviate imbalance when training the prediction the model, the data is down-sampled. CBGs in the negative class

(ones that were not de-energized) are randomly deleted from the training data such that an equal amount of positive and negative classes are included in the training data. The data is split 75% and 25% between the training and testing data.

Table 4.1 summarizes the key characteristics of the propensity-score prediction model. The model is fit separately for each utility-service territory. In the testing data, area under the receiver operating characteristic curve (AUC) values between 0.89 and 0.91 indicate the model predicts de-energization status accurately and consistently across each territory. The bottom panel of Table 4.1 shows the importance of using propensity-score weights in combination with the spatial discontinuity method. Note the propensity-scores for the adjacent and never de-energized CBGs are still lower than the de-energized CBGs. This suggests that relying on the spatial discontinuity method without propensity-score weighting may still be subject to selection bias.

Figure 4.2 shows how the combination of the spatial discontinuity approach and propensity-score weighting reduces covariate imbalance between de-energized and control CBGs. On average across the three utilities, CBGs that were de-energized tend to have a higher proportion of white households (76%). In comparison, the proportion of white households in CBGs that were not de-energized is 62%. Applying propensity-score weights and filtering to adjacent CBGs narrows this difference in the control group (74%).

In SDG&E's territory, median household income is meaningfully higher in de-energized CBGs than control CBGs ($95,000 vs. $75,000 per year). Given the important role income plays in determining electric vehicle adoption, this difference in income between treatment and control groups raises selection bias concerns. Applying the propensity-score weights and spatial discontinuity reduces this difference from $20,000 per year to $3,000 per year. In PG&E and SCE territories, median household income is also higher in de-energized CBGs, but the initial difference prior to propensity-score weighting and applying the spatial discontinuity method is smaller ($7,000 and $13,000, respectively).

Commute times are meaningfully longer when comparing de-energized CBGs against unaffected CBGs in SDG&E's territory. In the median de-energized CBG, half of households feature commute times of less than 30 minutes, while a higher two-thirds of households in unaffected CBGs feature commutes of 30 minutes or less. The longer commute times for de-energized CBGs reflects the tendency for de-energized CBGs to be located in rural and wildfire prone terrain. The empirical strategy reduces this proportion in the control group to 53% compared with 51% in the de-energized group. Given the importance of range anxiety in the BEV adoption literature, balancing commute times in the treatment and control groups is critical to alleviating selection bias concerns.

Parallel Trends

A foundational assumption to the differences-in-differences estimator is the conditional parallel trends assumption. As noted earlier, this assumption requires in the absence of de-energization that the BEV market share of CBGs that were de-energized to have evolved similarly to control CBGs, conditional on covariates. Figure 4.3 provides a visual inspection of the conditional parallel trends assumption for PG&E cohorts (cohorts are defined by initial exposure year in the first panel of Table 4.1).

Figure 4.3 shows that the conditional parallel trends assumption is unlikely to be violated for PG&E cohorts first exposed to de-energization in 2018 and 2019. For these first two cohorts, BEV market share grew at a similar pace compared with control CBGs in the years prior to de-energization. However, the conditional parallel trends assumption appears to be violated for the cohort that was first de-energized in 2020 (third panel of Figure 4.3). Between 2015 and 2018, the median CBG in this cohort had 0% BEV market share, while the control group saw positive growth during the same period. This raises concerns that the control group is not a valid comparison group for the specific set of CBGs that were de-energized in 2020 in PG&E's territory. Therefore, this treatment group is dropped from the differences-in-differences estimator. Table 4.1 shows the cohort makes up less than 1% of PG&E's de-energized CBGs.

One treatment cohort is dropped for SCE and SDG&E due to similar concerns regarding parallel trends. The CBGs that are dropped from the estimation process make up 0.1% and 7% of SCE and SDG&E's de-energized CBGs, respectively.

4.6 Results

Figures 4.4-4.6 summarize the estimated average treatment effects by electric utility, commute length, and income. A key advantage of Callaway and Sant'Anna's average treatment effect estimator is that it can be summarized flexibly across treatment groups, exposure duration, or other sources of heterogeneity. In Figure 4.4, average treatment effects are expressed as a population-weighted average across all of a utility's treated CBGs by time since de-energization, similar to an event study.

The first conclusion is that, when expressed as a population-weighted average across utilities, the effect of the de-energization policy on BEV market share is ambiguous. There is a small estimated reduction in BEV market share in PG&E and SCE territories, but the effect is not statistically significant. A portion of CBGs in PG&E's territory that have been exposed to the de-energization policy for three years (2018 cohort) show a large 40% reduction in BEV market share by the third year of exposure. This effect is clearly visible in the parallel trends plot (Figure 4.3). However, the 2018 PG&E cohort makes up 5% of the utility's de-energized CBGs, and thus may be an outlier.

The second conclusion, shown in Figure 4.5, is that the effect of the de-energization policy on BEV market share is correlated with commute time. In the first three years since experiencing a de-energization event, CBGs with the longest average commute times saw a 9-11% decrease in BEV adoption relative to CBGs in the control group. CBGs with shorter commute times, in contrast, show no statistically significant decrease in BEV adoption. This suggests that range anxiety and charge anxiety may interact in meaningful ways. Households with the longest commute times may be more reluctant to purchase a BEV if they experience electricity outages that disrupt their charging session and make it less feasible to complete a trip on a single charge.

The third conclusion, captured in Figure 4.6, is that income may also play a role in explaining how charge anxiety manifests across households. CBGs in the income bracket with the lowest median household income see a 15% reduction in BEV adoption in the first three years since experiencing a de-energization event, on average. However, the effect is not statistically significant. This effect differs markedly from CBGs in the higher income brackets, which display a 1% increase in BEV adoption in the first three years, on average. While the effects by income bracket are not statistically different from zero, they suggest lower income groups may be more sensitive to electricity outages and charge anxiety.

In the appendix, robustness tests are shown using a conventional linear regression and event-study framework. In terms of commute times, the robustness test reproduces a similar correlation between longer commute times and decreasing BEV adoption. Unlike with the group-time average treatment effect approach, this relationship is not statistically significant. See Figures B.1 and B.2.

4.7 Discussion

Widespread adoption of BEVs is largely seen as a centerpiece of efforts to decarbonize the economy and transition to net-zero. While some barriers to BEV adoption are well-documented, such as range anxiety and price, little is known about how electric service reliability may affect consumer willingness to adopt a BEV. A new policy to de-energize powerlines during periods of elevated fire risk in California provides a compelling setting to study charge anxiety. De-energization events are localized, which allows for a comparison of BEV adoption in CBGs that experienced electricity outages to adjacent CBGs that were unaffected. This spatial discontinuity research design, in combination with propensity-score weighting, creates a credible control group to evaluate BEV adoption.

A main conclusion of this study is that households with the longest commute times display the largest aversion to electricity outages and BEV adoption. These households see a 9-11% reduction in BEV adoption compared with households that did not experience a de-energization event. This suggests that households that are fearful of having sufficient range to complete their trip are also concerned about electricity outages that may disrupt

their charging session. The finding underscores the importance of a reliable electric grid and reliable charging infrastructure in achieving policy goals to decarbonize the transportation sector. Increasing the range of BEVs and deploying additional charging infrastructure can alleviate range anxiety, but addressing charge anxiety through reliable electricity service is critical, too.

A limitation of the analysis is that the potential for a reverse relationship between electric service reliability and BEV adoption is not considered. Some BEVs, notably the Ford F-150 Lightning under a partnership with Sunrun, offer bi-directional charging [124]. The technology allows BEV owners to supply power to their home during an electricity outage by using the battery-electric storage that powers the vehicle. With bi-directional charging, some households that face frequent electricity outages may prefer BEV ownership over an ICE vehicle. Given the limited amount of BEV models that currently offer the technology, it is unlikely that this relationship is meaningful during the study period. However, future research should seek to better understand the role bi-directional charging can play for households that face frequent electricity outages.

Another related limitation is that the presence of home battery-electric storage systems or other forms of backup generation are not accounted for. Households with access to backup generation may be less concerned about electricity outages when choosing to purchase a BEV.

The second finding of this analysis is that income may explain some heterogeneity in charge anxiety across households. While the results are not statistically significant, lower income households show an estimated 15% reduction in BEV adoption, on average, compared with households that were not de-energized. A possible explanation is that higher income households may be more likely to own additional vehicles per household. Access to a second vehicle, especially an ICE vehicle, would reduce concerns over charge anxiety. Another explanation is that systematic issues related to energy poverty and affordability may make lower income households more sensitive to interruptions to their charging session that disrupt travel. This finding speaks to well-established concerns that the most vulnerable socio-economic groups may bear the greatest costs of adapting to climate change [125].

Lastly, it is worth underscoring that the analysis does not offer a cost-benefit test of the de-energization program. Despite the conclusions that such proactive electricity outages reduce BEV adoption, reducing wildfire ignitions can provide substantial benefits in terms of avoided structure damages, fatalities, ecosystem impacts, and more. Rather, the findings emphasize the difficult trade-offs in the electric power sector between adapting to the heightened risks of climate change, such as wildfire, and pursuing deep de-carbonization goals. The long-run effects of new operational strategies that reduce wildfire risk at the expense of grid reliability need to be carefully studied to ensure harmony with electrification policies.

4.8 Figures and Tables

Figure 4.1: Spatial Discontinuity

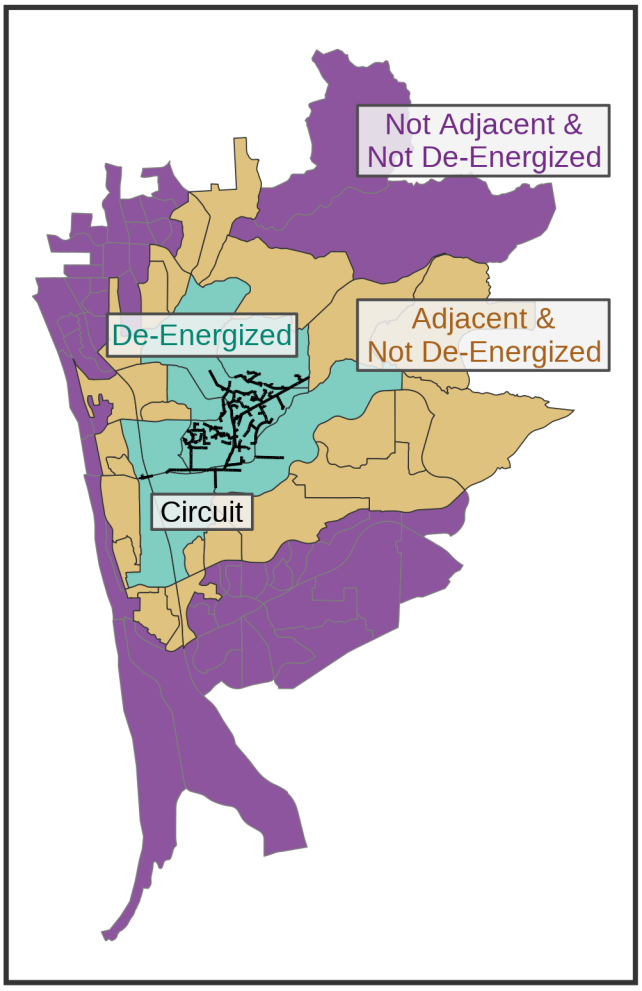

Notes: This map provides an example to visualize the spatial discontinuity method. It depicts one circuit that was de-energized and the census block groups (CBGs) that are intersected by the circuit. In addition, the map shows adjacent CBGs that were not affected by de-energization events. These adjacent CBGs are used as controls in the differences-in-differences estimator, in combination with propensity-score weights. CBGs that are not adjacent to a de-energized CBG (shown in purple) are excluded from the estimation.

Table 4.1: Propensity-Score Estimation

	PG&E	SCE	SDG&E
Number of CBGs De-Energized by Initial Exposure Year			
2017	-	-	22
2018	204	2	118
2019	3,642	563	63
2020	40	455	109
2021	197	320	-
CBGs De-Energized	4,083	1,340	312
All CBGs Never De-Energized	6,667	9,298	2,277
Adjacent CBGs Never De-Energized	1,845	1,290	351
Propensity-Score Model			
True Positive Rate	81%	83%	87%
False Positive Rate	16%	22%	18%
AUC	0.90	0.89	0.91
Mean Propensity-Score			
CBGs De-Energized	0.85	0.84	0.86
	(0.15)	(0.14)	(0.14)
All CBGs Never De-Energized	0.21	0.31	0.28
	(0.17)	(0.21)	(0.21)
Adjacent CBGs Never De-Energized	0.27	0.48	0.40
	(0.20)	(0.22)	(0.24)

Figure 4.2: Covariate Balance

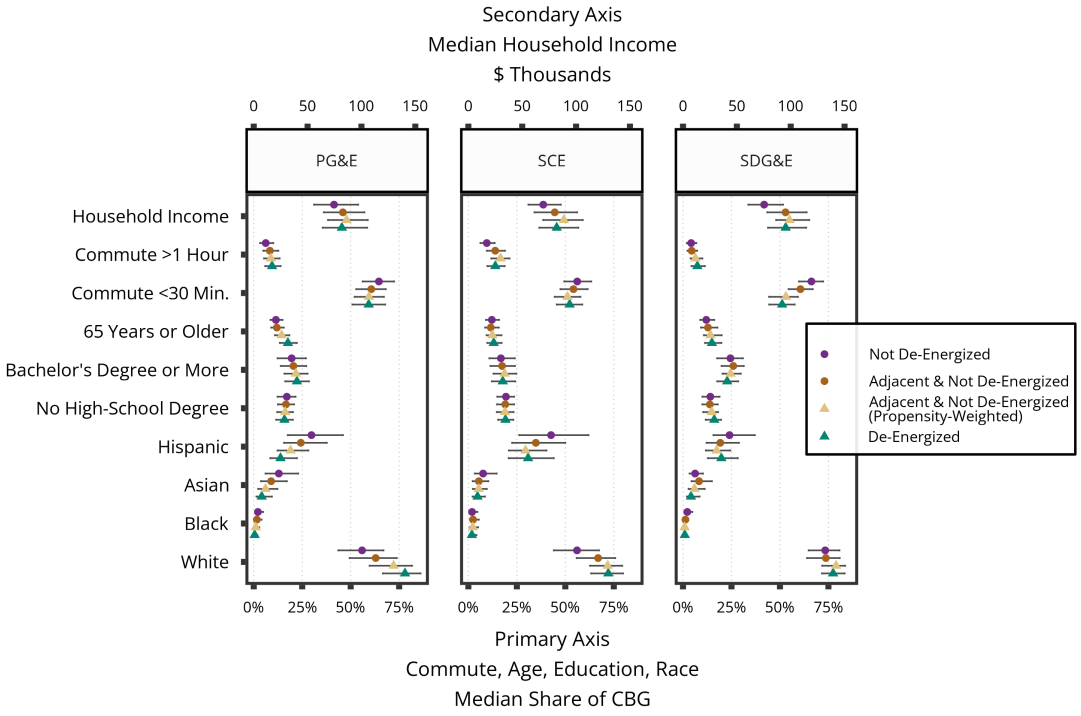

Notes: The plot shows how the spatial discontinuity method and propensity-score weighting alleviate covariate imbalance between de-energized CBGs and control CBGs.

Figure 4.3: Conditional Parallel Trends for PG&E Cohorts

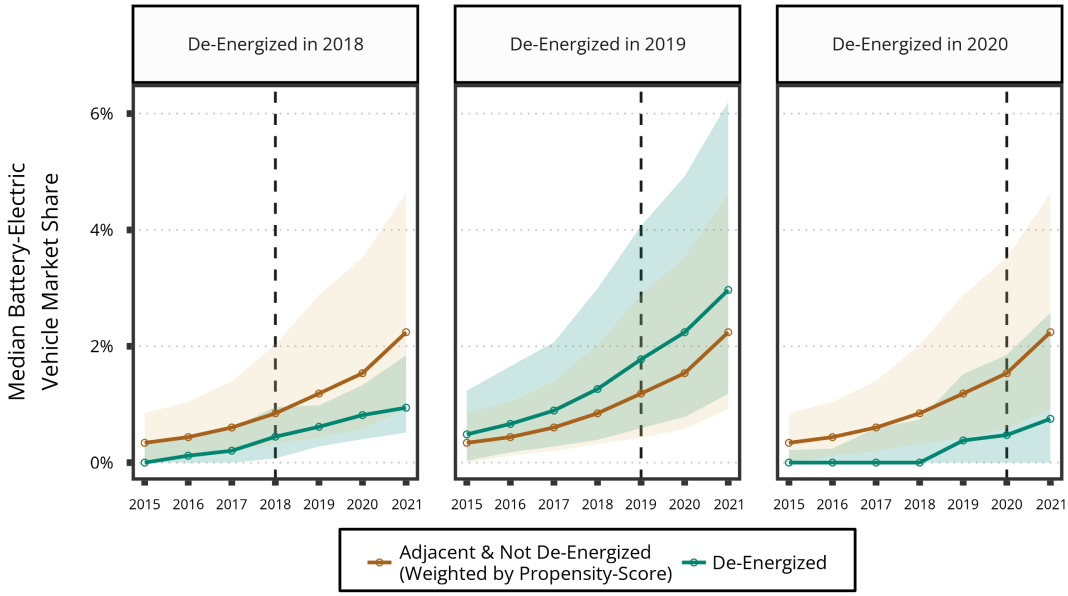

Notes: Shaded area represents interquartile range. Dashed lines indicate the first year each cohort experienced a de-energization event. The cohort that was first de-energized in 2020 (rightmost panel) is dropped from the differences-in-differences estimator due to concerns over violation of the conditonal parallel trends assumption.

Figure 4.4: Average Treatment Effect by Utility

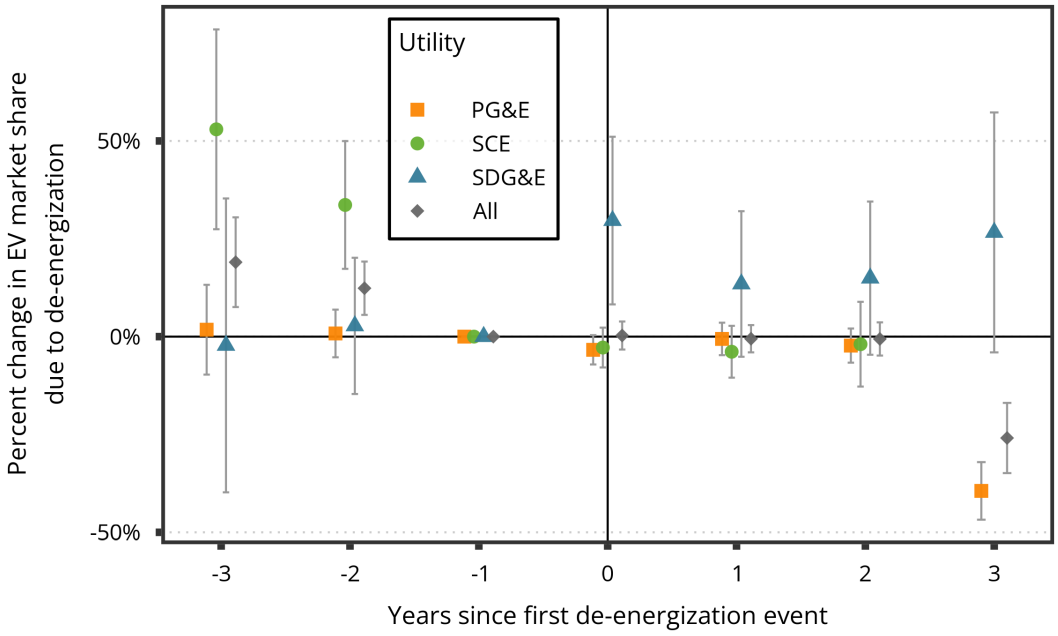

Notes: Error bars represent 95% confidence intervals.

Figure 4.5: Average Treatment Effect by Commute Length

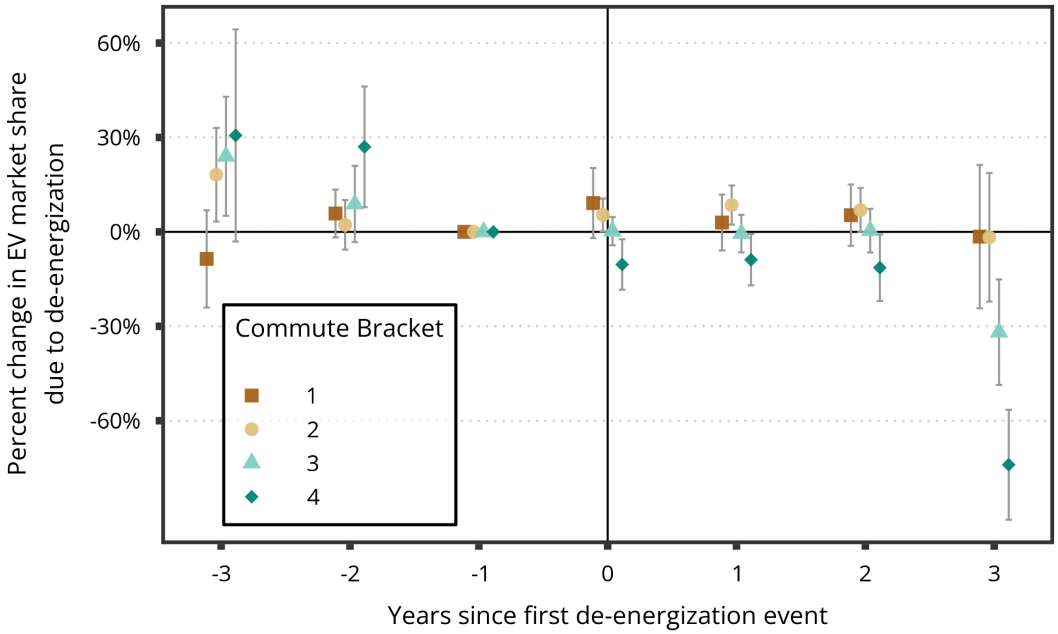

Notes: Commute brackets are expressed as quartiles. The first quartile represents CBGs with the shortest commute times, and the fourth quartile represents CBGs with the longest commute times. Error bars represent 95% confidence intervals.

Figure 4.6: Average Treatment Effect by Income Bracket

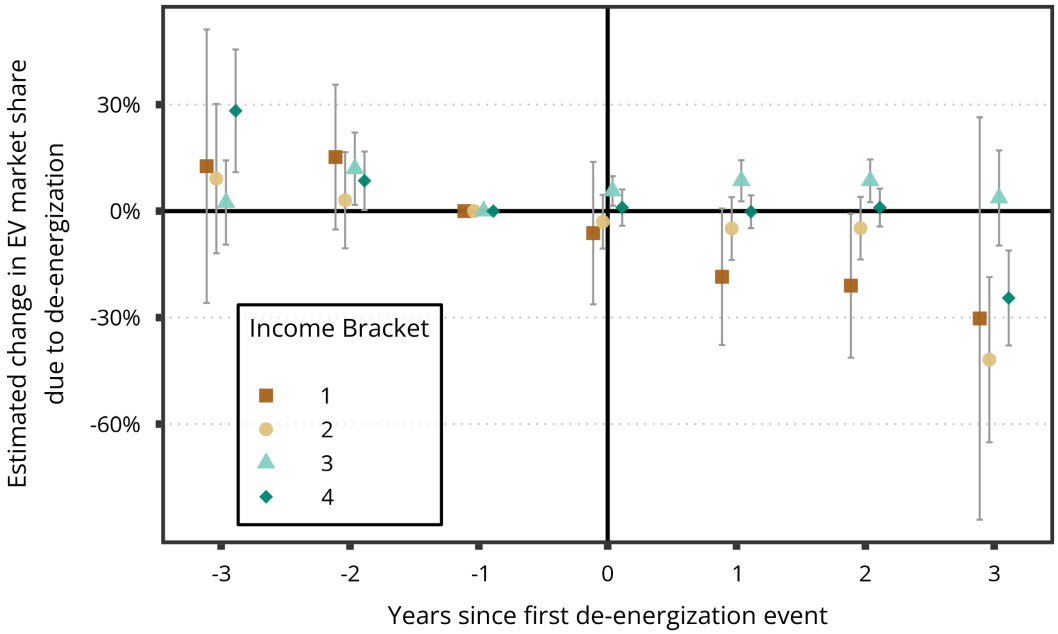

Notes: Income brackets are expressed as quartiles. The first quartile represents CBGs with the lowest median household income, and the fourth quartile represents CBGs with the highest median household income. Error bars represent 95% confidence intervals.

Chapter 5

Conclusion

Adapting to climate change presents significant economic and environmental challenges. This dissertation is guided by the critical question of "*what policies and investments can lead us to cost-effectively adapt to wildfire risk?*" In exploring this question, I focus on the electric power sector because its role is two-fold. It is both a critical agent in the push to de-carbonize the economy and it is responsible for a disproportionate share of the losses from catastrophic wildfire outcomes.

To reduce the losses from catastrophic wildfire, policymakers and communities need detailed assessments of the costs and benefits of adaptation strategies. A key contribution of the work presented in the preceding chapters is the rigorous measurement of the cost-effectiveness of electric power sector wildfire adaptation investments. The results of this cost-effectiveness analysis reveal that dynamic strategies to manage and operate the distribution grid during periods of elevated fire risk present promising opportunities to lower risk.

Fast-trip settings are one of these operational techniques. Their rapid and successful deployment across the distribution grid during the study period highlights the role of innovation in adapting to climate change. As the distribution grid is being upgraded to accommodate new controllable electric loads, including home battery systems and electric vehicles, a rare opportunity exists to coordinate innovation across electrification efforts and wildfire risk mitigation strategies.

Chapter 2 demonstrates that innovative ways to operate the distribution grid can significantly reduce the capital investment needed to achieve a given risk reduction. This finding is critical, not only for jurisdictions where adaptation strategies are well under-way, but also for jurisdictions that have yet to comprehensively assess their risk exposure. Fast-trip settings, for example, require little upfront capital investment and can be scaled quickly across the distribution grid. Thus, the benefits of operational strategies are two-headed: they can reduce capital costs and scale quickly.

Chapter 3 dives deeper into the uncertainty surrounding capital-intensive system hardening measures. Innovation is not limited to grid management and operations; future technology could improve the costs of burying powerlines underground. The analysis shows that system hardening measures with long lifespans (i.e., underground powerlines) are subject to significant uncertainty regarding their intended risk reduction benefits. Forecasted reductions in unit costs deliver improvements to cost-effectiveness, but a host of other factors drive uncertainty. For example, the amount of fuel treatments or the amount of structure hardening that property owners invest in can substantially affect the returns on electric power sector adaptation investments. This conclusion points to the need for cross-sector coordination when deploying capital-intensive adaptation strategies. Failure to do so could lead to the "stranded assets" problem, in which system hardening investments perform below their intended risk reduction goals and leave the customer base with higher costs.

Chapter 4 departs from the previous two and focuses on the possible unintended consequences of grid protocols that de-energize powerlines during periods of elevated risk. The chapter addresses how degrading grid reliability could affect a consumer's decision to adopt a battery-electric vehicle. This question is critical because innovative grid management techniques reduce wildfire risk but can come with the important caveat that they cause customers to lose power. The results of the analysis provide suggestive evidence that electricity outages have slowed the pace of battery-electric vehicle adoption among potential adopters with long commute times and in low-income locations. Despite the cost-effectiveness advantages operational mitigations present, the additional economic toll they enact on vulnerable population segments needs to be accounted for.

Many open questions remain on the topic of adapting to wildfire risk, both within the electric power sector and collectively across sectors. First, what role do we envision the electric power sector playing in the future wildfire risk adaptation regime? Currently, the electric power sector causes a disproportionate share of wildfire losses in California, but it also carries the largest weight in terms of adaptation investments. Part of the reason is that electric utilities are held financially liable for wildfire losses, even if those wildfire losses hinge on the effectiveness of adaptation investments outside of the power sector. Another explanation is that rate of return regulation encourages utilities to deploy capital-intensive investments due to favorable returns the utilities can accrue. Looking ahead, adaptation investments need to be pursued across sectors and stakeholders to avoid being concentrated in one sector.

A related question focuses on the future of the electric utility business model as it simultaneously adapts to wildfire risk and transforms itself to accommodate intermittent, low-carbon generation and growing electric loads. Historically, electric utilities have prioritized electric service reliability and financed growth through capital projects and its customer base. What changes to the traditional electric utility business model are needed to rise to these challenges? Is a new business model needed to ensure customers are not left with the rising costs of wildfire adaptation? Pairing distributed energy resources (DERs) at the

customer level with innovative grid management techniques could achieve dual adaptation and electrification goals.

Outside of the electric power sector, questions remain on what policies can encourage sustainable co-existence with fire. Answering these questions fundamentally requires an interdisciplinary approach. Adapting to wildfire is a complex natural resource management problem. Therefore, effective policy-making requires research from a range of disciplines– including ecologists and economists. The research community should prioritize interdisciplinary approaches when evaluating wildfire risk, management, and policy.

The long-term incidence of catastrophic wildfire also remains an open question. For example, how have the burdens of catastrophic fires in Paradise, CA or Lahaina, HI been distributed across socio-economic groups? What can be learned from the responses of socio-economic groups to catastrophic wildfire outcomes? Does the economy experience a short-run shock, or are there long-run disruptions or migrations to less risky areas? In studying the long-run impacts of catastrophic wildfires, much can be learned about how communities adapt to extreme climate shocks and consequently what policies can support adaptation.

The findings presented throughout this dissertation and the open questions above suggest one overarching point of emphasis: cross-sector collaboration is crucial in adapting to wildfire. The benefits of electric power sector adaptation depend fundamentally on the amount of adaptation outside of the electric power sector. Policymakers, electric utilities, forest managers, wildfire professionals, and academic researchers all should strive to develop and measure risk reduction goals in concert. Aided by rigorous measurement of wildfire risk, credible empirical data on adaptation investments, and sound policy-making, collaboration across stakeholders can deliver a landscape and an economy that is well-adapted to wildfire.

Bibliography

1. Westerling, A. L., Hidalgo, H. G., Cayan, D. R. & Swetnam, T. W. Warming and Earlier Spring Increase Western U.S. Forest Wildfire Activity. *Science* **313.** https://www.science.org/doi/10.1126/science.1128834 (Aug. 2006).
2. Westerling, A. L. Increasing western US forest wildfire activity: sensitivity to changes in the timing of spring. *Philosophical Transactions of the Royal Society B: Biological Sciences* **371.** Publisher: Royal Society, 20150178. https://royalsocietypublishing.org/doi/10.1098/rstb.2015.0178 (June 2016).
3. Higuera, P. E. & Abatzoglou, J. T. Record-setting climate enabled the extraordinary 2020 fire season in the western United States. en. *Global Change Biology* **27.** _eprint: https://onlinelibrary.wiley.com/doi/pdf/10.1111/gcb.15388, 1–2. ISSN: 1365-2486. https://onlinelibrary.wiley.com/doi/abs/10.1111/gcb.15388 (2021).
4. Radeloff, V. C. *et al.* Rapid growth of the US wildland-urban interface raises wildfire risk. *Proceedings of the National Academy of Sciences* **115.** Publisher: Proceedings of the National Academy of Sciences, 3314–3319. https://www-pnas-org.libproxy.berkeley.edu/doi/10.1073/pnas.1718850115 (Mar. 2018).
5. *Fire in California's Ecosystems* 2nd ed. en (eds Wagtendonk, J. W. v. *et al.*) ISBN: 978-0-520-28683-2 (June 2018).
6. Balch, J. K. *et al.* Human-started wildfires expand the fire niche across the United States. *Proceedings of the National Academy of Sciences* **114.** Publisher: Proceedings of the National Academy of Sciences, 2946–2951. https://www.pnas.org/doi/10.1073/pnas.1617394114 (Mar. 2017).
7. California Council on Science and Technology. *The Costs of Wildfire in California: An Independent Review of Scientific and Technical Information* tech. rep. (Oct. 2020). https://ccst.us/reports/the-costs-of-wildfire-in-california/.
8. Keeley, J. E., Syphard, A. D., Keeley, J. E. & Syphard, A. D. Historical patterns of wildfire ignition sources in California ecosystems. en. *International Journal of Wildland Fire* **27.** Publisher: CSIRO PUBLISHING, 781–799. ISSN: 1448-5516, 1448-5516. https://www.publish.csiro.au/wf/WF18026 (Nov. 2018).

9. Abatzoglou, J. T., Smith, C. M., Swain, D. L., Ptak, T. & Kolden, C. A. Population exposure to pre-emptive de-energization aimed at averting wildfires in Northern California. en. *Environmental Research Letters* **15.** Publisher: IOP Publishing, 094046. ISSN: 1748-9326. https://dx.doi.org/10.1088/1748-9326/aba135 (Aug. 2020).
10. Jazebi, S., De Leon, F. & Nelson, A. Review of Wildfire Management Techniques—Part I: Causes, Prevention, Detection, Suppression, and Data Analytics. en. *IEEE Transactions on Power Delivery* **35,** 430–439. ISSN: 0885-8977, 1937-4208. https://ieeexplore.ieee.org/document/8768218/ (Feb. 2020).
11. Pacific Gas and Electric Company. *2023-2025 Wildfire Mitigation Plan R1* tech. rep. (Apr. 2023).
12. Southern California Edison. *2023-2025 Wildfire Mitigation Plan* tech. rep. (Mar. 2023).
13. San Diego Gas & Electric. *2023-2025 Wildfire Mitigation Plan* tech. rep. (Oct. 2023).
14. Eric Macomber, Michael Wara & Michael Mastrandrea. *Wildfire: Assessing and Quantifying Risk Exposure and Mitigation Across Western Utilities* tech. rep. (Woods Institute for the Environment, May 2024).
15. First Street Foundation. *The fastest growing economic climate risk - wildfire* Aug. 2021. https://firststreet.org/research-library/the-fastest-growing-economic-climate-risk---wildfire.
16. Collins, K. M., Penman, T. D. & Price, O. F. Some Wildfire Ignition Causes Pose More Risk of Destroying Houses than Others. en. *PLOS ONE* **11.** Publisher: Public Library of Science, e0162083. ISSN: 1932-6203. https://journals.plos.org/plosone/article?id=10.1371/journal.pone.0162083 (Sept. 2016).
17. California Public Utilities Commission. *Fire Ignition Data* https://www.cpuc.ca.gov/industries-and-topics/wildfires.
18. Fortin, J. & Hassan, A. Death Toll of Maui Wildfire Rises to 101. en-US. *The New York Times.* ISSN: 0362-4331. https://www.nytimes.com/article/maui-wildfire-victims.html (Feb. 2024).
19. Smith, M. Maui Officials Blame Utility for Allowing Deadly Fire to Start. en-US. *The New York Times.* ISSN: 0362-4331. https://www.nytimes.com/2023/08/24/us/hawaii-lahaina-fire-lawsuit.html (Aug. 2023).
20. United Nations Environment Programme. *Adaptation Gap Report 2023: Underfinanced. Underprepared. Inadequate investment and planning on climate adaptation leaves world exposed* tech. rep. (United Nations Environment Programme, 2023). https://www.unep.org/adaptation-gap-report-2023.
21. Bhandary, R. R., Gallagher, K. S. & Zhang, F. Climate finance policy in practice: a review of the evidence. *Climate Policy* **21.** Publisher: Taylor & Francis _eprint: https://doi.org/10.1080/14693062.2020.1871313, 529–545. ISSN: 1469-3062. https://doi.org/10.1080/14693062.2020.1871313 (Apr. 2021).

22. Otto, I. M. *et al.* Social tipping dynamics for stabilizing Earth's climate by 2050. *Proceedings of the National Academy of Sciences* **117.** Publisher: Proceedings of the National Academy of Sciences, 2354–2365. https://www.pnas.org/doi/full/10.1073/pnas.1900577117 (Feb. 2020).

23. Allen, M. R. *et al.* Net Zero: Science, Origins, and Implications. en. *Annual Review of Environment and Resources* **47.** Publisher: Annual Reviews, 849–887. ISSN: 1543-5938, 1545-2050. https://www.annualreviews.org/content/journals/10.1146/annurev-environ-112320-105050 (Oct. 2022).

24. Auffhammer, M. Climate Adaptive Response Estimation: Short and long run impacts of climate change on residential electricity and natural gas consumption. *Journal of Environmental Economics and Management* **114,** 102669. ISSN: 0095-0696. https://www.sciencedirect.com/science/article/pii/S0095069622000432 (July 2022).

25. Jaglom, W. S. *et al.* Assessment of projected temperature impacts from climate change on the U.S. electric power sector using the Integrated Planning Model®. *Energy Policy* **73,** 524–539. ISSN: 0301-4215. https://www.sciencedirect.com/science/article/pii/S0301421514002675 (Oct. 2014).

26. Rose, S. *Understanding the Social Cost of Carbon: A Technical Assessment* en. Tech. rep. (Electric Power Research Institution, 2014).

27. Davis, L. W. & Gertler, P. J. Contribution of air conditioning adoption to future energy use under global warming. *Proceedings of the National Academy of Sciences* **112.** Publisher: Proceedings of the National Academy of Sciences, 5962–5967. https://www.pnas.org/doi/10.1073/pnas.1423558112 (May 2015).

28. Gabriel Petek. *The 2022-23 Budget: Wildfire and Forest Resilience Package* tech. rep. (Legislative Analyst's Office (LAO), Jan. 2022).

29. U.S. Department of Agriculture. *Fiscal Year 2025 Budget Justification* tech. rep. (Mar. 2024).

30. Baylis, P. & Boomhower, J. The Economic Incidence of Wildfire Suppression in the United States. en. *American Economic Journal: Applied Economics* **15,** 442–473. ISSN: 1945-7782. https://www.aeaweb.org/articles?id=10.1257/app.20200662 (Jan. 2023).

31. Baylis, P. W. & Boomhower, J. Mandated vs. Voluntary Adaptation to Natural Disasters: The Case of U.S. Wildfires. *National Bureau of Economic Research. Working Paper Series* https://www.nber.org/papers/w29621 (Dec. 2021).

32. Plantinga, A. J., Walsh, R. & Wibbenmeyer, M. Priorities and Effectiveness in Wildfire Management: Evidence from Fire Spread in the Western United States. *Journal of the Association of Environmental and Resource Economists* **9.** Publisher: The University of Chicago Press, 603–639. ISSN: 2333-5955. https://www.journals.uchicago.edu/doi/full/10.1086/719426 (July 2022).

33. Miller, R. K., Field, C. B. & Mach, K. J. Barriers and enablers for prescribed burns for wildfire management in California. en. *Nature Sustainability* **3.** Publisher: Nature Publishing Group, 101–109. ISSN: 2398-9629. https://www.nature.com/articles/s41893-019-0451-7 (Feb. 2020).

34. Boomhower, J. Adapting to growing wildfire property risk. *Science* **382.** Publisher: American Association for the Advancement of Science, 638–641. https://www.science.org/doi/abs/10.1126/science.adk7118 (Nov. 2023).

35. Larsen, P. H. A method to estimate the costs and benefits of undergrounding electricity transmission and distribution lines. *Energy Economics* **60,** 47–61. ISSN: 0140-9883. https://www.sciencedirect.com/science/article/pii/S0140988316302493 (Nov. 2016).

36. Wang, Z., Wara, M., Majumdar, A. & Rajagopal, R. Local and utility-wide cost allocations for a more equitable wildfire-resilient distribution grid. en. *Nature Energy* **8.** Number: 10 Publisher: Nature Publishing Group, 1097–1108. ISSN: 2058-7546. http://www.nature.com/articles/s41560-023-01306-8 (Oct. 2023).

37. Taylor, W. O., Watson, P. L., Cerrai, D. & Anagnostou, E. A Statistical Framework for Evaluating the Effectiveness of Vegetation Management in Reducing Power Outages Caused during Storms in Distribution Networks. en. *Sustainability* **14.** Number: 2 Publisher: Multidisciplinary Digital Publishing Institute, 904. ISSN: 2071-1050. https://www.mdpi.com/2071-1050/14/2/904 (Jan. 2022).

38. Malloy, C. *The Consequences of Wildfire Liability for Firm Precaution: Evidence from Power Shutoffs in California* en. 2024. https://www.ssrn.com/abstract=4780392.

39. Mildenberger, M., Howe, P. D., Trachtman, S., Stokes, L. C. & Lubell, M. The effect of public safety power shut-offs on climate change attitudes and behavioural intentions. en. *Nature Energy* **7.** Number: 8 Publisher: Nature Publishing Group, 736–743. ISSN: 2058-7546. http://www.nature.com/articles/s41560-022-01071-0 (Aug. 2022).

40. Wong-Parodi, G. When climate change adaptation becomes a "looming threat" to society: Exploring views and responses to California wildfires and public safety power shutoffs. *Energy Research & Social Science* **70,** 101757. ISSN: 2214-6296. https://www.sciencedirect.com/science/article/pii/S2214629620303327 (Dec. 2020).

41. Mitchell, J. W. Analysis of utility wildfire risk assessments and mitigations in California. *Fire Safety Journal* **140,** 103879. ISSN: 0379-7112. https://www.sciencedirect.com/science/article/pii/S0379711223001479 (Oct. 2023).

42. Vazquez, D. A. Z., Qiu, F., Fan, N. & Sharp, K. Wildfire Mitigation Plans in Power Systems: A Literature Review. *IEEE Transactions on Power Systems* **37.** Conference Name: IEEE Transactions on Power Systems, 3540–3551. ISSN: 1558-0679. https://ieeexplore-ieee-org.libproxy.berkeley.edu/document/9677975 (Sept. 2022).

43. California Public Utilities Commission. *Protective Equipment and Device Settings (PEDS)* https://www.cpuc.ca.gov/industries-and-topics/wildfires/protective-equipment-device-settings.

44. Ivan Penn. PG&E, Troubled California Utility, Emerges From Bankruptcy. en-US. *The New York Times.* ISSN: 0362-4331. https://www.nytimes.com/2020/07/01/business/energy-environment/pge-bankruptcy-ends.html (July 2020).

45. Pacific Gas and Electric Company. *System Hardening & Undergrounding* https://www.pge.com/en/outages-and-safety/safety/community-wildfire-safety-program/system-hardening-and-undergrounding.html.

46. Blunt, K. *PG&E Wins Approval to Bury More Than 1,200 Miles of Power Lines* en-US. Section: US. Nov. 2023. https://www.wsj.com/us-news/climate-environment/pg-e-wins-approval-to-bury-more-than-1-200-miles-of-power-lines-3ab460d4.

47. Pacific Gas and Electric Company. *2023 General Rate Case Exhibit (PG&E-4) Electric Distribution Workpapers Supporting Prepared Testimony Chapters 2-13* tech. rep. Application 21-06-021 (June 2021).

48. California Public Utilities Commission. *Decision on Test Year 2023 General Rate Case of Pacific Gas and Electric Company* tech. rep. Application 21-06-021 (Sept. 2023).

49. Yao, M., Bharadwaj, M., Zhang, Z., Jin, B. & Callaway, D. S. Predicting electricity infrastructure induced wildfire risk in California. en. *Environmental Research Letters* **17.** Publisher: IOP Publishing, 094035. ISSN: 1748-9326. https://dx.doi.org/10.1088/1748-9326/ac8d18 (Sept. 2022).

50. DW Hosmer & S Lemeshow. *Applied Logistic Regression* 2nd (New York, NY, 2000).

51. Pozzolo, A. D., Caelen, O., Johnson, R. A. & Bontempi, G. *Calibrating Probability with Undersampling for Unbalanced Classification* in *2015 IEEE Symposium Series on Computational Intelligence* (Dec. 2015), 159–166. http://ieeexplore.ieee.org/document/7376606.

52. Mark Filip. *Re: Information Request Regarding Monitor Team Field Inspections* Oct. 2020. https://www.courthousenews.com/wp-content/uploads/2020/10/PGEMonitor10202020.pdf.

53. California Public Utilities Commission. *Resolution M-4852: Placing Pacific Gas and Electric Company Into Step 1 of the "Enhanced Oversight and Enforcement Process" Adopted in Decision 20-05-053* tech. rep. (Apr. 2021).

54. Lazar, J., Chernick, P., Marcus, W. & LeBel, M. *Electric Cost Allocation for a New Era: A Manual* en. Tech. rep. (Regulatory Assistance Project (RAP), Jan. 2020).

55. California Public Utilities Commission. *Historical Electric Cost Data* https://www.cpuc.ca.gov/industries-and-topics/electrical-energy/electric-costs/historical-electric-cost-data.

56. Karl Dunkle Werner & Stephen Jarvis. *Rate of Return Regulation Revisited* tech. rep. (Energy Institute at Haas Working Paper, Aug. 2023). https://haas.berkeley.edu/wp-content/uploads/WP329.pdf.

57. Averch, H. & Johnson, L. L. Behavior of the Firm Under Regulatory Constraint. *The American Economic Review* **52.** Publisher: American Economic Association, 1052–1069. ISSN: 0002-8282. http://www.jstor.org/stable/1812181 (1962).

58. Abatzoglou, J. T. Development of gridded surface meteorological data for ecological applications and modelling. en. *International Journal of Climatology* **33.** _eprint: https://onlinelibrary.wiley.com/doi/pdf/10.1002/joc.3413, 121–131. ISSN: 1097-0088. https://www.climatologylab.org/gridmet.html (2013).

59. Mesowest, University of Utah. *RAWS Weather Station Network* https://mesowest.utah.edu/.

60. *gridMET*

61. U.S. Department of Agriculture & U.S. Department of the Interior. *LANDFIRE* https://landfire.gov/index.php.

62. Pacific Gas and Electric Company. *Attachments to 2020 Wildfire Mitigation Plan ("EDGIS2-12.gdb")* https://www.pge.com/en/outages-and-safety/safety/community-wildfire-safety-program.html.

63. California Public Utilities Commission. *Fire-Threat Maps and Fire-Safety Rulemaking* https://www.cpuc.ca.gov/industries-and-topics/wildfires/fire-threat-maps-and-fire-safety-rulemaking.

64. Pacific Gas and Electric Company. *2023 Wildfire Mitigation Plan Discovery WMP-Discovery2023_DR_SPD_004-Q001Atch01* May 2023.

65. California Public Utilities Commission. *Utility Company PSPS Reports: Post-Event, Post-Season and Pre-Season* https://www.cpuc.ca.gov/consumer-support/psps/utility-company-psps-reports-post-event-and-post-season.

66. Pacific Gas and Electric Company. *2023 Wildfire Mitigation Plan Appendix D ACI PG&E-22-32_Atch01_Redacted* Mar. 2023.

67. Pacific Gas and Electric Company. *2023 Wildfire Mitigation Plan Discovery WMP-Discovery2023_DR_MGRA_002-Q008Atch01* Apr. 2023.

68. Pacific Gas and Electric Company. *2022 Wildfire Mitigation Plan Discovery WMP-Discovery2022_DR_MGRA_002-Q01Atch01* Mar. 2022.

69. Pacific Gas and Electric Company. *2022 Wildfire Mitigation Plan Discovery WMP-Discovery2022_DR_MGRA_002-Q02* Mar. 2022.

70. Pacific Gas and Electric Company. *2020 Wildfire Mitigation Plan Supplemental Data Request 3.4 Table 7 Veg* 2020.

71. Pacific Gas and Electric Company. *2021 Wildfire Mitigation Plan Discovery WildfireMitigationPlans_DR_CalAdvocates_035-Q04-Atch01* Feb. 2021.

72. Pacific Gas and Electric Company. *2022 Wildfire Mitigation Plan Discovery WMP-Discovery2022_DR_MGRA_002-Q16Atch01* Mar. 2022.

73. Pacific Gas and Electric Company. *2023 Wildfire Mitigation Plan Discovery WMP-Discovery2023_DR_CalAdvocates_006-Q003Atch01* Mar. 2023.

74. Pacific Gas and Electric Company. *2023 Wildfire Mitigation Plan Discovery WMP-Discovery2023_DR_CalAdvocates_003-Q001Atch01* Mar. 2024.

75. Pacific Gas and Electric Company. *2023 General Rate Case Exhibit (PG&E-4) Electric Distribution Chapters 1-6* tech. rep. Application 21-06-021 (Feb. 2022).

76. Ariel Jacoby. BURNING DOWN THE HOUSE: ANALYZING CALIFORNIA'S INVERSE CONDEMNATION STRICT LIABILITY RULE FOR UTILITY-CAUSED WILDFIRES. *Southern California Interdisciplinary Law Journal* **31** (Feb. 2022).

77. Boomhower, J., Fowlie, M. & Plantinga, A. J. Wildfire Insurance, Information, and Self-Protection. en. *AEA Papers and Proceedings* **113,** 310–315. ISSN: 2574-0768. https://www.aeaweb.org/articles?id=10.1257/pandp.20231104 (May 2023).

78. Bos, K. & Gupta, J. Stranded assets and stranded resources: Implications for climate change mitigation and global sustainable development. *Energy Research & Social Science* **56,** 101215. ISSN: 2214-6296. https://www.sciencedirect.com/science/article/pii/S2214629618305383 (Oct. 2019).

79. Rode, D. C., Fischbeck, P. S. & Páez, A. R. The retirement cliff: Power plant lives and their policy implications. *Energy Policy* **106,** 222–232. ISSN: 0301-4215. https://www.sciencedirect.com/science/article/pii/S0301421517302136 (July 2017).

80. Pfeiffer, A., Hepburn, C., Vogt-Schilb, A. & Caldecott, B. Committed emissions from existing and planned power plants and asset stranding required to meet the Paris Agreement. en. *Environmental Research Letters* **13.** Publisher: IOP Publishing, 054019. ISSN: 1748-9326. https://dx.doi.org/10.1088/1748-9326/aabc5f (May 2018).

81. Caldecott, B., Tilbury, J. & Yuge, M. Stranded Down Under? Environment-related factors changing China's demand for coal and what this means for Australian coal assets. en. *Stranded Down Under?* ISBN: 9780992761806 Publisher: Smith School of Enterprise and the Environment, University of Oxford. https://ora.ox.ac.uk/objects/uuid:27d52eb8-0c8b-44a6-b395-31c660e32855 (2013).

82. Davis, L. W. & Hausman, C. Who Will Pay for Legacy Utility Costs? *Journal of the Association of Environmental and Resource Economists* **9.** Publisher: The University of Chicago Press, 1047–1085. ISSN: 2333-5955. https://www.journals.uchicago.edu/doi/full/10.1086/719793 (Nov. 2022).

83. Gorman, W., Jarvis, S. & Callaway, D. Should I Stay Or Should I Go? The importance of electricity rate design for household defection from the power grid. *Applied Energy* **262,** 114494. ISSN: 0306-2619. https://www.sciencedirect.com/science/article/pii/S0306261920300064 (Mar. 2020).

84. Melissa R. Jaffe *et al. Wildfire Risk to Communities: Spatial datasets of wildfire risk for populated areas in the United States (2nd Edition)* en. 2024. https://www.fs.usda.gov/rds/archive/catalog/RDS-2020-0060-2.

85. Melissa R. Jaffe *et al. Wildfire Risk to Communities 2.0: Updated methods for geospatial datasets for populated areas in the United States* Forest Service Research Data Archive (US Department of Agriculture, Fort Collins, Colorado, 2024).

86. Wang, D. *et al.* Economic footprint of California wildfires in 2018. en. *Nature Sustainability* **4.** Number: 3 Publisher: Nature Publishing Group, 252–260. ISSN: 2398-9629. http://www.nature.com/articles/s41893-020-00646-7 (Mar. 2021).

87. Marshall Burke *et al.* The changing risk and burden of wildfire in the United States. en. *Proceedings of the National Academy of Sciences* **118.** https://www.pnas.org/doi/10.1073/pnas.2011048118 (2021).

88. Wen, J., Heft-Neal, S., Baylis, P., Boomhower, J. & Burke, M. Quantifying fire-specific smoke exposure and health impacts. *Proceedings of the National Academy of Sciences* **120.** Publisher: Proceedings of the National Academy of Sciences, e2309325120. https://www.pnas.org/doi/abs/10.1073/pnas.2309325120 (Dec. 2023).

89. Weitzman, M. L. in *The Theory and Practice of Command and Control in Environmental Policy* Num Pages: 15 (Routledge, 2003). ISBN: 978-1-315-19729-6.

90. Abatzoglou, J. T. *et al.* Projected increases in western US forest fire despite growing fuel constraints. en. *Communications Earth & Environment* **2.** Number: 1 Publisher: Nature Publishing Group, 1–8. ISSN: 2662-4435. http://www.nature.com/articles/s43247-021-00299-0 (Nov. 2021).

91. Goss, M. *et al.* Climate change is increasing the likelihood of extreme autumn wildfire conditions across California. en. *Environmental Research Letters* **15.** Publisher: IOP Publishing, 094016. ISSN: 1748-9326. https://dx.doi.org/10.1088/1748-9326/ab83a7 (Aug. 2020).

92. Fischer, E. M., Sippel, S. & Knutti, R. Increasing probability of record-shattering climate extremes. en. *Nature Climate Change* **11.** Publisher: Nature Publishing Group, 689–695. ISSN: 1758-6798. https://www.nature.com/articles/s41558-021-01092-9 (Aug. 2021).

93. Zhang, R. & Fujimori, S. The role of transport electrification in global climate change mitigation scenarios. en. *Environmental Research Letters* **15.** Publisher: IOP Publishing, 034019. ISSN: 1748-9326. https://dx.doi.org/10.1088/1748-9326/ab6658 (Feb. 2020).

94. Larson, E. *et al. Net-Zero America: Potential Pathways, Infrastructure, and Impacts* en. Tech. rep. (Princeton University, Oct. 2021). https://netzeroamerica.princeton.edu/the-report.

95. International Energy Agency. *Global EV Outlook 2024* en. Tech. rep. (2024). https://www.iea.org/reports/global-ev-outlook-2024.

96. Needell, Z. A., McNerney, J., Chang, M. T. & Trancik, J. E. Potential for widespread electrification of personal vehicle travel in the United States. en. *Nature Energy* **1.** Publisher: Nature Publishing Group, 1–7. ISSN: 2058-7546. https://www.nature.com/articles/nenergy2016112 (Aug. 2016).

97. Brownstone, D., Bunch, D. S. & Train, K. Joint mixed logit models of stated and revealed preferences for alternative-fuel vehicles. *Transportation Research Part B: Methodological* **34,** 315–338. ISSN: 0191-2615. https://www.sciencedirect.com/science/article/pii/S0191261599000314 (June 2000).

98. Tran, M., Banister, D., Bishop, J. D. K. & McCulloch, M. D. Realizing the electric-vehicle revolution. en. *Nature Climate Change* **2.** Publisher: Nature Publishing Group, 328–333. ISSN: 1758-6798. https://www.nature.com/articles/nclimate1429 (May 2012).

99. Miele, A., Axsen, J., Wolinetz, M., Maine, E. & Long, Z. The role of charging and refuelling infrastructure in supporting zero-emission vehicle sales. *Transportation Research Part D: Transport and Environment* **81,** 102275. ISSN: 1361-9209. https://www.sciencedirect.com/science/article/pii/S1361920919309149 (Apr. 2020).

100. Lee, J. H., Hardman, S. J. & Tal, G. Who is buying electric vehicles in California? Characterising early adopter heterogeneity and forecasting market diffusion. *Energy Research & Social Science* **55,** 218–226. ISSN: 2214-6296. https://www.sciencedirect.com/science/article/pii/S2214629618312258 (Sept. 2019).

101. Muehlegger, E. & Rapson, D. S. Subsidizing low- and middle-income adoption of electric vehicles: Quasi-experimental evidence from California. *Journal of Public Economics* **216,** 104752. ISSN: 0047-2727. https://www.sciencedirect.com/science/article/pii/S0047272722001542 (Dec. 2022).

102. Borenstein, S. & Davis, L. W. The Distributional Effects of US Clean Energy Tax Credits. *Tax Policy and the Economy* **30.** Publisher: The University of Chicago Press, 191–234. ISSN: 0892-8649. https://www.journals.uchicago.edu/doi/full/10.1086/685597 (Jan. 2016).

103. Do, V. *et al.* Spatiotemporal distribution of power outages with climate events and social vulnerability in the USA. en. *Nature Communications* **14,** 2470. ISSN: 2041-1723. https://www.nature.com/articles/s41467-023-38084-6 (Apr. 2023).

104. Andresen, A. X., Kurtz, L. C., Hondula, D. M., Meerow, S. & Gall, M. Understanding the social impacts of power outages in North America: a systematic review. en. *Environmental Research Letters* **18.** Publisher: IOP Publishing, 053004. ISSN: 1748-9326. https://dx.doi.org/10.1088/1748-9326/acc7b9 (May 2023).

105. Axsen, J., TyreeHageman, J. & Lentz, A. Lifestyle practices and pro-environmental technology. *Ecological Economics* **82,** 64–74. ISSN: 0921-8009. https://www.sciencedirect.com/science/article/pii/S0921800912002777 (Oct. 2012).

106. Krause, R. M., Carley, S. R., Lane, B. W. & Graham, J. D. Perception and reality: Public knowledge of plug-in electric vehicles in 21 U.S. cities. *Energy Policy* **63,** 433–440. ISSN: 0301-4215. https://www.sciencedirect.com/science/article/pii/S0301421513009427 (Dec. 2013).

107. Powell, S., Cezar, G. V., Min, L., Azevedo, I. M. L. & Rajagopal, R. Charging infrastructure access and operation to reduce the grid impacts of deep electric vehicle adoption. en. *Nature Energy* **7.** Publisher: Nature Publishing Group, 932–945. ISSN: 2058-7546. https://www.nature.com/articles/s41560-022-01105-7 (Oct. 2022).

108. He, F., Yin, Y. & Zhou, J. Deploying public charging stations for electric vehicles on urban road networks. *Transportation Research Part C: Emerging Technologies* **60,** 227–240. ISSN: 0968-090X. https://www.sciencedirect.com/science/article/pii/S0968090X15003198 (Nov. 2015).

109. Woo, S., Bae, S. & Moura, S. J. Pareto optimality in cost and service quality for an Electric Vehicle charging facility. *Applied Energy* **290,** 116779. ISSN: 0306-2619. https://www.sciencedirect.com/science/article/pii/S0306261921002816 (May 2021).

110. Bailey, M. R., Brown, D. P., Shaffer, B. C. & Wolak, F. A. *Show Me the Money! Incentives and Nudges to Shift Electric Vehicle Charge Timing* Working Paper. Aug. 2023. https://www.nber.org/papers/w31630.

111. Westerling, A. L. *et al.* Climate change and growth scenarios for California wildfire. en. *Climatic Change* **109,** 445–463. ISSN: 1573-1480. https://doi.org/10.1007/s10584-011-0329-9 (Dec. 2011).

112. California Department of Forestry and Fire Protection. *Statistics — CAL FIRE* 2024. https://www.fire.ca.gov/our-impact/statistics.

113. California Public Utilities Commission. *DECISION GRANTING PETITION TO MODIFY DECISION 09-09-030 AND ADOPTING FIRE SAFETY REQUIREMENTS FOR SAN DIEGO GAS & ELECTRIC COMPANY* tech. rep. (Apr. 2012).

114. California Public Utilities Commission. *Order Instituting Rulemaking to Examine Electric Utility De-Energization of Power Lines in Dangerous Conditions* tech. rep. (Dec. 2018).

115. California Air Resources Board. *EMFAC Fleet Database* 2024. https://arb.ca.gov/emfac/.

116. Angrist, J. D. & Pischke, J.-S. The Credibility Revolution in Empirical Economics: How Better Research Design Is Taking the Con out of Econometrics. en. *Journal of Economic Perspectives* **24,** 3–30. ISSN: 0895-3309. https://www-aeaweb-org.libproxy.berkeley.edu/articles?id=10.1257/jep.24.2.3 (June 2010).

117. Callaway, B. & Sant'Anna, P. H. C. Difference-in-Differences with multiple time periods. *Journal of Econometrics. Themed Issue: Treatment Effect 1* **225,** 200–230. ISSN: 0304-4076. https://www.sciencedirect.com/science/article/pii/S0304407620303948 (Dec. 2021).

118. Kahn-Lang, A. & Lang, K. The Promise and Pitfalls of Differences-in-Differences: Reflections on 16 and Pregnant and Other Applications. *Journal of Business & Economic Statistics* **38.** Publisher: Taylor & Francis _eprint: https://doi.org/10.1080/07350015.2018.1546591, 613–620. ISSN: 0735-0015. https://doi.org/10.1080/07350015.2018.1546591 (July 2020).

119. Ito, K. Do Consumers Respond to Marginal or Average Price? Evidence from Nonlinear Electricity Pricing. en. *American Economic Review* **104,** 537–563. ISSN: 0002-8282. https://www.aeaweb.org/articles?id=10.1257/aer.104.2.537 (Feb. 2014).

120. Wuepper, D. & Finger, R. Regression discontinuity designs in agricultural and environmental economics. *European Review of Agricultural Economics* **50,** 1–28. ISSN: 0165-1587. https://doi.org/10.1093/erae/jbac023 (Jan. 2023).

121. Heckman, J. J., Ichimura, H. & Todd, P. E. Matching As An Econometric Evaluation Estimator: Evidence from Evaluating a Job Training Programme. *The Review of Economic Studies* **64,** 605–654. ISSN: 0034-6527. https://doi.org/10.2307/2971733 (Oct. 1997).

122. Hirano, K., Imbens, G. & Ridder, G. Efficient Estimation of Average Treatment Effects Using the Estimated Propensity Score. *Econometrica* **71.** Publisher: Econometric Society, 1161–1189. https://econpapers.repec.org/article/ecmemetrp/v_3a71_3ay_3a2003_3ai_3a4_3ap_3a1161-1189.htm (2003).

123. Fowlie, M., Holland, S. P. & Mansur, E. T. What Do Emissions Markets Deliver and to Whom? Evidence from Southern California's NOx Trading Program. en. *American Economic Review* **102,** 965–993. ISSN: 0002-8282. https://www.aeaweb.org/articles?id=10.1257/aer.102.2.965 (Apr. 2012).

124. Lewis, M. *Sunrun launches the US's first vehicle-to-home power plant using customer-owned Ford F-150 Lightnings* en-US. July 2024. https://electrek.co/2024/07/29/sunrun-vehicle-to-home-power-plant-ford-f-150-lightning/.

125. *Climate Change 2022: Impacts, Adaptation and Vulnerability. Contribution of Working Group II to the Sixth Assessment Report of the Intergovernmental Panel on Climate Change.* tech. rep. (Intergovernmental Panel on Climate Change, 2022).

126. Prest, B., Rennert, K., Newell, R., Pizer, W. & Anthoff, D. *Updated Estimates of the Social Cost of Greenhouse Gases for Usage in Regulatory Analysis* en. Tech. rep. (Resources for the Future, Feb. 2023). https://media.rff.org/documents/EPA_SCC_Report_Comments.pdf.

127. Pacific Gas and Electric Company. *2022 Wildfire Mitigation Plan Update* tech. rep. (Feb. 2022).

128. Goodson, H., Long, T. & Hawiger, M. *Sur-Reply Brief of the Utility Reform Network Regarding the Revised Undergrounding Proposal of Pacific Gas and Electric Company* en. Tech. rep. (Jan. 2023).

129. Gorman, W. The quest to quantify the value of lost load: A critical review of the economics of power outages. *The Electricity Journal* **35,** 107187. ISSN: 1040-6190. https://www.sciencedirect.com/science/article/pii/S1040619022001130 (Oct. 2022).

130. Energy Information Administration. *Residential Energy Consumption Survey (RECS)* tech. rep. (). https://www.eia.gov/consumption/residential/data/2020/.

131. Pacific Gas and Electric Company. *Office of Energy Infrastructure Safety Attachment 3: Wildifire Mitigation Plan Quarterly Data Report - non-spatial data template May 2022* May 2022.

132. Missoula Fire Sciences Laboratory. *Missoula Fire Lab Command Line Applications* Sept. 2023. https://www.alturassolutions.com/FB/FB_API.htm.

133. Finney, M. A. Fire growth using minimum travel time methods. en. *Canadian Journal of Forest Research* **32,** 1420–1424. ISSN: 0045-5067, 1208-6037. http://www.nrcresearchpress.com/doi/10.1139/x02-068 (Aug. 2002).

134. Scott, J. H. & Reinhardt, E. D. Assessing crown fire potential by linking models of surface and crown fire behavior. en. *Res. Pap. RMRS-RP-29. Fort Collins, CO: U.S. Department of Agriculture, Forest Service, Rocky Mountain Research Station. 59 p.* **29.** https://www.fs.usda.gov/research/treesearch/4623 (2001).

Appendix A

A.1 Cost Data

Enhanced Vegetation Management

Following Workpaper Table 9-15 from Exhibit PG&E 4, Chapter 9 - Vegetation Management, PG&E recorded average per mile costs of $245K between 2018 and 2020[47]. In addition, the utility cites forecasted per mile costs of $298K from 2021 to 2026. Therefore, the cost analysis assumes a central per mile estimate of $250K per mile and low and high estimates of $200K and $300K, respectively.

Enhanced vegetation management is modeled as an operational expense that is incurred in the year the work is performed. However, the benefits of the vegetation management work in terms of risk reduction continue to accrue in subsequent years until the vegetation grows back. Due to data support, the analysis does not estimate empirically the rate at which these benefits attenuate to zero. In the central case, the ignition benefits of enhanced vegetation management are assumed to linearly decline to zero over a ten year lifetime. The sensitivity analysis in Figure 2.8 varies this assumption between five and fifteen years. Because some of the ignition benefits of enhanced vegetation management work are realized in future years, avoided ignitions are discounted to 2022 terms using a real social discount rate of 2.5%[126]. The discount rate varies in the sensitivity analysis between 1% and 4%.

While the vast majority of enhanced vegetation management costs are incurred at the time the work is performed, there are ongoing maintenance costs that the utility likely incurs. For instance, the utility may need to reinspect segments of the circuit to determine if sufficient clearance still exists between the overhead line and vegetation. The cost analysis assumes annual per mile maintenance costs equal to 1% of the assumed unit cost.

Undergrounding

In terms of per mile costs, Workpaper Table 4-23 from Exhibit PG&E 4, Chapter 4, Wildfire Risk Mitigation cites forecasted underground costs of $4.3M per mile in 2022 dollars[47]. However, PG&E's wildfire mitigation plan filed in February 2022 cites costs of $3.75M per mile[127]. A decision on PG&E's general rate case proceeding noted that the utility forecasts $3.3M per mile in 2023 and $2.8M by 2026 for a four-year average of $3M per mile. The decision continued by noting that the utility faces "significant uncertainty and variability associated with wildfire mitigation activities and their associated costs."[48]. The cost analysis uses $3.7M per mile as the central assumption and varies the per mile costs between $2.9M and $4.3M. It is worth noting that it may take more than one mile of undergrounding investment to replace one mile of overhead conductor, due to rerouting underneath the ground to avoid existing underground infrastructure or natural obstacles. One source cites that one mile of undergrounding only replaces 0.64-0.80 miles of overhead conductor[128]. This conversion factor is omitted from the cost analysis, but it would decrease the estimates of the cost-effectiveness of undergrounding investments.

Unlike enhanced vegetation management, underground lines are considered capital assets. Under rate of return regulation, the utility earns an authorized rate of return on its rate base, which consists of the utility's total assets net of accumulated depreciation[54]. This rate of return on capital investment enters into the utility's revenue requirement and is recovered by ratepayers via retail electricity rates. Therefore, the cost to underground a line includes both the capital cost (i.e., $3.7M per mile) and the rate of return the utility earns on the newly underground line.

The cost analysis only models this additional return on capital when it considers the "regulator" perspective in Figure 2.8. In the societal perspective, rate of return regulation is ignored and the cost of undergrounding consists solely of the per-mile unit cost and ongoing maintenance costs. In practice, there is likely a non-zero cost of financing the capital investment that is less than the utility's authorized return on capital.

To model the utility's return on capital investment, the cost analysis linearly depreciates the undergrounding asset over its assumed lifetime of 40 years. In each year, the value of the depreciated undergrounding asset is multiplied by the utility's cost of capital– 7.5%[55]. The cost model then discounts each of these annual returns into 2022 terms using a ratepayer-centric discount rate of 5% and sums them. The sensitivity analysis in Figure 2.8 varies the assumed cost of capital between 5% and 10% and varies the ratepayer-centric discount rate symmetrically between 2.5% and 7.5%.

In the "regulator" perspective, the cost analysis does not assume the entire capital cost of the underground work is recovered by the utility in the year the undergrounding work is

completed. If this was the case, retail electricity rates would have to adjust significantly in the year the work was completed, rather than adjusting smoothly over the lifetime of the asset. To model this, the cost analysis assumes each year the utility recovers the portion of the undergrounding asset that is depreciated. By the end of the asset's lifetime, it has fully depreciated to zero, and the utility has recovered the full cost of the asset. Because these costs are incurred in future years, they are discounted to 2022 terms and summed. In contrast, in the societal perspective, the per-mile costs of undergrounding are incurred solely in the year the work is completed and not spread out across future years.

Similar to enhanced vegetation management, ongoing maintenance costs associated with the underground lines are accounted for. They are expressed as ongoing annual maintenance costs equal to 1% of the per mile capital cost. However, unlike enhanced vegetation management, the analysis assumes the undergrounding investment obviates the need for the utility to complete routine vegetation management and tree mortality work on the line. Per mile routine vegetation management costs are approximated using the utility's recorded costs in 2016 and 2017, prior to the implementation of the enhanced vegetation management program. The utility spent approximately $400M per year on routine vegetation management and tree mortality in 2016 and 2017[47]. To calculate per mile costs, the analysis spreads the $400M per year across the utility's 25K miles in the HFTD to obtain a per mile estimate of $16K. This likely overstates per mile routine vegetation management costs as the $400M annual budget includes circuit-miles outside the HFTD. Discounted across the lifetime of the undergrounding asset, this annual avoided routine vegetation management cost equals approximately 11% of the $3.7M per mile undergrounding capital cost.

Given the longevity of the underground asset, a critical assumption concerns the potential for future changes to ignition and wildfire risk. Relying on 30 different climate models, one study estimates that the vast majority of climate projections lead to at least a 50% annual increase in burned area in the Western U.S. in the period 2021-2050 relative to 1991-2020[90]. However, there is considerable uncertainty surrounding future increases to annual burned area, not only due to uncertain climate projections but also due to feedback effects between burned area and fuel availability. The cost model coarsely approximates this increase in future wildfire risk by linearly increasing the measure of baseline ignition probability each year until it reaches a 50% increase by the year 2050. The analysis continues to increase ignition probability at the same linear rate after 2050 until the end of the undergrounding asset's lifetime. The sensitivity analysis varies this future risk increase between 25% and 75%. Though projections of future burned area are not equivalent to projections of powerline ignition risk, there is a relationship between burned area and ignition probabilities, as the model is strongly influenced by climate and fuel variables such as vapor pressure deficit and dead fuel moisture.

As ignition risk increases in future years, the quantity of high-wildfire risk days may

increase similarly. This is especially pertinent to fast-trip settings because fast-trip settings are only enabled when elevated wildfire conditions are identified along a segment of a distribution circuit. This means an increase in ignition risk in future years will likely raise the costs of the fast-trip program because the settings will be enabled more frequently and subsequently increase the number of fast-trip induced outages.

To project an increase in high-fire risk days (when the utility's fire potential index is at R3 or greater), the analysis takes the following steps. For each circuit, calculate the average number of high-fire risk days per year during 2015-2022. For example, suppose a hypothetical circuit, which I refer to as Circuit A, experienced 80 high-risk days per year on average from 2015-2022. Next, for each circuit, calculate the annual increase in ignition risk relative to 2015-2022 as a percentage. For example, in 2023 Circuit A's ignition risk increased by 1% compared to 2015-2022 average, and in 2040, Circuit A's ignition risk increased by 20%. Then calculate the number of high-risk days for each circuit based on its cumulative increase in ignition risk. For example, in Circuit A would have 81 (80 * [1.0+1%]) high-fire risk days in 2023, and in 2040, Circuit A would have 96 (80 * [1.0+20%]) high-fire risk days. Finally, after rounding high-risk days to the nearest whole number, rank each day in terms of ignition risk and assign the top "X" circuit-days as high-risk days where "X" is the quantity calculated in the previous step. For example, for Circuit A in 2040, the top 96 days in terms of ignition risk would be considered high-risk days.

Fast-Trip Settings

Due to the dynamic nature of fast-trip settings, their costs are modeled differently than enhanced vegetation management and undergrounding. Fast-trip settings are inexpensive to deploy, but when they are enabled on a circuit and an outage occurs, the utility must dispatch ground patrols to inspect the circuit for damage before restoring power to customers. In some cases, the utility may dispatch air resources, such as helicopters and drones, to improve restoration times.

To assess the cost-efficiency of fast-trip settings, the cost model relies on PG&E's forecasted annual budget for the fast-trip program of approximately $150M in 2022[75]. The utility forecasts $151M in fast-trip expenses for 2023, declining to $134M by 2026. The cost model assumes the $150M fast-trip budget applies only to the utility's 25K HFTD circuit-miles. In practice, due to the topology of the utility's distribution network, circuit-miles outside of the HFTD may be enabled with fast-trip settings when a circuit-segment within the HFTD is enabled. In addition to the $150M fast-trip budget in 2022, the cost model accounts for the utility's recorded $18M in fast-trip expenses for the 2021 pilot program[75].

In evaluating the cost-efficiency of fast-trip settings on reducing structures burned, the

analysis focuses on a smaller sample of approximately 6K HFTD circuit-miles (discussed in the next section). The analysis apportions the $150M fast-trip budget to the reduced 6K circuit-mile sample based on the share of fast-trip outages that occurred in the 6K sample relative to the full 25K HFTD sample. The 6K circuit-mile sample accounted for approximately 20% of fast-trip caused outages in terms of customer-hours and 25% of ignitions.

Fast-trip settings create additional costs to customers in the form of unplanned electricity outages. In 2022 and 2023, fast-trip settings caused approximately six to seven million customer-hours of outages per year. The cost model applies a constant value of lost load (VoLL) to estimate the economic cost of these outages to customers. The central VoLL parameter is $5/kWh, and the cost model varies this between $2.5/kWh and $7.5/kWh. Key sources of heterogeneity in VoLL parameter estimates include the duration of the outage, customer type, end-use, and whether the outage was expected or not[129]. Customer-hours of fast-trip outages are mapped to end-use consumption using state survey data from the U.S. Energy Information Administration[130].

Lastly, when the cost-efficiency of the fast-trip program is modeled in Figure 2.8, it is modeled assuming that no undergrounding and enhanced vegetation management had taken place. A finding from the reliability analysis is that these two measures reduce the duration and frequency of fast-trip outages (see Table A.7). The costs of the fast-trip program are adjustd upwards when no undergrounding and vegetation management efforts are deployed, given more outages would have occurred in their absence. To make this adjustment, the reliability model is used to predict the number of customer-hours of fast-trip outages absent the vegetation management and undergrounding investments. The reliability model is described in Table A.7. The model finds that there would have been an additional 700K customer-hours of fast-trip outages in 2022 absent these investments.

Public-Safety Power Shutoffs (PSPS)

Cost-effectiveness results for PSPS are not reported because of a lack of confidence in the reported cost data. There are two reasons for lacking confidence. First, attachments to the utility's wildfire mitigation plan cite approximately $180 million and $264 million in actual PSPS operational expenses in 2019 and 2020, respectively (Table 12)[131]. However, the utility's general rate case filings indicate only $141 million in recorded PSPS operations in 2020 (Workpaper Table 2-11)[75]. This is nearly half the reported costs in the utility's wildfire mitigation plan in 2020. The effect of this wide range of actual recorded PSPS costs is that ignition cost-effectiveness estimates will be highly uncertain. Second, the duration of PSPS events declined considerably in 2020 compared with 2019, but the utility reports increased PSPS costs. Customer-hours of PSPS outages declined by 76% between the two years[131] (92 million customer-hours in 2019 versus 22 million customer-hours in 2020),

and yet the utility reports a 46% increase in PSPS costs. This relationship does not inspire confidence in reported PSPS costs because such operational expenses should be positively correlated to PSPS use.

A.2 Modeling the Enablement of Fast-Trip Settings

Fast-trip settings are only enabled on circuits and days when the utility's fire potential index exceeds a threshold. PG&E combines data on weather, fuel moisture, topography, and fuel type to predict the probability of large and catastrophic wildfires, and uses a random forest classifier to predict wildfire risk, which is then summarized into six risk levels: R1, R2, R3, R4, R5, and R5+. R1 and R2 correspond to very little or moderate fire danger. R3 denotes high fire danger, R4 and R5 both denote critical fire danger, and R5+ is the greatest level of fire danger. Fast-trip settings are enabled when the risk level is R3 and above. In rare cases, PG&E enables fast-trip settings at R2, or on an R1 day if it occurs between two high-risk days, but the analysis ignore these rare cases. PSPS events are typically called on R5+ days. For more detail on PG&E's fire potential index, see section 8.3.6 of PG&E's wildfire mitigation plan[11].

To identify the effect of fast-trip settings on ignition outcomes, the analysis restricts the sample only to those fast-trip enabled days (those with fire potential index above R3). However, data on the utility's fire potential index is only available on a fraction of circuit-days, and therefore a model is trained to predict the circuit-days on which the fire potential index was above R3, and therefore fast-trip settings are enabled. Specifically, the model uses a sample of 997 observations of the utility's fire potential index at the circuit-day level[64], along with historical weather, fuel moisture, topography, and fuel type, to train a random forest classifier that predicts when the fire potential index is high enough to enable fast-trip settings, i.e. at R3 or greater on each circuit. As with the risk-score prediction model discussed earlier, the model uses 3-repeat 10-fold cross validation and tunes hyperparameters. Training and testing data are split75/25%. The model achieves an AUC value of 0.93 with the testing data. Furthermore, PG&E reported that fast-trip settings were enabled on approximately 60% of the circuit-days from May to October in 2022; using a classification threshold of 0.5, our prediction model produces a result of 62%.

Only 11,500 HFTD circuit-miles had fast-trip settings enabled in 2021. These circuits are identified through incident-specific data on fast-trip outages in 2021[68]. After 2021, all HFTD circuits had fast-trip settings enabled.

A.3 Simulating Wildfire Perimeters Using the Minimum Travel Time Method

To estimate the potential number of structures burned by an ignition at a distribution circuit on a given day, the analysis combines data on the actual acreages of utility-caused wildfires with simulations of wildfire perimeters. As shown in Equation A.1, structures burned (Y_{it}) at distribution circuit i on day t are modeled as a function of (1) the probability that an ignition grows to wildfire size s, (2) the number of residential and commercial parcels intersected (δ) by wildfire size s, and (3) the proportion of structures burned per residential and commercial parcel intersected by a wildfire (ω). Covariates include weather and environmental variables (X_{it}) and fixed circuit variables (C_i).

$$Y_{it} = \sum_{s}^{S} \Pr(s|X_{it}, C_i) * \delta_{i,s,t}(\bar{\text{A}}_s, X_{it}, C_i) * \omega \tag{A.1}$$

The four wildfire class sizes (s) considered are:

1. Small: $<$ 10 acres
2. Medium: [10 acres, 300 acres)
3. Large: [300 acres, 10,000 acres)
4. Extreme: [10,000 acres, ∞)

To estimate the first term of Equation A.1, $\Pr(s|X_{it}, C_i)$, the approach relies on empirical data on the acreages of 1,893 grid-caused ignitions between 2014 and 2022. 95% of the ignitions are considered "small" wildfires, 4% of the ignitions are considered "medium," 1% are considered "large," and 0.5% are considered "extreme." To predict which size bin s each ignition falls into, a random forest classification model is trained on historical ignition size categories as the target, and weather and environmental variables and circuit variables as features. The training and testing data is split 75/25%. Repeated 10-fold cross-validation is performed, and hyperparameters are tuned. The resulting model produces an AUC value of 0.70. Key weather and environmental variables (X_{it}) and fixed circuit variables (C_i) that influence model performance include average forest canopy height, relative humidity, wind speed, and elevation. See Figure 2.10 for a comparison of actual wildfire sizes and predicted wildfire sizes. Figure 2.11 shows how the distribution of predicted wildfire size probabilities varies across each day of the year.

The second term in Equation A.1, $\delta_{i,s,t}(\bar{A}_s, X_{it}, C_i)$, reflects the potential number of residential and commercial parcels intersected by an average wildfire in size bin ($\bar{A}_s$) conditional

on weather and circuit characteristics. In other words, if a "medium"-sized wildfire is ignited at a given circuit, how many residential and commercial parcels would we expect that wildfire to intersect, conditional on the prevailing wind direction, dead and live fuel moistures, and other covariates? Some circuits may be located near major roadways or natural fuel breaks while others may be located in densely forested areas downhill from populated areas. In addition, circuits can span hundreds of miles, and an ignition along one segment of a circuit may produce a wildfire that is more or less likely to intersect a populated area than an ignition along a different segment of the same circuit. A given wildfire size at the same ignition point can produce different structure risk, too, depending on wind direction and the locations of nearby structures.

Wildfire simulations are used to model the second term in Equation A.1, capturing important variation across circuits, within circuits, and across weather covariates by simulating many wildfire perimeters. To do this, the Minimum Travel Time (MTT) model is implemented using the command line applications developed by the Missoula Fire Sciences Laboratory[132]. The approach follows the methodology of research on the effectiveness and priorities of fire suppression in California[32]. The MTT model serves as the foundation for more complex wildfire simulation applications. Unlike the more complex physical models such as FARSITE and FlamMap, the MTT model's low computational cost makes it well-suited for running many wildfire simulations[133].

The MTT model uses a detailed landscape file from the U.S. Geological Survey's LANDFIRE program that includes remotely-sensed vegetation and topographic data at a 30-meter resolution. The landscape file uses the 40 Scott and Burgan Fire Behavior Fuel Model. For each circuit, the nearest RAWS weather station is found and corresponding wind speeds and fuel moisture data are inputted. For computational efficiency, wildfire perimeters are not simulated for all days of the year for each circuit. Rather, two high-wildfire risk days per month are selected if available and one median day per month based on fuel moisture levels, wind speeds, and relative humidity. A high-risk day is defined based on two of the three conditions being met: peak wind speeds exceeding 22 miles per hour, 10-hour dead fuel moistures being less than 5%, and relative humidity less than 25%. We then randomly create ignition points along each circuit at a density of 1 ignition point every 5 miles, but do not allow fewer than 3 or more than 15 ignition points.

Using the MTT model, wildfire perimeters are simulated at each ignition point and each weather slice. The analysis allows the MTT model to grow wildfires over a duration of 24 hours and then records the wildfire perimeters at intervals of 1-hour, 8-hours, and 24-hours to generate variation in wildfire sizes. Though a 24-hour duration is smaller than the duration of extreme wildfires, the lack of fire suppression in the MTT model and the fact that these extreme weather conditions are held constant across the entire 24-hour duration of the simulation encourages the MTT model to produce relatively large wildfire perimeters. The

average acreage of a 24-hour wildfire simulated between July and September is 72,000 acres and the maximum is 340,000 acres. Figure A.2 provides example wildfire simulation output for one circuit across two different weather slices, all ignition points along the circuit, and the three duration intervals. Additional assumptions needed to run the simulations include an ember spot probability of 0.01, 300-meter resolution, and use of the Scott-Reinhardt crown fire method[134].

Next, each wildfire perimeter is intersected with the locations of residential and commercial parcels obtained from county GIS services. Non-residential and non commercially-zoned parcels, such as timber production zones, open space areas, and agricultural plots are excluded. These types of parcels are excluded to simplify the assessment of the potential number of structures burned, acknowledging at the same time that wildfires generate significant economic impacts outside of direct structure loss.

At this point, the sample has on average 430 simulated wildfire perimeters – and corresponding number of residential and commercial parcels intersected – for every circuit, taking into account approximately 36 (12x3) weather slices, 3-15 ignition points, and 3 time intervals (1-hour, 8-hours, and 24-hours) that act as a proxy for wildfire size. Because simulations were not conducted for every day in the dataset, a random forest model is trained to predict the number of residential and commercial parcels intersected across all circuit-days. The key variables used to predict parcels intersected are wildfire size in acres, a circuit-specific effect, and detailed weather characteristics. The prediction model produces an R-squared value of 0.872.

The prediction model is then used to estimate the number of parcels intersected by an average wildfire in each wildfire size bin ("small," "medium", "large," and "extreme") for all circuit-days in the sample. The estimated number of parcels intersected for a given wildfire size bin on a circuit-day is captured by $\delta_{i,s,t}$ in the second term of Equation A.1. We calculate the expected number of parcels intersected for a given circuit-day by multiplying δ by the corresponding probability weights of each wildfire size bin s and summing the results up across each wildfire size bin.

Our wildfire simulations do not account for the effects of fire suppression. However, by deriving wildfire size probability weights using the empirical distribution of grid-caused wildfires, we implicitly account for the ability of fire suppression resources to contain wildfires during the wetter months of the year and to be less effective at containing fires during late summer and early autumn.

Lastly, the third term of Equation A.1, ω, represents the proportion of structures burned for every residential or commercial parcel intersected by a wildfire. In practice, it is not

uncommon for a mapped wildfire perimeter to intersect a parcel boundary and produce no structure damage or only partial structure damage because firefighting resources protected the structure and/or the parcel owner removed fuels in the immediate vicinity of the structure. A value of 0.4 is assumed for this parameter based on reviewing incident-specific data from CALFire. The sensitivity analysis varies this parameter from 0.2 to 0.6. Table 3.3 in Chapter Two uses a geo-spatial data product from the U.S. Forest Service (conditional risk to potential structures), and finds an average value of 0.33 to 0.36 depending on the size of the wildfire footprint.

Due to the computational intensity of the simulations, structures burned are estimated only for two key regions in the utility's service territory. Chapter Two uses a similar approach, without simulating wildfire perimeters, to conduct this analysis across all high-risk circuits. The first region is based on CALFire's Lake-Sonoma-Napa (LNU) administrative unit. The second region is based on two adjacent CALFire administrative units, Nevada-Yuba-Placer (NEU) and Amador-El Dorado (AEU) units. These two regions are prioritized based on their recent history of grid-caused wildfires and their differing fire regimes. Because circuits or simulated wildfire perimeters in these regions may extend into neighboring counties, parcel data is collected from additional counties such as Mendocino and Marin counties. The circuits in these regions span approximately six thousand HFTD miles, or about 25% of the utility's total overhead exposure in the HFTD.

A.4 Supplementary Figures and Tables

Table A.1: Covariate Balance, All Days, 2 Matches

		Controls	**Veg. Mgmt.**		**Matched Controls**		**Matched Veg. Mgmt.**	
		All HFTD	High	Moderate	High	Moderate	High	Moderate
Covariate	Units	<10%	≥50%	[10-50%)	<10%	<10%	≥50%	[10-50%)
Ignition Risk Covariates								
Ignition Risk Score	Daily Circuit Probability	0.00034	0.00084*	0.00064*	0.00079	0.0006	0.00079	0.0006
		(0.00028)	(0.00039)	(0.00033)	(0.00034)	(0.00028)	(0.00037)	(0.00028)
Circuit Length	Miles	39.8	91.5*	78.6*	88.2	62.7	87.7	71.6
		(40.9)	(59.7)	(60.7)	(60.5)	(49.8)	(58.5)	(50.4)
Relative Humidity	Daily Minimum (%)	39.0	34.4*	37.3*	35.3	35.9	34.5	37.5*
		(7.5)	(4.7)	(5.6)	(5.3)	(6.0)	(4.8)	(5.6)
Vapor Pressure Deficit	kPa	1.0	1.34*	1.16*	1.24	1.19	1.32*	1.15
		(0.3)	(0.25)	(0.27)	(0.25)	(0.28)	(0.25)	(0.27)
100 Hr. Dead Fuel Moisture	%	14.3	12.7*	13.7*	13.3	13.3	12.8*	13.8*
		(2.0)	(1.6)	(1.9)	(1.7)	(1.9)	(1.6)	(1.9)
1,000 Hr. Dead Fuel Moisture	%	15.8	14.3*	15.5	14.9	15.0	14.4*	15.6*
		(2.1)	(1.7)	(2.1)	(1.9)	(2.1)	(1.7)	(2.1)
Energy Release Component	Index	38.7	46.0*	41.0*	43.5	43.1	45.7*	40.5*
		(9.3)	(7.3)	(8.8)	(8.0)	(8.9)	(7.4)	(8.8)
Wind Speed	Meters/Second	3.8	3.3*	3.8	3.5	3.6	3.3*	3.8*
		(0.7)	(0.6)	(0.9)	(0.7)	(0.8)	(0.6)	(0.9)
Mean Forest Canopy Height	Meters	7.1	9.1*	9.4*	10.4	10.1	9.1	9.2
		(6.4)	(5.3)	(6.3)	(6.8)	(7.0)	(5.4)	(6.2)
Circuit Age	Years	34.9	31.4*	36.6	38	36.7	31.5*	37.2
		(13.0)	(11.3)	(13.8)	(10.7)	(11.7)	(11.6)	(13.7)
Elevation	Ft. Above Sea-Level	1,068	1,237	1,313*	1,394	1,430	1,247	1,294
		(1,241)	(691)	(934)	(944)	(1,084)	(693)	(944)
Precipitation	Millimeters/Day	2.0	2.1	2.4*	2.3	2.3	2.1	2.4*
		(0.8)	(0.7)	(0.9)	(0.8)	(0.8)	(0.7)	(0.9)
Mean Absolute Percent Difference		-	25.9%	19.2%	-	-	6.7%	6.4%
Wildfire Prevention Measures (Per Circuit)								
Fast-Trip	Customer-Hrs/Day	3.3	7.6*	6.5*	5.9	5.5	7.6	5.1
		(8.7)	(11.9)	(14.6)	(10.9)	(9.8)	(12.0)	(10.6)
PSPS De-Energization	Customer-Hrs/Day	37.5	88.1*	90.7*	79.7	61.3	87.7	80.9*
		(60.8)	(78.7)	(116.8)	(79.7)	(66.0)	(80.2)	(95.1)
Enhanced Vegetation Mgmt.	Miles Completed ('18-'22)	0.4	66.1*	22.5*	1.1	0.8	64.9*	20.0*
		(1.7)	(45.6)	(23.9)	(2.4)	(2.3)	(46.6)	(19)
Undergrounding	Miles Completed ('18-'22)	0.9	1.42	1.72*	0.46	0.53	1.49*	1.73*
		(2.93)	(3.76)	(5.19)	(0.74)	(0.88)	(3.88)	(5.3)

Table A.2: Covariate Balance, R3+ Days, 2 Matches

		Controls	**Veg. Mgmt.**		**Matched Controls**		**Matched Veg. Mgmt.**	
Covariate	Units	All HFTD <10% Length	High ≥50% Length	Moderate [10-50%)	High <10%	Moderate <10%	High ≥50%	Moderate [10-50%)
Ignition Risk Covariates								
Ignition Risk Score	Daily Circuit Probability	0.00067	0.00168*	0.00129*	0.0016	0.00118	0.00158	0.00121
		(0.0006)	(0.00083)	(0.00071)	(0.00076)	(0.00059)	(0.00078)	(0.00059)
Circuit Length	Miles	39.8	91.5*	78.6*	88.2	62.7	87.7	71.6
		(40.9)	(59.7)	(60.7)	(60.5)	(49.8)	(58.5)	(50.4)
Relative Humidity	Daily Minimum (%)	22.3	18.5*	20.2*	19.0	19.6	18.6	20.3
		(5.7)	(3.2)	(4.4)	(4.0)	(4.3)	(3.3)	(4.5)
Vapor Pressure Deficit	kPa	1.8	2.25*	2.03*	2.12	2.04	2.23*	2.02
		(0.41)	(0.34)	(0.38)	(0.34)	(0.38)	(0.35)	(0.38)
100 Hr. Dead Fuel Moisture	%	10.3	8.2*	9.2*	8.6	8.9	8.2	9.3
		(2.6)	(1.9)	(2.4)	(2.0)	(2.3)	(1.9)	(2.4)
1,000 Hr. Dead Fuel Moisture	%	11.3	9.0*	10.1*	9.5	9.8	9.1	10.3
		(2.7)	(1.9)	(2.4)	(2.1)	(2.4)	(1.9)	(2.4)
Energy Release Component	Index	58.5	70.3*	64.4*	67.8	66.4	69.9	63.7*
		(9.3)	(7.3)	(8.8)	(8.0)	(8.9)	(7.4)	(8.8)
Wind Speed	Meters/Second	3.6	3.2*	3.6	3.3	3.4	3.2	3.6*
		(0.8)	(0.7)	(1.0)	(0.8)	(0.7)	(0.7)	(0.9)
Mean Forest Canopy Height	Meters	7.0	9.1*	9.4*	10.4	10.1	9.1	9.2
		(6.4)	(5.3)	(6.3)	(6.8)	(7.0)	(5.4)	(6.2)
Circuit Age	Years	34.9	31.4*	36.6	38	36.7	31.5*	37.2
		(13.0)	(11.3)	(13.8)	(10.7)	(11.7)	(11.6)	(13.7)
Elevation	Ft. Above Sea-Level	1,068	1,237	1,313*	1,394	1,430	1,247	1,294
		(1,241)	(691)	(934)	(944)	(1,084)	(693)	(944)
Precipitation	Millimeters/Day	0.1	0.1	0.1	0.1	0.1	0.1	0.1
		(0.1)	(0.1)	(0.1)	(0.1)	(0.1)	(0.1)	(0.1)
Mean Absolute Percent Difference		-	28.9%	20.1%	-	-	6.0%	6.4%
Wildfire Prevention Measures (Per Circuit)								
Fast-Trip	Customer-Hrs/Day	12.2	19.4	23.7*	19.2	19.9	19.6	20.6
		(35.8)	(31.3)	(67.5)	(47.1)	(44.4)	(32.0)	(63.9)
PSPS De-Energization	Customer-Hrs/Day	142.5	232.6*	280.5*	227.0	194.9	234.2	257.6*
		(244.2)	(217)	(370.4)	(223.7)	(231.5)	(222.3)	(333.3)
Enhanced Vegetation Mgmt.	Miles Completed ('18-'22)	0.4	66.1*	22.5*	1.1	0.8	64.9*	20.0*
		(1.7)	(45.6)	(23.9)	(2.4)	(2.3)	(46.6)	(19)
Undergrounding	Miles Completed ('18-'22)	0.9	1.42	1.72*	0.46	0.53	1.49*	1.73*
		(2.93)	(3.76)	(5.19)	(0.74)	(0.88)	(3.88)	(5.3)

Figure A.1: Comparison of Predicted and Actual Ignitions

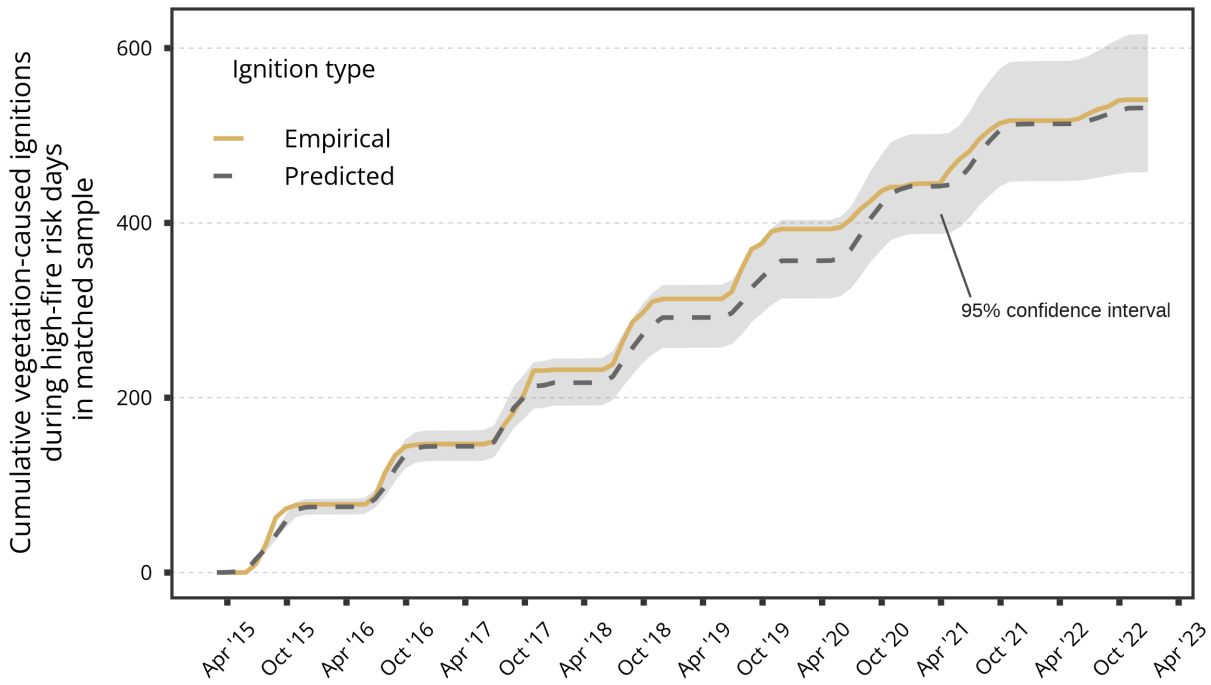

Notes: Comparison of predicted and empirical ignitions. Using our preferred specification in column (3) of Table 2.5, we compare the number of ignitions predicted by our econometric model against the number of ignitions observed in our matched treatment and control sample on high-fire risk days. We find that the fitted values of our econometric model reasonably predict actual observed ignitions, which is also supported by an AUC value in Table 2.5 of 0.75. Our econometric model tends to under-predict powerline-caused ignitions in 2019 and over-predict ignitions in 2020. The former period was a relatively low risk year for wildfires given record snowfall totals while the latter period saw a record number of acres burned across the state.

Table A.3: Intertemporal Covariate Balance

		High-Fire Risk Days	
Covariate	Units	Pre Fast-Trip (2015-21)	Post Fast-Trip (2021-22)
Ignition Risk Score	Daily Circuit Probability	0.00133 (0.00070)	0.00137 (0.00071)
Relative Humidity	Daily Minimum (%)	19.1 (3.9)	20.01* (4.75)
Vapor Pressure Deficit	kPa	2.08 (0.36)	2.19* (0.41)
100 Hr. Dead Fuel Moisture	%	8.8 (2.2)	8.8 (2.3)
1,000 Hr. Dead Fuel Moisture	%	9.8 (2.3)	9.8 (2.4)
Energy Release Component	Index	66.5 (12.1)	66.0 (13.2)
Maximum Temperature	Celsius	30.2 (2.1)	31.1* (2.3)
Wind Speed	Meters/Second	3.4 (0.8)	3.5 (0.8)
Precipitation	Millimeters/Day	0.05 (0.04)	0.11* (0.21)

Notes: High-fire risk days before and after fast-trip settings were deployed. Asterisks denote statistical significance of a two-sided t-test.

Table A.4: Robustness Test - Inclusion of Regional Fixed Effects

	Incidence Rate - Vegetation-Caused Ignitions		
	No Matching	Matching	Matching & High Fire Risk
	(1)	(2)	(3)
Fast-Trip (F_{it})	−0.25	−0.57*	−0.73*
	(−0.57, 0.31)	(−0.74, −0.29)	(−0.83, −0.55)
Veg. Mgmt. (D_i=High x T_{it}=Post)	−0.62*	−0.59*	−0.59*
	(−0.80, −0.29)	(−0.78, −0.22)	(−0.82, −0.04)
Veg. mgmt. (D_i=Moderate x T_{it}=Post)	−0.01	0.01	0.30
	(−0.25, 0.33)	(−0.25, 0.37)	(−0.12, 0.91)
Veg. mgmt. (D_i=High)	1.04*	0.17	0.28
	(0.63, 1.56)	(−0.06, 0.45)	(−0.003, 0.63)
Veg. mgmt. (D_i=Moderate)	0.75*	−0.12	−0.11
	(0.44, 1.12)	(−0.27, 0.07)	(−0.31, 0.14)
Combined Effect (D_i=High x F_{it} x T_{it}=Post)	−0.89	−0.87	−0.92
	(−1.00, 1.95)	(−0.99, 2.34)	(−1.00, 1.85)
Combined Effect (D_i=Moderate x F_{it} x T_{it}=Post)	−0.75	−0.80	−0.87
	(−0.97, 1.14)	(−0.98, 1.04)	(−0.99, 0.45)
Risk-score matching	No	Yes	Yes
High-fire risk days only	No	No	Yes
Region FEs	Yes	Yes	Yes
Matched control neighbors (N)	-	2	2
Risk-score, undergrounding, PSPS, and covered conductor controls	Yes	Yes	Yes
AUC	0.776	0.757	0.752
Observations	2,400,342	1,890,015	665,868
Log Likelihood	−6,679.31	−8,039.28	−4,519.75

Table A.5: Robustness Test - One Matched Control Circuit

	Incidence Rate - Vegetation-Caused Ignitions		
	No Matching	Matching	Matching & High Fire Risk
	(1)	(2)	(3)
Fast-Trip (F_{it})	−0.27	−0.36	−0.56*
	(−0.58, 0.26)	(−0.62, 0.05)	(−0.74, −0.27)
Veg. Mgmt. (D_i=High x T_{it}=Post)	−0.62*	−0.59*	−0.58*
	(−0.79, −0.29)	(−0.78, −0.22)	(−0.82, −0.02)
Veg. Mgmt. (D_i=Moderate x T_{it}=Post)	−0.03	−0.03	0.26
	(−0.27, 0.29)	(−0.28, 0.31)	(−0.14, 0.86)
Veg. Mgmt. (D_i=High)	1.18*	−0.11	−0.05
	(0.77, 1.70)	(−0.28, 0.11)	(−0.26, 0.23)
Veg. Mgmt. (D_i=Moderate)	1.23*	−0.10	−0.12
	(0.87, 1.67)	(−0.25, 0.09)	(−0.31, 0.13)
Combined Effect (D_i=High x F_{it} x T_{it}=Post)	−0.89	−0.87	−0.92
	(−1.00, 1.89)	(−1.00, 2.19)	(−1.00, 1.70)
Combined Effect (D_i=Moderate x F_{it} x T_{it}=Post)	−0.77	−0.81	−0.88
	(−0.97, 0.94)	(−0.98, 0.86)	(−0.99, 0.38)
Risk-score matching	No	Yes	Yes
High-fire risk days only	No	No	Yes
Matched control neighbors (N)	-	1	1
Region FEs	No	No	No
Risk-score, undergrounding, PSPS, and covered conductor controls	Yes	Yes	Yes
AUC	0.782	0.785	0.732
Observations	2,400,342	1,282,899	446,254
Log Likelihood	−6,776.30	−5,979.78	−3,397.59

Note:

Table A.6: Robustness Test - Inclusion of Unmatched High-Risk Circuits

	Incidence Rate - Vegetation-Caused Ignitions		
	No Matching	Matching	Matching & High Fire Risk
	(1)	(2)	(3)
Fast-Trip (F_{it})	−0.27	−0.55*	−0.72*
	(−0.58, 0.26)	(−0.71, −0.30)	(−0.82, −0.56)
Veg. Mgmt. (D_i=High x T_{it}=Post)	−0.62*	−0.63*	−0.62*
	(−0.79, −0.29)	(−0.80, −0.31)	(−0.83, −0.13)
Veg. mgmt. (D_i=Moderate x T_{it}=Post)	−0.03	−0.03	0.20
	(−0.27, 0.29)	(−0.27, 0.29)	(−0.16, 0.72)
Veg. mgmt. (D_i=High)	1.18*	0.07	0.13
	(0.77, 1.70)	(−0.11, 0.29)	(−0.09, 0.41)
Veg. mgmt. (D_i=Moderate)	1.23*	0.05	0.09
	(0.87, 1.67)	(−0.11, 0.23)	(−0.12, 0.34)
Combined Effect (D_i=High x F_{it} x T_{it}=Post)	−0.89	−0.88	−0.93
	(−1.00, 1.89)	(−0.99, 1.74)	(−1.00, 1.14)
Combined Effect (D_i=Moderate x F_{it} x T_{it}=Post)	−0.77	−0.74	−0.85
	(−0.97, 0.94)	(−0.96, 0.83)	(−0.98, 0.17)
Risk-score matching	No	Yes	Yes
High-fire risk days only	No	No	Yes
Region FEs	No	No	No
Matched control neighbors (N)	-	2	2
Risk-score, undergrounding, PSPS, and covered conductor controls	Yes	Yes	Yes
AUC	0.782	0.794	0.754
Observations	2,400,342	2,037,012	724,765
Log Likelihood	−6,776.30	−9,491.70	−5,481.75

Note:

Table A.7: Effect of Wildfire Mitigations on Fast-Trip Outages

	OLS Model	
	Daily Fast-Trip Customer-Hours	
	(1)	(2)
Fast-trip (F_{it})	87.8*	74.9*
	(5.0)	(3.7)
Veg. mgmt. (D_i=High)	-0.5	-0.5
	(0.4)	(0.3)
Combined effect (D_i=High x F_{it})	−12.8	2.1
	(8.3)	(7.6)
Veg. mgmt. (D_i=Moderate)	-0.6	-0.5
	(0.4)	(0.4)
Combined effect (D_i=Moderate x F_{it})	−18.4*	-3.7
	(8.1)	(7.4)
Underground miles (10s mi)	0.03	0.01
	(0.02)	(0.01)
Combined effect (Underground x F_{it})	−26.2*	−21.3*
	(6.1)	(5.4)
Ignition risk score (θ)	2,744.2	2,356.8
	(1,924.9)	(1,660.6)
Matched controls	1	2
Observations	149,550	220,324
Adjusted R^2	0.02	0.01

Notes: The reliability model regresses daily customer-hours of fast-trip outages on the set of wildfire prevention measures, an interaction of each wildfire prevention measure and whether fast-trip settings were enabled or not, and our measure of ignition risk probability. Only data from 2022 is used in both columns– when fast-trip settings were deployed across the entire HFTD. The first column uses the sample where circuits treated with vegetation management are matched to a single control circuit based on ignition risk, and the second column uses the sample where circuits are matched to at most two control circuits. We use a linear regression model here, in contrast to the logistic regression model earlier, because customer-hours of fast-trip outages is a continuous variable. We find that when fast-trip settings are enabled on a given day, a circuit will experience 75-88 customer-hours of outages, on average. In the first column, the enhanced vegetation management combined effects show that when fast-trip settings are enabled and a circuit has received high or moderate vegetation management, we expect 13-18 fewer customer-hours of fast-trip outages. This is a 15-21 percent reduction in reliability impacts relative to circuits without enhanced vegetation management. However, as the second column shows, the effect is not robust. Adding a second matched control reduces the magnitudes of the effects and the statistical significance. In contrast, the effect of undergrounding on expected fast-trip customer hours is robust. On days when fast-trip settings are enabled, we find that a circuit with 10 miles of overhead conductor placed underground experiences 21-26 (28-30%) fewer customer-hours of fast-trip outages compared to circuits with zero miles. These results demonstrate that undergrounding and vegetation management can reduce the reliability impact of operational measures that de-energize powerlines.

Figure A.2: Illustration of Wildfire Simulation

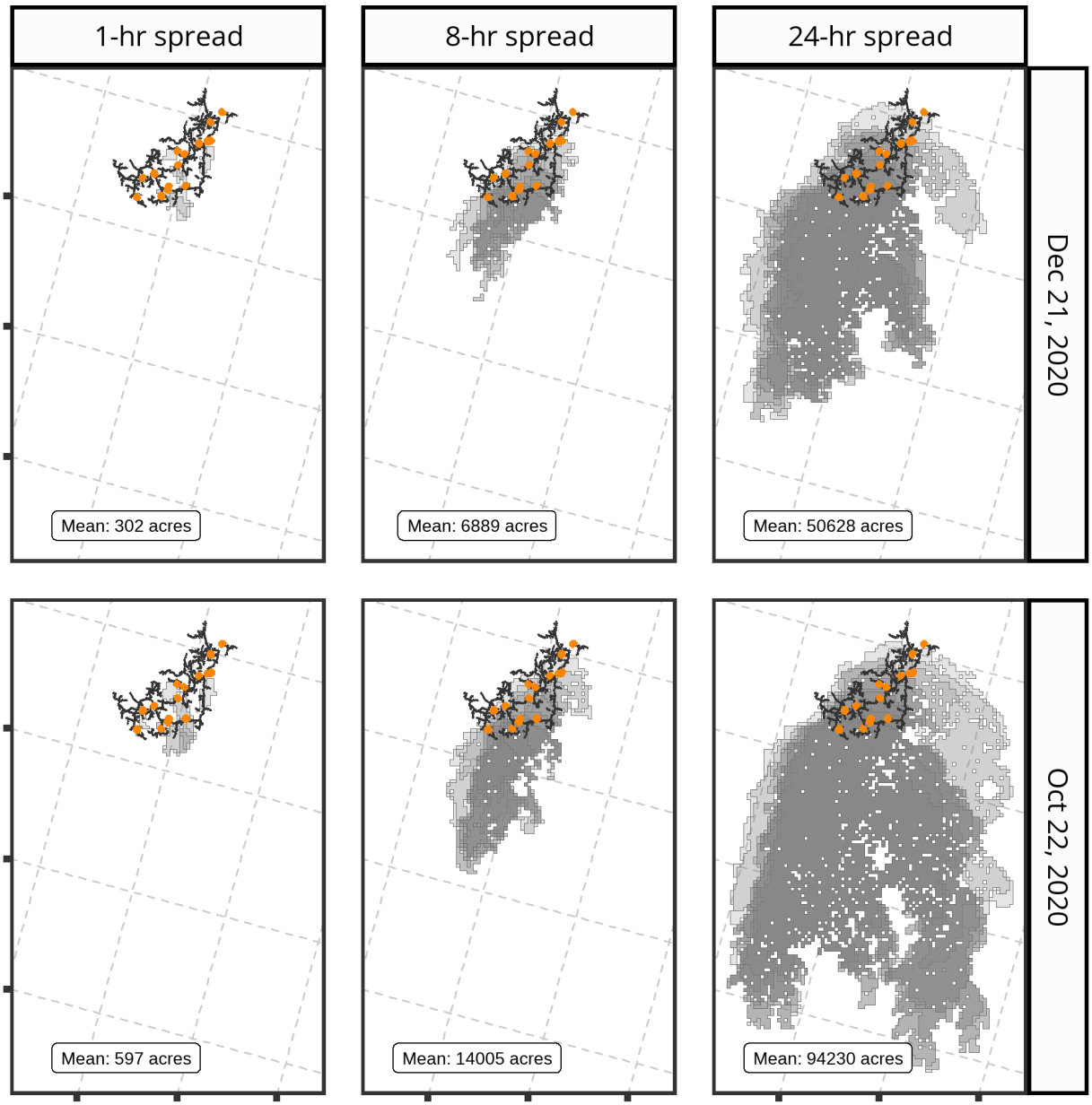

Notes: The plot shows pixels burned by wildfires simulated using the Minimum Travel Time (MTT) model. Here we show the wildfires simulated for one distribution circuit across multiple ignition points and two weather slices (October 22, 2020 and December 21, 2020). Ignition points are randomly sampled across each distribution circuit to capture variation in wildfire risk within a distribution circuit. As a proxy for variation in wildfire size, wildfires grow for a maximum of 24 hours but the perimeters of the simulated fires are recorded at 1-hour, 8-hour, and 24-hour intervals. The perimeters are then intersected with spatial data on the locations of residential and commercial parcels.

Appendix B

B.1 OLS Robustness Tests

Figure B.1: OLS Robustness Test Average Treatment Effect by Utility

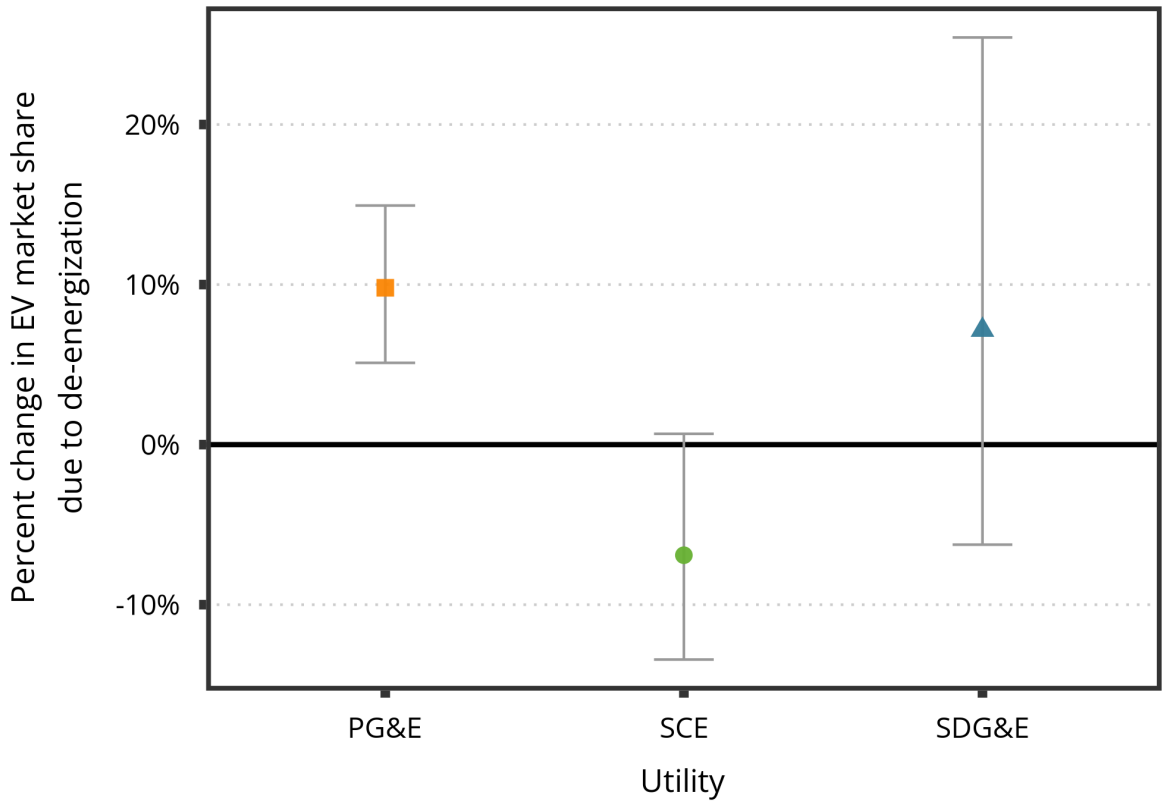

Notes:

Figure B.2: OLS Robustness Test Average Treatment Effect by Commute Bracket

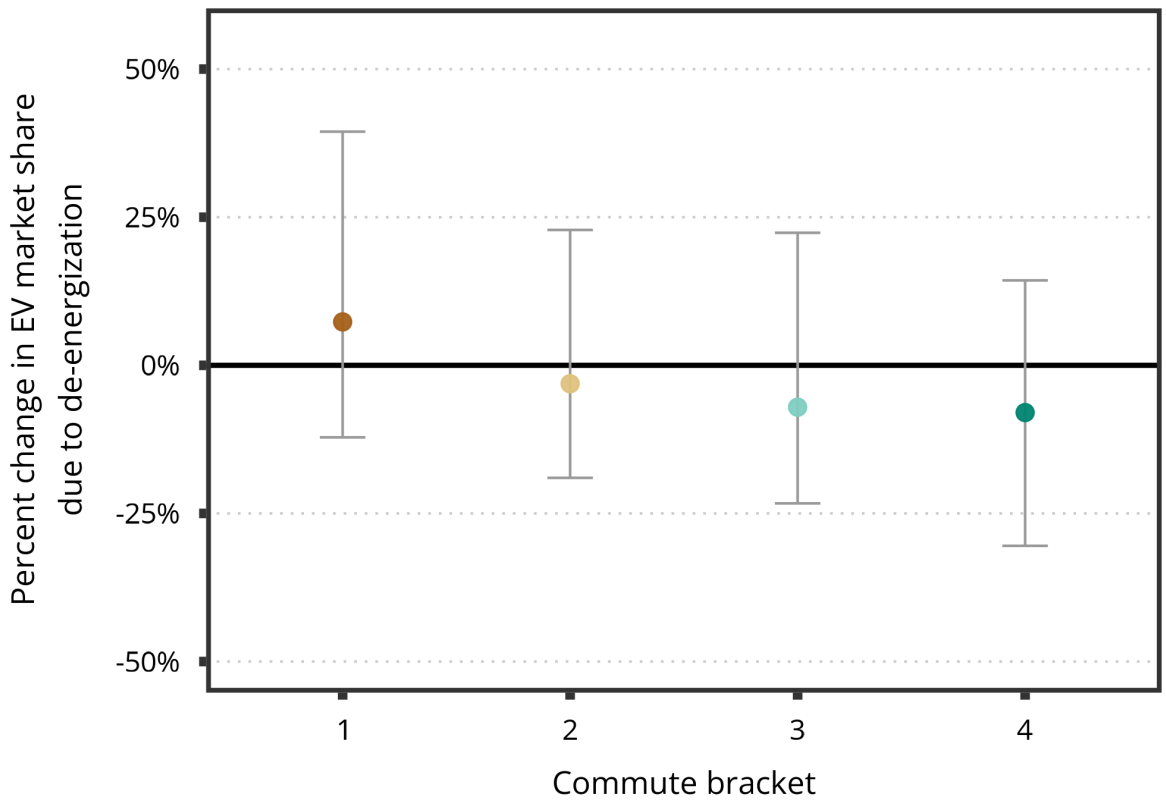

Notes: